Faculty of Aerospace Engineering

Effect of ADS-B Limitations and Inaccuracies on CD&R Performance

T.P. Langejan

September 7, 2016

Delft University of Technology

Challenge the future

Effect of ADS-B Limitations and Inaccuracies on CD&R Performance

Master of Science Thesis

For obtaining the degree of Master of Science in Aerospace Engineering
at Delft University of Technology

T.P. Langejan

September 7, 2016

Faculty of Aerospace Engineering · Delft University of Technology

Delft University of Technology

Copyright © T.P. Langejan
All rights reserved.

Delft University Of Technology
Department Of
Control and Simulation

The undersigned hereby certify that they have read and recommend to the Faculty of Aerospace Engineering for acceptance a thesis entitled **"Effect of ADS-B Limitations and Inaccuracies on CD&R Performance"** by **T.P. Langejan** in partial fulfillment of the requirements for the degree of **Master of Science**.

Dated: September 7, 2016

Readers:

____
Prof. Dr. Ir. J.M. Hoekstra

____
Dr. Ir. J. Ellerbroek

____
Ir. E. Sunil

Preface

First of all I would like to thank you for reading my Thesis research. This graduation project contains the results of the final deliverable for my Master of Science Thesis Aerospace Engineering, Control and Simulation at the Delft University of Technology.

I would like to thank Emmanuel Sunil, my daily supervisor, for his feedback and enthusiasm. Through the whole project Emmanuel invested time and energy to support me continuously, ranging from small questions to elaborate Python sessions and tips for a good paper structure. Next to that I, would like to thank Joost Ellerbroek and Jacco Hoekstra for their feedback and support during my thesis work.

Finally I would like to thank my friends and family for their moral support, both during my Bachelor and Master.

Thom Langejan
August, 2016

Outline Report

This thesis consists of several parts. During the preliminary phase a reports has been written of the results so far. The preliminary phase is followed by the main phase of the thesis. For the final phase a scientific paper has been written in IEEE style, containing the main results. The appendices contain a more elaborated literature review and a project plan, including a Gantt chart.

The outline of this report is as follows:

- **Paper** The main results are presented in a paper written in IEEE lay-out in the first part of the report.
- **Preliminary report** The preliminary report is shown in the second part of this report.
- **Appendices** The appendices contain a more extensive literature review and a project plan, including a Gantt chart. Additionally a shortened paper is included, that is submitted to the SESAR innovation days 2016.

Acronyms

ADS-B	Automatic Dependent Surveillance-Broadcast
ASAS	Airborne Separation Assurance System
ATC	Air Traffic Control
ATM	Air Traffic Management
CA	Collision Avoidance
CD	Conflict Detection
CD&R	Conflict Detection & Resolution
CPA	Closest Point of Approach
CPR	Compact Position Reporting
CR	Conflict Resolution
DEP	Domino Effect Parameter
ES	Extended Squitter
FC	Flock Centering
FMS	Flight Management System
FSPL	Free Space Path Loss
GNSS	Global Navigation Surveillance System
GPS	Global Positioning System
IFR	Instrument Flight Rules
LOS	Loss Of Separation
LVNL	Lucht Verkeersleiding Nederland
MTL	Minimum Triggering Level
MVP	Modified Voltage Potential
NM	Nautical Mile
PPM	Pulse Position Modulation
TCAS	Traffic Collision Avoidance System
UAS	Unmanned Aircraft System
UAV	Unmanned Aerial Vehicle

VM	Velocity Matching
WAAS	Wide Area Augmentation System

List of Symbols

Greek Symbols

τ	ADS-B message duration [s]
λ	Longitude [rad]
λ	Number of events occuring in 1 unit length of time for Poisson distribution.
μ	Mean normal distribution
ϕ	Latitude[rad]
σ	Standard deviation normal distribution

Roman Symbols

c	speed of light [$\frac{m}{s}$]
d	Distance in meter [m]
dB	Decibel
f_{ES}	ADS-B carrier frequency [Hz]
FSPL	Free Space Path Loss [dBi]
N_{ac}	Number of aircraft within range [-]
N_{LOS}	Total number of Loss of separation in scenario [LOS]
N_{total}	Total number of aircraft in scenario [Aircraft]
r	Distance in Nautical Miles [NM]
s	Distance [m]
S_{rec}	Received Power [dBm]
S_{rec0}	Received Power with 0 reception probability [dBm]
S_{rec_1NM}	Received Power at 1 NM distance [dBm]

S_T	Transmit Power [dBm]
t_{CPA}	Time to closest approach [s]
$\mathbf{T}$	Thrust [N]
$\vec{V}$	Swarming method vector, corresponding swarming element indicated in subscript.
R	Earths radius [m]
W	Swarming method weight, corresponding swarming element indicated in subscript. [-]
X	Number of events occuring in interval length of Poisson distribution [-]

List of Figures

List of Tables

Contents

Part I

Paper

Effect of ADS-B Limitations and Inaccuracies on Conflict Detection and Resolution methods

Thom Langejan, Emmanuel Sunil, Joost Ellerbroek and Jacco Hoekstra

Abstract—**The current Air Traffic Management (ATM) system is reaching its capacity limits. Additionally the growing Unmanned Aerial Vehicle (UAV) market results in new Air Traffic Control (ATC) challenges in the near future. A possible solution is a Free Flight environment, where all restrictions of ATC are lifted. This requires Airborne Conflict Detection & Resolution (CD&R) methods, using the Automatic Dependent Surveillance-Broadcast (ADS-B) system for direct state information exchange between aircraft. Limitations of ADS-B are system related, affecting state information quality and situation related, resulting in reduced detect and decode probability due to range and interference. In this project these limitations are assessed against two CD&R methods and three air traffic densities. This research aims to quantify the impact of these limitations on airborne CD&R and the feasibility using the ADS-B system in Free Flight. Three experiment are conducted to obtain safety, efficiency and stability metrics. The goal of the first experiment is to differentiate between the effect of ADS-B based and perfect state information on CD&R. The second and third experiment assess the contribution of individual aspects, such as interference and transmit power (i.e. range). The Modified Voltage Potential (MVP) method showed better results than the swarming method, and is very robust. The effect ADS-B limitations are small when compared to assuming perfect state information for airborne CD&R purposes. However, increasing traffic and transmit power lower the detect and decode probability due to interference and should be considered for high traffic densities.**

I. Introduction

RECENT and on-going developments in aviation require a modernization of the ATM system. First of all; due to the steady and continuous growth of air traffic, the current ATM system is reaching its capacity limits [1]. Secondly the current developments in UAVs require a novel approach to ATC. Current technologies rely on communication between the pilots and ground-based controllers, both actively involved to prevent conflicts. A trend in the UAV area is observed from pilot guided UAVs to vehicles with a higher level of autonomy [2]. A restructuring of airspace and novel ATC systems are required to fulfill future airspace demand and to safely integrate UAVs [3], [4].

Free Flight, using airborne self separation, is identified as a promising concept to increase capacity and integrate UAVs [5], [6]. Additional benefits of Free Flight are increases in safety as well as economical and environmental gains [7], [8]. In Free Flight, airborne CD&R methods are used to predict conflicts between aircraft and provide possible resolutions to the aircrew, or even autonomously resolve conflicts. In this research domain, the ADS-B system is identified as a key enabling technology for Free Flight, providing direct state information exchange between aircraft [9], [10]. However, in the simulations performed in most CD&R related research, the availability of perfect state information of surrounding aircraft is assumed. Previous research has not considered the effect of ADS-B limitations and inaccuracies on CD&R methods. The questions arises if the ADS-B system is actually capable of providing usable state information for CD&R purposes. It is concluded by several studies that the ADS-B system has limitations [11]. The main degrading factors are aircraft state inaccuracy, as well as transmission latency and reception limitations [12]. ADS-B reception models are derived in [9], [13]. The authors model the effect of range and interference between aircraft on ADS-B detect and decode probability. A gap in literature is found where the use of CD&R methods for airborne self separation are evaluated using realistic ADS-B limitations.

This paper aims to link the limitations of the ADS-B system and study its effect on CD&R methods in a Free Flight environment. An ADS-B model is created and different CD&R methods are subjected to ADS-B limitations. Two CD&R methods are selected; the MVP and swarming method, described in [14]. Additionally it is assessed which factors affect the quality of the ADS-B signal and to what extent. Therefore three experiments are created. The goal of the first experiment is to assess the effect of different ADS-B models on CD&R performance. The second experiment aims to study the impact of two individual ADS-B signal degrading properties, range and interference. Increasing the maximum ADS-B reception range has two opposing effects: increase of range related detect and decode probability and increase of interference severity. Therefore the goal of the third experiment is to assess the effect of different ADS-B reception ranges on CD&R performance.

This paper is organized as follows: an overview of the CD&R methods is given in Section II. Subsequently the ADS-B system is discussed in Section III. A detect and decode probability model for ADS-B messages is created based on situational related properties. Also system related inaccuracies are discussed. The implementation of the ADS-B model in the BlueSky simulator is explained in Section IV. Also the experimental dependent an independent variables for each experiment are discussed in Section IV. The results of the three experiments are discussed in Section V, Section VI and Section VII. This paper is concluded with a discussion in Section VIII and a conclusion in Section IX.

II. Conflict Detection and Resolution

In this section the Conflict Detection (CD) is discussed in Section II-A. Subsequently two Conflict Resolution (CR) methods, MVP and Swarming, are described in Section II-B.

A. Conflict Detection

A conflict occurs when an aircraft is predicted to enter the Intruder Protected Zone (IPZ) of another aircraft in case no additional actions are taken. Another aircraft entering this zone results in an intrusion, also called Loss Of Separation (LOS). In this study state based conflict detection is chosen over intent based conflict detection. This method uses the current positions of aircraft and extrapolates speeds vector of itself and surrounding aircraft to detect possible conflicts. This method has a low false-alarm rate and high fidelity for en-route air traffic [15]. Additionally nominal trajectory planning is chosen over worst-case or probabilistic projection, discussed in [16]. The dimensions of the IPZ are defined by the RTCA. For en-route air traffic a 5 nautical miles separation in the horizontal plane and 1000 feet separation in the vertical plane need to be maintained, to ensure safe flight [17]. Only conflicts occurring within 5 minutes will result in CR. The 5 minutes look-ahead time is typical and most suitable for velocity vector extrapolation [6], [18].

B. Conflict resolution

In [14] it was found that two CD&R methods showed promising result as application for airborne self separation, the MVP and Swarming method (discussed in [19] and [20] respectively in more detail). While subjected to perfect state information, the MVP method showed better performance than the swarming method (lower number of LOS). However, with stochastic factors introduced, the swarming showed a decrease in numbers of LOS, while the MVP methods showed an increase in number of LOS. Therefore these two methods are selected for further research and presented below.

MVP

The MVP method is based on modeling aircraft as similarly charged particles that repel each other, described in [7], [19]. This method contains of three steps [21]:

1) Conflict detection
2) Obtain MVP based resolution vector
3) Conflict resolution

The determination of the MVP based resolution vector is shown in more detail in Figure 1 and discussed below.

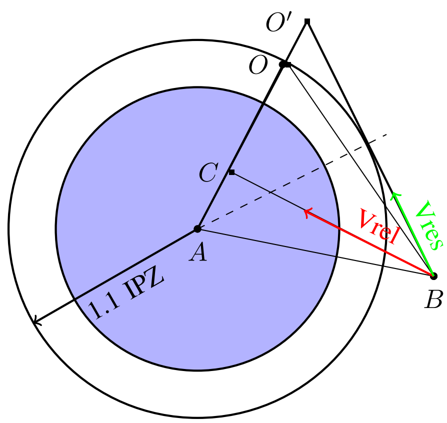

Figure 1: Top view of two aircraft (A and B) on collision course with MVP based resolution in the horizontal plane. Shown are the relative velocity vector (V_{rel}) and the MVP based resolution vector (V_{res}).

The Intruder Protected Zone is shown and an additional safety margin of 10% is added. The relative velocity vector with respect to a conflicting aircraft (A) is calculated (V_{rel}). This relative velocity vectors results in a loss of separation without any intervention. Using this relative velocity and distance between the two aircraft, the Closest Point of Approach (Point C) can be determined. Subsequently the closest distance out of the IPZ (O) is determined. It can be obtained the resolution vector CO still results in a LOS. Therefore Equation (1) is used to obtain the final resolution vector (V_{res}).

$$\frac{|CO'|}{CO} = \frac{1}{|cos(arcsin(\frac{R}{AB}) - arcsin(\frac{AC}{AB})|} \quad (1)$$

Now the distance vector CO' is determined, the new velocity vector is calculated using Equation (2) [21]. In this equation t_C is the time it is predicted for aircraft B to be at point C.

$$V_{MVP} = \frac{CO'}{t_C} + V_{current} \quad (2)$$

The swarming method

Swarming intelligence, discussed in [20], is a bio-inspired interaction between animals in large groups, such as a school of fish or a flock of birds. In this research the goal was to apply the swarming method to UAVs. The behavior of each individual agent consists of three elements and is adapted to use as a CD&R method for en-route traffic, shown in [14]:

1) **Collision Avoidance (CA) component**. Uses the MVP method to obtain a resolution vector.
2) **Velocity Alignment (VA) component**. Match the velocity direction and magnitude of surrounding aircraft.
3) **Flock Centering (FC) component**. Obtain the graphical center of surrounding aircraft (with aircraft in the same heading range) and steer in that direction. This results in grouping of aircraft.

The swarming method employs a weighted combination of the three actions described above, shown in Equation (3). The subscripts in the symbols correspond with the different swarming elements.

$$\vec{V}_{SW} = \frac{W_{CA} \cdot \vec{V}_{CA} + W_{VA} \cdot \vec{V}_{VA} + W_{FC} \cdot \vec{V}_{FC}}{W_{CA} + W_{VA} + W_{FC}} \quad (3)$$

The velocity alignment and flock centering components are constantly activated during flight. The collision avoidance component becomes active in case a conflict is detected. The swarming weights are tuned based on a "super-8 conflict" and "wall conflict", discussed in [14], [22], [19]. The values shown in Table I resulted in satisfactory results. It was found that collision avoidance should have the largest weight, and flock centering the smallest, for a stable result.

Table I: Swarming weights

Swarming weights		
Swarming Element	Symbol	Weight
Collision Avoidance	W_{CA}	20
Velocity Alignment	W_{VA}	3
Flock Centering	W_{FC}	1

Two additional rules were added to increase the swarming performance:

- Aircraft only swarm when their current heading difference is $\leq$ 30 °.
- Aircraft only swarm if their way-point heading is $\leq$ 45 °.
- Aircraft only swarm if their distance is $\leq$ 20 NM.

The first rule makes sure that only aircraft with a similar current heading swarm together. The second rule enables aircraft to "escape" a group of aircraft when they are close to their destination (way-point heading becomes $\geq$ 45 °). It should be noted that the swarming method is MVP extended with a swarming element.

Trajectory recovery

After a successful conflict resolution, aircraft are required to follow the heading back to their original destination. Aircraft do not return to their original track. The Closest Point of Approach (CPA) of a conflict is determined. After this point the conflict is solved and the aircraft determines its new heading to arrive at its destination. Other aircraft states, such as altitude and velocity, are also restored.

III. ADS-B Model

In this research the focus is on the airborne ADS-B link between aircraft, enabled by ADS-B IN/OUT. ADS-B transmits specific state information in an omnidirectional manner called squitter. Different type of squitter messages exist, with their corresponding transmit rate:

- Airborne positions squitter (2/sec)
- Surface position squitter (1/sec)
- Airborne velocity squitter (2/sec)
- Aircraft identification squitter (0.2/sec)
- Operational Status (0.4/sec)
- Target state (0.8/sec)

The reports are transmitted using a 1090 MHz carrier frequency using Pulse Position Modulation (PPM). Each message contains 120 bits and is transmitted with 1 Mbps, resulting in a message duration of 120 μs.

Two main elements can be identified affecting the system performance; situational and system related elements. Situation related elements mostly affect the probability of proper detection and decoding of an ADS-B report. System related elements affect the actual content of the ADS-B report. A schematic overview is shown in Figure 2.

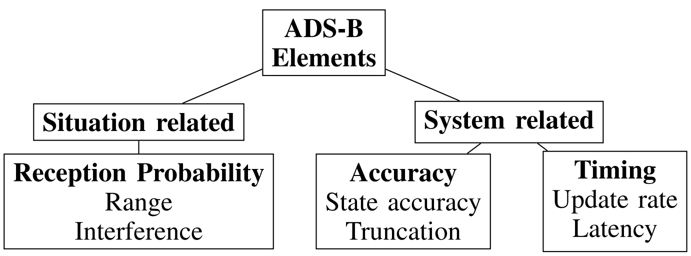

Figure 2: Schematic overview of elements degrading ADS-B performance.

Both system and situation related elements are discussed in Section III-A and Section III-B respectively. An analytical model is developed and explained for both.

A. System related ADS-B elements

Several system related elements affect the quality of an ADS-B report. Only a limited number of bits are available, affecting the level of accuracy in the ADS-B message, caused by truncation.

Truncation

The position reports contain latitude and longitude locations. The latitude and longitude are both transmitted using 6 significant digits. The offset, caused by truncation, is the distance between two locations where the 6th digit is changed. The Haversine function, shown in Equation (4), is used to calculate the great-circle distance between two points in meters, expressed in latitude and longitude. In this equation ϕ is latitude (rad), λ is longitude (rad), and R (m) is the earth radius.

$$a = sin(\frac{\Delta\phi}{2}) + cos(\phi_1) \cdot cos(\phi_2) \cdot sin^2(\frac{\Delta\lambda}{2}) \tag{4a}$$

$$c = atan2(\sqrt{a}, \sqrt{1-a}) \tag{4b}$$

$$d = R \cdot c \tag{4c}$$

Using the Haversine function and a position described in longitude and latitude with a six digit significance level results in a accuracy ranging from 9 to 17 m, depending on the location on the earth.

State accuracy

In addition to the truncation effect, the state accuracy of the on-board measurement equipment affects the location precision. Location determination is done using the Global Navigation Surveillance System (GNSS). Altitude and airspeed are obtained using on-board sensors. These two states are expected to be highly accurate compared to position. Position is the state that depends on an external system, such as GNSS or Wide Area Augmentation System (WAAS). In [23] it is that found a GPS measurement has an accuracy of $\leq$7.8 meter with a 95% confidence interval.

Update rate and latency

Generating and transmitting an ADS-B reports results in a latency in the order of 20 milliseconds. A much larger effect is the limited update or transmit rate of an ADS-B report, which is in the order of seconds. This system delay does result in a position error in the order of tens of meters in the ADS-B position report.

Different system related properties contribute to the position error:

1) **GPS error:** $\pm$8 m with a 95 % confidence interval.
2) **Latency:** 20 milliseconds, resulting in $\pm$5 m (assuming cruise speeds of 800 km/h).
3) **Truncation:** $\pm$15 meters.

B. Situation related ADS-B elements

The situation related elements affect the reception and decode probability of the content of an ADS-B report, caused by range and interference. An analytical model of these two is discussed in the following two paragraphs.

Range

The derivation of an analytical model between distance and detect/decode probability is based on the 1090 Extended Squiter (ES) Minimum Operational Performance Specifications (MOPS) [12]. The general approach, described in [9], [24], is followed. It is assumed that the noise level on the 1090 MHz frequency is constant. An increasing distance between transmitter and receiver results in a decrease in Signal to Noise Ratio (SNR). An illustration is shown in Figure 3.

This derivation consists of the following steps:

1) **Step 1:** Calculate the Free Space Path Loss (FSPL) per Nautical Mile for the 1090 MHz frequency.
2) **Step 2:** A fixed transmit power (S_{trans}) is assumed for the ADS-B transmitter. A relation between received power (S_{rec}) and distance in NM between two aircraft is obtained, using the FSPL equation from Step 1.
3) **Step 3:** Detect and decode probability is exponentially modeled with respect to received power. A constant noise level on the 1090 MHz frequency is assumed. The minimum triggering level is based on [12].
4) **Step 4:** Step 2 is substituted in step 3. The detect and decode probability relation as function of received power is rewritten as function of distance.
5) **Step 5:** Parameters for specific transmit power and minimum triggering level are derived based on [12].

Step 1:

The derivation is based on the link budget between a transmitting and receiving aircraft. The decrease in power level due to the Free Space Path Loss (FSPL) is shown in Equation (5) and rewritten to dB.

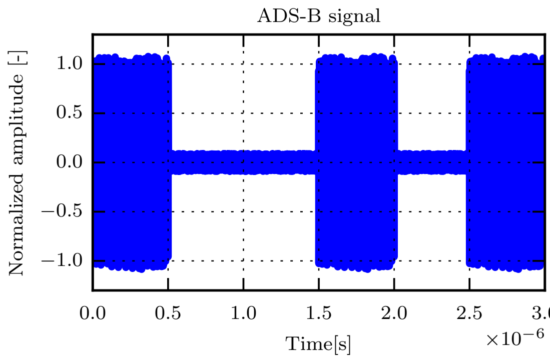

(a) Large SNR (normalized). Message can be decoded.

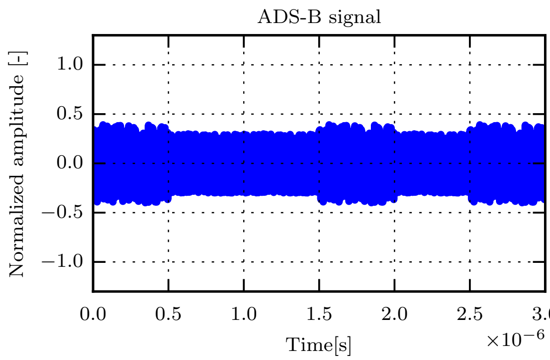

(b) Low SNR (normalized wrt (a)). Message cannot be decoded.

Figure 3: Two normalized SNR ratios. SNR decreases with increasing distance between transmitter and receiver.

$$FSPL = (\frac{4\pi df}{c})^2 \tag{5a}$$

$$FSPL(dB) = 10 \cdot log_{10}((\frac{4\pi df}{c})^2) \tag{5b}$$

$$FSPL(dB) = 20 \cdot log_{10}(\frac{4\pi df}{c}) \tag{5c}$$

In Equation (5) c (speed of light) and f (carrier frequency) are constant. The FSPL per NM can be obtained from Equation (5), resulting in Equation (6). It should be noted that the distance parameter d [m], in meters, is replaced with r [NM], indicating the distance in nautical miles.

$$FSPL_{NM} = 20 \cdot log_{10}\frac{f 4\pi r}{c} \tag{6a}$$

$$FSPL_{1NM} = 20 \cdot log_{10}\frac{1090 \cdot 10^6 \cdot 4 \cdot \pi \cdot 1852}{2.9979 \cdot 10^8} = 95.55 \tag{6b}$$

$$FSPL_{NM}(r) = 95.55 + 20 \cdot log_{10}(r)[\frac{dB}{NM}] \tag{6c}$$

Step 2:

Using Equation (5) the received power (S_{rec}) for a specific transmit power (S_{trans}) is obtained for a distance (r) in NM, shown in Equation (7).

$$S_{rec} = S_{trans} - FSPL_{1NM} - 20 \cdot log(r) \tag{7a}$$

$$S_{rec} = S_{rec\_1NM} - 20 \cdot log(r) \tag{7b}$$

In Equation (7) $(S_{trans} - FSPL_{1NM})$ equals the received power at a distance of 1 Nautical Mile (NM), called S_{rec_1NM} with a transmitted power of S_{trans}. Rewriting this equation, a relation between distance and received power is obtained, shown in Equation (8). This equation is substituted in step 4 to determine the maximum reception distance r_0.

$$r = 10^{\frac{-(S_{rec} - S_{rec\_1NM})}{20}} \tag{8a}$$

$$r = e^{-(S_{rec} - S_{rec\_1NM})(\frac{ln(10)}{20})} \tag{8b}$$

Step 3:

The detect and decode probability of an ADS-B report without interference is modeled as an exponential function of received signal power (S_{rec}). A specific signal power where the detect and decode probability is 0 (S_{rec0}) is defined (due to background noise and sensor sensitivity). This signal power is received at the maximum reception distance, r_0 [12]. The variable k is added to scale the curve of the probability function, resulting in Equation (9).

$$P(S_{rec}) = 1 - e^{-k(S_{rec} - S_{rec0})(\frac{ln(10)}{20})}, S_{rec} \geq S_{rec0} \tag{9a}$$

$$P(S_{rec}) = 1 - 10^{-k\frac{(S_{rec} - S_{rec0})}{20}}, S_{rec} \geq S_{rec0} \tag{9b}$$

Step 4:

The zero detect and decode distance between transmitter and receiver, as a function of range instead of received power, can be obtained by substituting Equation (8) in Equation (9).

$$P(r) = 1 - (r \cdot e^{-(S_{rec\_1NM} - S_{rec0})(\frac{ln(10)}{20})})^k, r \geq r_0 \tag{10a}$$

$$P(r) = 1 - (r \cdot 10^{-\frac{(S_{rec\_1NM} - S_{rec0})}{20}})^k, r \geq r_0 \tag{10b}$$

The received power S_0 results in a zero detect and decode probability with the corresponding distance r_0. Using Equation (8), r_0 is obtained as shown in Equation (11)

$$r_0 = 10^{\frac{-(S_{rec0} - S_{rec\_1NM})}{20}} \tag{11}$$

The inverse of Equation (11) is substituted in Equation (10) to obtain Equation (12).

$$P(r) = 1 - (\frac{r}{r_0})^k, r \geq r_0 \tag{12}$$

Equation (12) is used to determine the no-interference reception probability as a function range, using a fixed transmit power, S_{trans}.

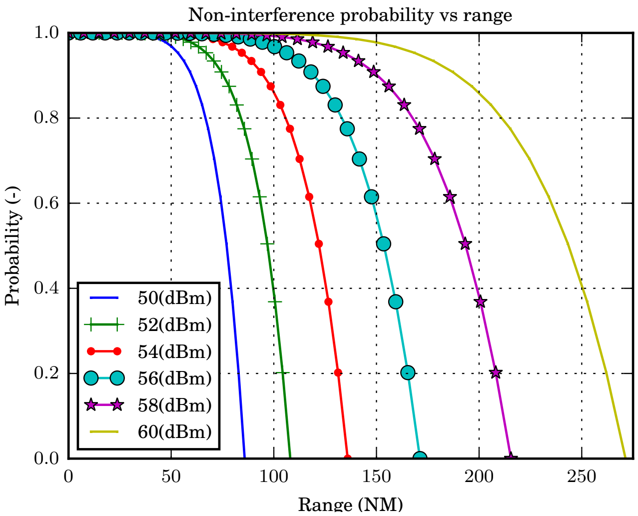

Figure 4: Effect of range (x-axis) on detect and decode probability for different transmit powers (legend). Based on [12].

Step 5:

The variable k is introduced to scale the curve of the probability equation. In [12] a minimum triggering level (S_{MTL}) of -90 dBm for Class A3 equipped commercial transport is defined with the following requirements:

1) If link margin ($S_{rec} - S_{MTL}$) = 3dB the minimum reception probability should be ≥ 0.99.
2) If link margin ($S_{rec} - S_{MTL}$) = -3dB the minimum reception probability should be ≥ 0.15.

Substituting these values in Equation (9) results in a scaling factor k of 6.4314. The maximum reception distance, r_0, is a function of transmit power (S_{trans}) and sensor sensitivity (S_{rec0}), as shown in Equation (13).

$$r_0 = \left(\sqrt{S_{trans} - S_{rec0}} \cdot \frac{c}{4\pi f}\right) \cdot \frac{1}{1852} \tag{13}$$

The relation of different transmit powers versus the detect and decode probability is shown in Figure 4.

The following assumptions are made in this model:

1) Omni-directional antenna used on transmitting and receiving aircraft.
2) A constant noise level on the 1090 MHz frequency is assumed, based on[12].
3) No multi-path effects.
4) Weather related effects are not taken into account.
5) No shielding by aircraft of ADS-B transmitter/receiver antenna.

Interference

The above defined reception probability does not take into account interference of other aircraft. Since all ADS-B reports are transmitted on the same frequency the interference effect needs to be accounted for. The effect of receiving two messages in the same time interval is shown in Figure 5; the bits from the original (blue) signal cannot be decoded anymore.

To model the effect of interference on detect and decode probability the Poisson distribution, shown in Equation (14), has been used. This probability distribution is generally used to calculate the number off occurrences during a specified time interval with the following variables:

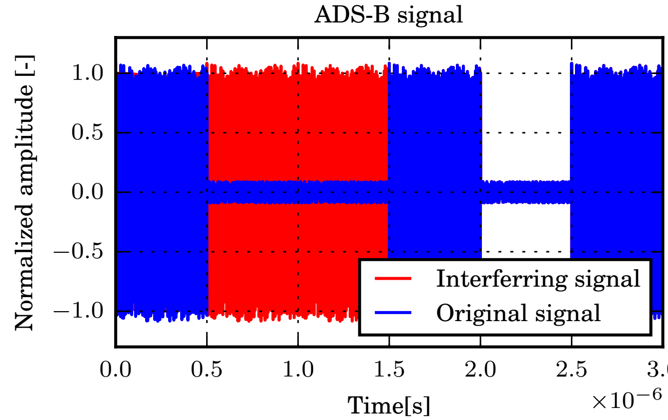

Figure 5: Interference effect; bits from the original signal cannot be decoded anymore due to interference.

$$P[X = k] = (\lambda t)^k \frac{e^{-\lambda t}}{k!}, k = 0, 1, 2, ... \tag{14}$$

- λ = Expected number of events occurring in 1 unit length of time.
- t = Interval length.
- X = Number of events occurring in an interval of length t.
- P = Probability of X occurrences in an interval of length t.

The different transmit rates, discussed in the previous section for the 6 different ADS-B reports, are considered. Each message has a duration of 120μ seconds. Not every message is being used for CD&R, but all the messages must be taken into account for the interference analysis. This results in a summed ADS-B transmission frequency of 6.4 Hz, contributing to interference. In addition to the different type of ADS-B messages, an aircraft also transmits a Traffic Collision Avoidance System (TCAS) signal on the 1090 MHz frequency. A TCAS signal has a duration of $64\mu s$ and is transmitted with a frequency of 4 Hz [24]. Using the characteristics stated above the probability of a message collision can be determined using the Poisson distribution from Equation (14). Additionally the following assumptions are made:

1) No de-garbling is used. Multiple received ADS-B messages can sometimes be de-garbled using software so both messages can be decoded. De-garbling can be modeled by selecting a lower message duration.
2) ADS-B message is modeled as 1 message, containing all the state information, instead of several different messages.

λ can be calculated by the summation of the message update frequencies (F_{update}), multiplied by the number of aircraft within range (N_{ac}), shown in Equation (15). This represents the expected number of instances (ADS-B messages received) in a specified time interval (1 s). The number of aircraft within range is the number of aircraft with a distance smaller than the maximum reception range, as discussed in the previous section.

$$\lambda = N_{ac} \cdot \sum F(Hz) = N \cdot F \tag{15a}$$

$$\lambda = N_{ac} \cdot F_{update} \tag{15b}$$

Assume a message is received at t=0. The duration of an ADS-B message τ is $120\mu s$, equal to the time variable in Equation (14).

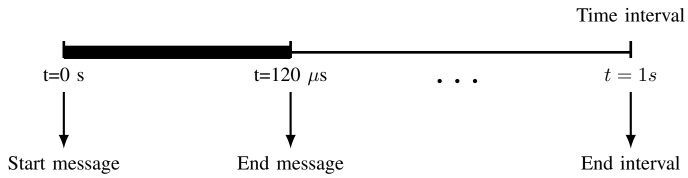

Figure 6: Schematic interference modeling overview (not in scale).

To obtain the probability no other messages are received in this time interval the variable X in Equation (14) is set equal to 0, resulting in Equation (16). This is visualized in Figure 6. The same principle holds for a TCAS message, with a duration of $64\mu s$.

Since x^0 = 1 and 0! = 1 the final equation to determine the probability of no message collision for N_{ac} within range and a message duration of τ seconds is shown in Equation (16).

$$P[X=0] = (\lambda t)^0 \frac{e^{-\lambda t}}{0!} \tag{16a}$$

$$P[X=0] = e^{-N_{ac}(\cdot F_{ADS-B}\cdot \tau_{ADS-B} + F_{TCAS}\cdot \tau_{TCAS})} \tag{16b}$$

To incorporate the reception probability, the number of aircraft within range (k) is weighted with respect to the specific aircraft (i). Aircraft closer than aircraft i are given a full weight, aircraft at a greater distance, according to the relative reception probability, as shown in Equation (17).

$$\begin{aligned} N_{acscaled} = N_{ac}(P_{R(i,k)} \geq P_{R(i,j)}) + \\ \sum \frac{P_{R(i,k)}}{P_{R(i,j)}}, \forall k (P_{R(i,k)} < P_{R(i,j)}) \end{aligned} \tag{17}$$

So to calculate the interference effect for aircraft i with respect to aircraft j, Equation (18) is being used.

$$P_{I(i,j)} = P_I(N_{acscaled}) \tag{18}$$

C. Situation related ADS-B model

The detect and decode probabilities described in Section III-B can be combined. The corresponding detect and decode probability is shown in Equation (19). The probability $P_{T(i,j)}$ resembles the combined detect and decode probability of aircraft i receiving an ADS-B message from aircraft j. $P_{R(i,j)}$ is the detect and decode probability of aircraft i wit respect to aircraft j due to range between the two aircraft. $P_{I(i,j)}$ is the scaled decreased detect and decode probability due to interference of surrounding aircraft.

$$\overbrace{P_{T(i,j)}(r, AC)}^{\text{Total probability}} = \overbrace{P_{R(i,j)}}^{\text{Range}} \cdot \overbrace{P_{I(i,j)}(N_{acscaled})}^{\text{Scaled Interference}} \tag{19}$$

IV. Experiment design

From the analysis in the previous section it is found that multiple factors affect the proper reception of an ADS-B message. The simulation environment is introduced in Section IV-A and the implementation of the ADS-B model in Section IV-B. The assessed traffic scenarios are discussed in Section IV-C. Three experiments are performed with different goals. The goal of the first experiment is to compare the effect of using ADS-B based state information with perfect state information on CD&R, discussed in Section IV-D. The second experiment is a sensitivity analysis to determine the contribution of the individual situation related properties, namely range and interference. The dependent variables are discussed in Section IV-E. The final experiment aims to assess the effect of a varying transmission power, resulting in different maximum reception distances. These independent variables are discussed in Section IV-F. The dependent variables are discussed in Section IV-G. This section is concluded with hypotheses in Section IV-H.

Table II: Verification quadratic computational power ADS-B module. Simulations performed on Intel Duo Core T9600 2.8GHz with 4 GB RAM.

Simulation time vs number of aircraft	
Aircraft in simulation [ac]	ADS-B module time [s]
75	0.038
150	0.15
300	0.62
600	2.3

A. Simulation Environment

BlueSky, an open-source Python based ATC simulator developed at the Delft University of Technology, is used as simulation environment. Many useful features are already available in the simulator, such as CD and CR in the Airborne Separation Assurance System (ASAS) module. DataLog options, way-point routing and aircraft performance limitations (accelerations, bank angles etc.) are also implemented. The open-source characters enables easy implementation of new modules in the simulator. For this research, the simulation update rate was set to 10 Hz. Further information regarding the simulator can be found in [25].

B. ADS-B Software implementation

Currently the real state of the aircraft is used for CD&R in the ASAS module, shown with (0) in Figure 7. This CD&R module uses airspeed, heading and position of surrounding aircraft for conflict detection and resolution. The open-source character of the BlueSky simulator allows it to implement the ADS-B module, also shown in Figure 7, on the right side.

The ADS-B model uses the real states of each aircraft(1). The actual position of each aircraft is used to determine the reception probability between each aircraft pair, based on the model described in Section III (2). This results in a NxN relative reception probability for each aircraft pair. The content of an ADS-B messages is created for each aircraft, containing position, velocity and heading information. In the content of this report, accuracy, truncation and latency error is introduced (3). Each ADS-B report is updated according to the set ADS-B update frequency (3). Different seeds are used, resulting in asynchronous transmission of the ADS-B message. Based on the calculated reception probability (4) it is determined which "in-air"' ADS-B report (5) is received by which aircraft (6). This collection of NxN ADS-B reports are the received ADS-B reports for each aircraft pair. This ADS-B report is used in the ASAS module for CD&R (7). All ADS-B calculations are performed every time-step. It should be noted that the number of calculations increases quadratically, due to the new NxN structure of the ADS-B states. The quadratic relation between number of aircraft and calculation time of the ADS-B module is shown in Table II.

C. Traffic Scenarios

A specific traffic scenario is created. The testing region is discussed first, followed by the traffic demand.

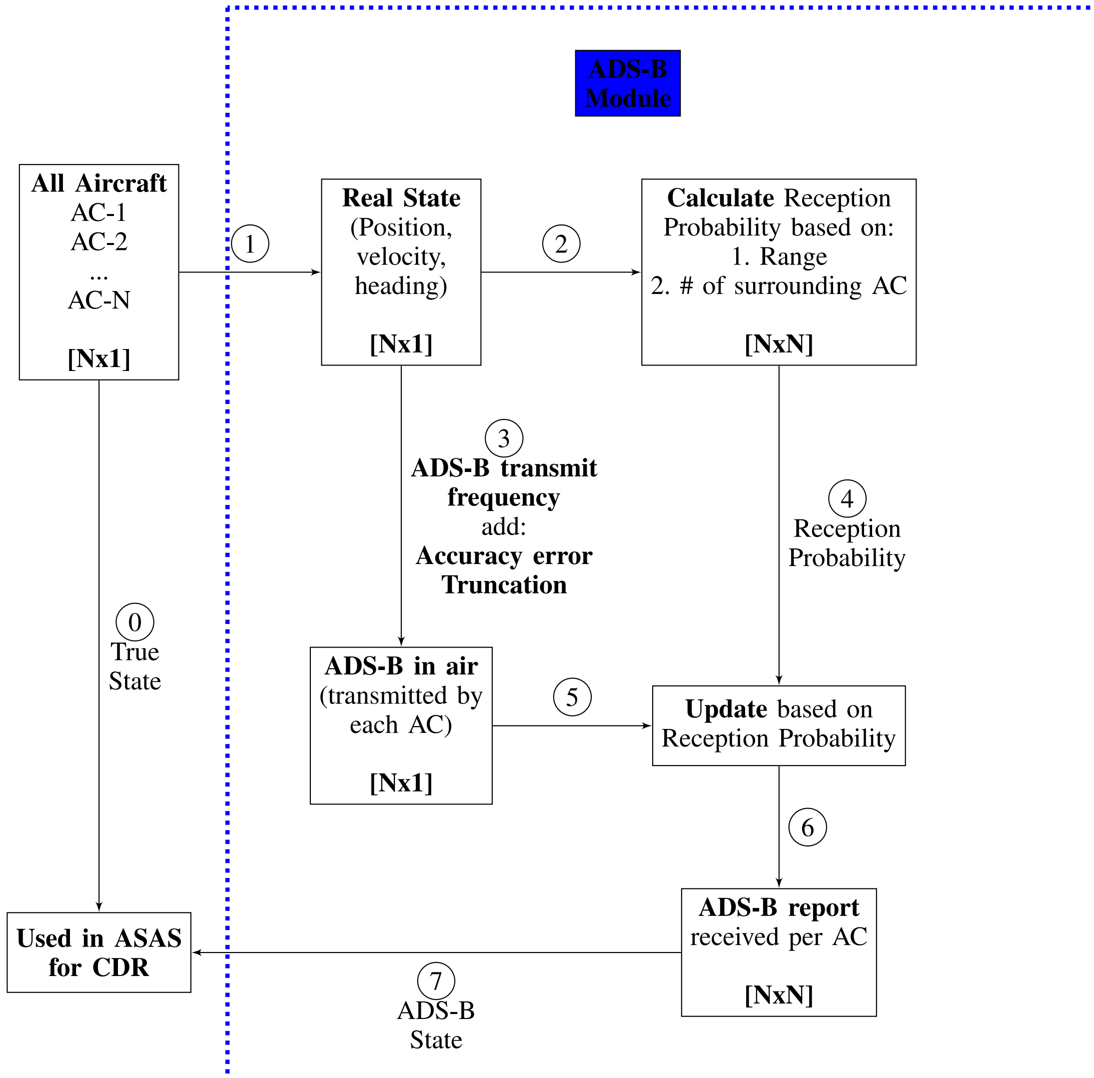

Figure 7: Schematic overview of implementation ADS-B model in the BlueSky simulator for N aircraft. Start at left top and end at left bottom. ADS-B model is shown in blue. Size of the elements are indicated between brackets

***Testing Region**:* A circular region is used, consisting of an initialization boundary and test boundary. The aircraft are only logged while they are within the experiment area and deleted when leaving the experiment area. To maintain a constant air traffic density the experiment is divided in three phases.

1) **Pre-logging phase:** Aircraft are created until a constant density is reached.
2) **Logging phase:** Aircraft created during this period are logged until the end of the experiment.
3) **Run-out phase:** Aircraft created during this phase are not logged, but contribute on maintaining a constant air traffic density. Aircraft created during the logging phase are allowed to finish their flight and are still logged.

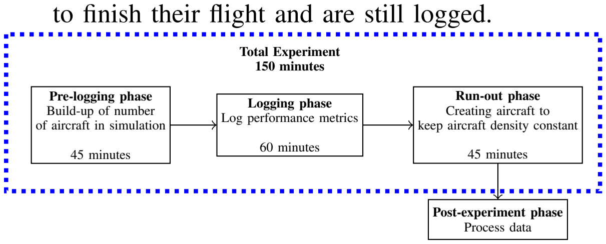

***Traffic demand**:* A scenario generator is constructed to create similar air traffic scenarios with a different seed randomization. Aircraft are created on the edge of the initialization boundary at one of the 40 discrete points. A way-point destination is defined, located on the other side of the circle within a 45° heading band. This limitation prevents aircraft from being pushed out of the test-area and ensures a minimum travel distance of $\frac{1}{\sqrt{2}}$ of the initialization diameter. Aircraft are created on three different flight levels and will randomly climb or descend to a different flight level or cruise at the current flight level. This results in intruding aircraft from all possible directions. An overview is shown in Figure 8.

The dimensions of the experiment area are shown in Table III. It should be noted that the experiment radius is customized to the MOPS maximum reception distance. This ensures full use of the MOPS detect and decode probability.

Table III: Experiment Area settings

Experiment area dimensions	
Parameter	Value
Test Radius [NM]	95
Test Radius Area [NM^2]	57 255
Initialization radius [NM]	135
Δ flight levels [ft]	3 000
Number of flight levels [-]	3
Altitude middle flight level [ft]	10 000

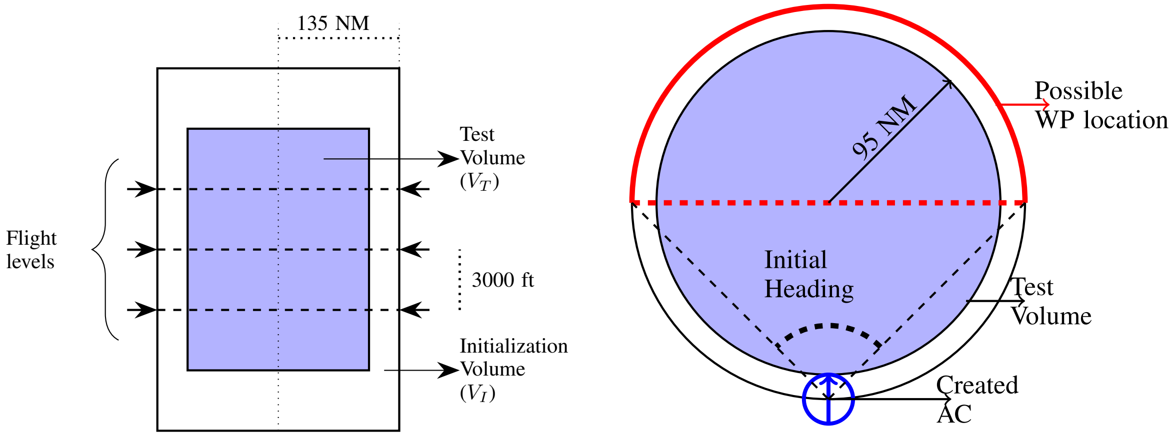

(a) Three flight levels

(b) Initialization of AC with 45° heading caption.

Figure 8: Scenario initialization.

To assess the different CD&R methods in a wide variety of conflict possibilities, aircraft are being created with a different airspeed and heading. These aircraft initialization parameters are shown in Table IV.

Table IV: Aircraft initialization variables

Parameter	Aircraft initialization properties	
	Distribution	Value
Initialization Location [$^\circ$]	Uniform	0-360
Initial Heading [$^\circ$]	Uniform	-45 - +45
Average distance [NM]	Uniform	162
Initial FL [FL]	Uniform	70, 100 or 130
Destination [FL]	Uniform	70, 100 or 130
True Air Speed [$\frac{m}{s}$]	Uniform	100-200
AC type [-]	-	B747-400

Three different scenarios are created, with Low, Medium and High density. The mean expected time of an aircraft in the experiment area is calculated using the variables from Table IV (CR off). The aircraft create rate is adapted accordingly to obtain the desired air traffic density. An overview is shown in table Table V.

Table V: Aircraft Scenarios: Low, Medium and High. (With resolution off)

Aircraft Scenarios			
	Scenario names		
Parameter	Low	Medium	High
Steady state nr of AC [AC]	50	75	100
Steady state AC / 10 000NM^2 FL [$\frac{AC}{NM^2}$]	2.8	4.4	5.6
AC create update interval [s]	42	31	21

D. Independent Variables - Experiment I

The goal of the first experiment is to assess the effect of different ADS-B model on the two CD&R methods. Three different independent variable are selected, namely CD&R method, air traffic density and state information quality. Each independent variable has three different levels, as shown in Table X.

Table VI: Independent variables. Experiment - I

Independent variables			
	Settings		
Independent variable	1	2	3
CDR	MVP	Swarming	None
AC density	Low	Medium	High
ADS-B	MOPS	Realistic	Perfect

CD&R method
The first independent variable, CD&R method, is introduced in Section II; the MVP method and swarming method. As a benchmark and for further analysis also simulations with CD&R switched off are assessed.

Air traffic density
Previous literature shows that the performance of CR methods depends on air traffic density [14], [26]. Therefore also three different traffic densities are assessed. The number of aircraft and densities per 10 000 NM^2 corresponding with the Low, Medium and High traffic density are stated in Table V.

State information
The last dependent variable is state information quality. In Section III it is found that system related and situation related properties affect the ADS-B system. In total three different independent variables are selected regarding state information; perfect state information and two ADS-B models. The settings of these two ADS-B models are discussed below.

It was found in Section III-A that the position is the most affected state. The two system related cases are summarized in Table VII.

Table VII: System related inaccuracies

System related inaccuracies			
		Cases	
Parameters	Distribution	Realistic	MOPS
Position [m]	Normal	$\mu = 0, \sigma = 30$	$\mu = 0, \sigma = 50$
Velocity $\frac{m}{s}$	Normal	-	$\mu = 0, \sigma = 10$
Heading [$^\circ$]	Normal	-	$\mu = 0, \sigma = 3$

Additionally two cases with respect to interference level and range effect are selected as independent variables. A worst-case

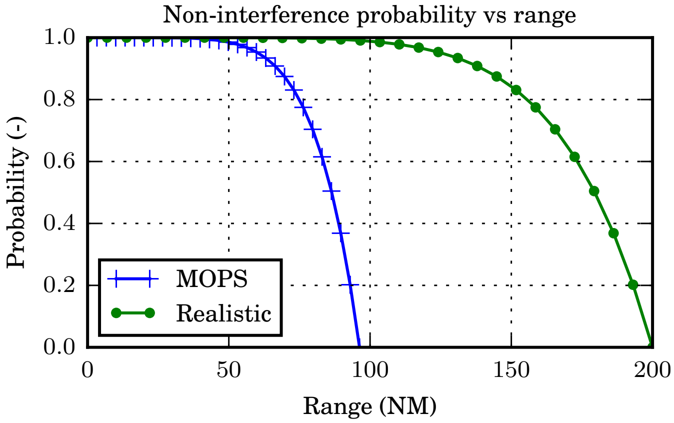

Figure 9: Range only detect en decode probability of ADS-B messages for MOPS and realistic scenario as function of range.

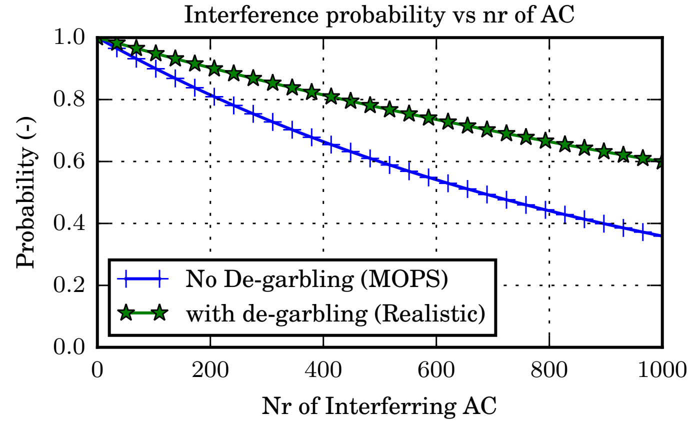

Figure 10: Interference only detect and decode probability based on Poisson distribution. With and without garbling.

scenario, based on MOPS specifications [9], [24] and a realistic model, based on measurements in literature are defined [3], [11].

Range
The range related parameters of these models are both shown in Table VIII.

Table VIII: Parameters describing ADS-B detect and decode probability versus range, based on MOPS [12] and measurements[11].

	ADS-B Assumptions Type	
	MOPS [12]	Realistic
$R_0[km]$	176	370
$R_0[NM]$	95	200
S_{trans} [dBm]	51	57
S_{trans} [W]	125	500 [11]
S_{MTL} [dBm][12]	-88.67	-88.67
S_{MTL} [W] [12]	$3.686 \cdot 10^{-5}$	$3.686 \cdot 10^{-5}$
State accuracy (Table VII)	MOPS	Realistic

The corresponding detect en decode probability with respect to range for these two cases regarding range are shown in Figure 9.

Interference
In addition to the range effect, two interference situations are identified; with de-garbling (Realistic) and without de-garbling (Worst-Case/MOPS). De-garbling enables distinguishing between two partly overlapping messages using software. De-garbling can be modeled by changing the message duration, τ in the interference model. The corresponding modeling parameters are stated in Table IX. The effect of de-garbling is shown in Figure 10. The no de-garbling results are used in the MOPS case. The case where de-garbling is applied is used in the realistic case.

Table IX: Parameters describing ADS-B interference model with and without garbling.

	ADS-B Assumptions Type	
	No Garbling	Garbling
$F_{ADS-B}[Hz]$	6.4	6.4
$F_{TCAS}[Hz]$	4	4
$\tau_{ADS-B}[\mu s]$	120	60
$\tau_{TCAS}[\mu s]$	64	32

The corresponding ADS-B detect and decode probability models are shown in Figure 11.

The 3 independent variables, with each 3 levels, result in 27 experiment conditions. Each experiment condition is repeated 5 times, with each repetition a traffic scenario with a different random seed.

E. Independent Variables - Experiment II

A second experiment is performed to asses the individual contribution of the two situation related properties; range and interference. The same three traffic densities and CD&R methods are used as in the previous experiment. The MOPS model, discussed in Section III, is used as benchmark.

The following ADS-B settings are used as independent variables:

1) **ADS-B MOPS settings**, both interference and range effect.
2) **Range effect only**.
3) **Interference effect only**.

Again the situation where no CDR is applied are assessed. An overview is shown in Table X.

Table X: Independent variables. Experiment - II

	Independent variables		
	Settings		
Independent variable	1	2	3
CDR	MVP	Swarming	None
AC density	Low	Medium	High
ADS-B	MOPS	MOPS interference only	MOPS range only

F. Independent Variables - Experiment III

The goal of the third experiment is to study the effect of a changing maximum reception distance on the MVP method. Only

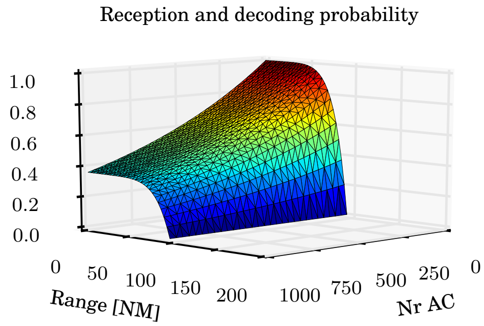

(a) Worst case ADS-B model, MOPS based. Maximum reception distance of 96 NM. No de-garbling used in interference probability.

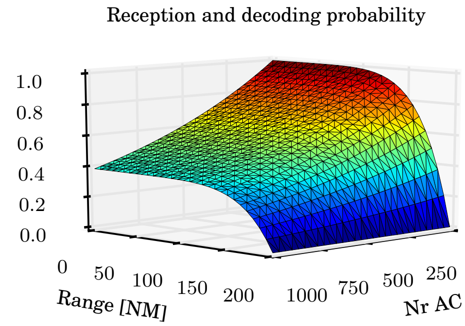

(b) Realistic case ADS-B model, measurement based. Maximum reception distance of 200 NM. De-grabling used in interference probability.

Figure 11: ADS-B detect and decode probability (z-axis) model with respect to range between aircraft (x-axis) an number of interfering aircraft (y-axis).

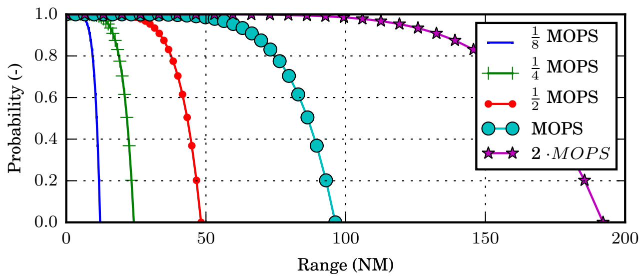

Figure 12: MOPS based reception models defined as fraction of MOPS range. Non-interference probability vs range.

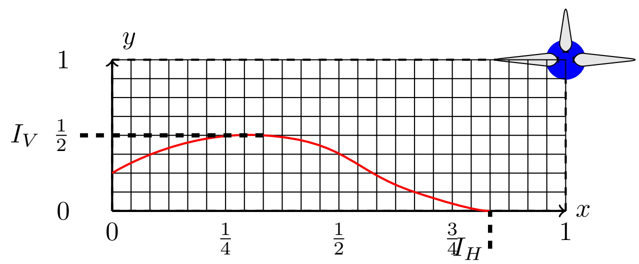

Figure 13: Figure showing normalized path of intruding aircraft through the $\frac{1}{4}^{th}$ Intruder Protected Zone (IPZ) of another aircraft.

this method is selected since it shows better results than the swarming method. From Section III it can be obtained that an increase in range results in a stronger interference effect. Therefore different ADS-B ranges are assessed and compared. The same traffic densities are used. The range of these ADS-B models, based on the MOPS model, are shown in Table XI. The maximum reception range can be modified by adapting the transmit power.

Table XI: Independent variables range analysis

Independent variables range analysis					
	Settings				
Independent variable	1	2	3	4	5
ADS-B Range fraction	$\frac{1}{8}$ Mops	$\frac{1}{4}$ Mops	$\frac{1}{2}$ Mops	1· Mops	2· Mops
ADS-B Range [NM]	12	24	48	96	192
ADS-B Range [km]	22	44	89	178	356
CDR	MVP	None	-	-	-
AC density	Low	Medium	High	-	-

The corresponding reception probability curves (defined as fractions of the MOPS range) are shown in Figure 12.

G. Dependent Variables

The CD&R performance can be assessed using different metrics. These metrics are divided in several different groups; safety, efficiency and airspace stability, each discussed below.

Safety: The conflicts detected, based on ADS-B state information are being logged. Additionally the conflicts detected when perfect state information would be available are logged. From these two metrics the false alerts (false positives) and missed conflicts (false negatives) can be obtained. Besides conflicts detected, the numbers of LOS are logged. Subsequently the severity of each LOS is logged. A normalized number between 0 and 1 indicates the severity of the LOS, as shown in Figure 13.

The total severity of a LOS can be calculated using Equation (20)[27]. This results in a number representing the severity of the intrusion.

$$LOS_{severity} = max[min(I_H, I_V)] \tag{20}$$

Efficiency: During the experiment the covered distance of each aircraft is logged. The resolution maneuvers causes an increase in covered distance (S_{ON}). Therefore the route efficiency is calculated with respect to the straight (great-circle) (S_{OFF}) distance as shown in Equation (21).

$$\eta = \frac{\sum S_{OFF}}{\sum S_{ON}} \tag{21}$$

Airspace stability: Resolving a conflict using CD&R can result in creating one or multiple different conflicts. Conflicts can be divided in two groups S_1 and S_2 as shown in Figure 19. S_1 and S_2 represent the set of detected conflicts with resolution off and on respectively (for the same traffic scenario). These groups share the subset R_2, conflicts that occurred with CD&R on and off.

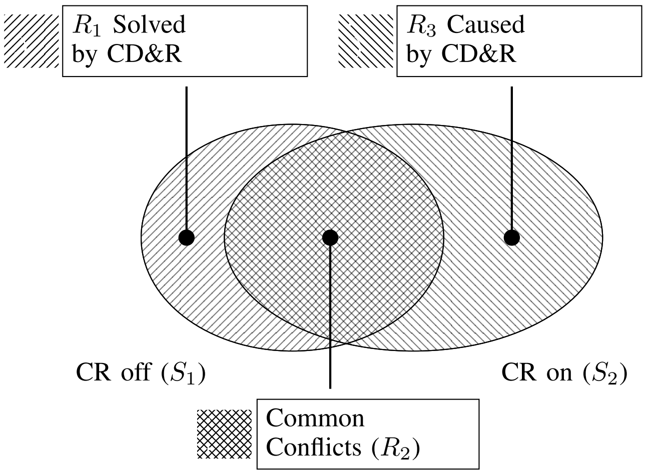

Figure 14: Venn diagram illustrating the Domino Effect Parameter.

If $R_3 > R_1$, the performed conflict resolutions have a destabilizing effect (as in the figure). If $R_3 < R_1$, the conflict resolutions have a stabilizing effect. The Domino Effect Parameter (DEP), gives an indication of the stability of the airspace [6] when conflict resolution is used. The DEP can be calculated using Equation (22). C_{ON} represents the number of detected conflicts with CD&R on and C_{OFF} the number of detected conflicts with CD&R off.

$$DEP = \frac{C_{ON}}{C_{OFF}} - 1 = \frac{S_2}{S_1} - 1 \tag{22}$$

***Data representation**:* Each observed dependent variable is shown in two figures, one each for the two CD&R methods. The different traffic densities are shown on the x-axis. The obtained dependent variable on the y-axis. The legend indicate the ADS-B model. The 95% confidence interval is indicated with the error bar for the 5 repetitions of each experiment setting.

H. Hypotheses

From Figure 9 it can be observed that for both ADS-B models the first 50 NM have a linear non-interference detect and decode probability, close to 1. In addition to the range effect, the interference effect is a constant factor, depending on the traffic density. Therefore it is hypothesized that the difference between the two ADS-B models (MOPS and realistic) are small regarding all metrics **(H-1)**. In addition, the effect of position error is small with respect to the dimensions of the IPZ. Therefore it is hypothesized the negative effect of ADS-B based state information will be small, compared with perfect state information, regarding efficiency and safety metrics for both CD&R methods**(H-2)**. The nature of the swarming method requires close coordination between aircraft and accurate state position. ADS-B degrades the state information quality. The third hypothesis is that the use of ADS-B based state information has a more negative effect on swarming than MVP regarding number of intrusions and intrusion severity **(H-3)**.

V. Results - Experiment I

The goal of the first experiment was to identify the differences of using ADS-B based state information on CD&R performance. The results are shown in Figure 16 to Figure 19. The detected conflicts are discussed in Section V-A. The safety metrics are shown in Section V-B. Subsequently the efficiency and stability results are shown in Section V-C and Section V-D respectively.

A. Conflict Detection

The ratio of detected real conflicts versus false positive conflicts detected can be obtained from Table XII. It is observed that the percentage of false positives increases with traffic density. Also the percentage of false alerts is larger for the MOPS based ADS-B model than the realistic ADS-B model. The false negatives, or missed conflicts, are a small portion of the total detected conflicts. The differences between the two CD&R methods is small. These observations supports hypothesis **(H-1)**.

Table XII: Type of conflicts detected as percentage of total detected conflicts.

ADS-B model	Conflict type	Traffic density			Cumulative
MVP method					
		Low	Medium	High	
MOPS	Real Conflict	92	88	89	89
	False Positive	8	12	11	11
	False Negative	5	4	5	5
Realistic	Real Conflict	95	94	94	94
	False Positive	5	6	6	6
	False Negative	3	3	4	4
Swarming method					
		Low	Medium	High	
MOPS	Real Conflict	93	90	89	91
	False Positive	7	10	11	9
	False Negative	3	4	3	3
Realistic	Real Conflict	96	96	95	96
	False Positive	4	4	5	4
	False Negative	3	2	3	3

Additionally the detected number of conflicts per aircraft are shown in Figure 15. It is obtained that the number of conflicts detected for both ADS-B models is higher than when using perfect state information. The differences between the two ADS-B models is small, supporting (**H-1**).

B. Safety

The number of unique intrusions per aircraft are shown for the MVP and swarming method in Figure 16a and Figure 16b respectively. The number of intrusions per aircraft is reduced significantly for all cases with respect to no CDR applied. It is observed that the MVP method performs better for all traffic densities than the swarming method. When perfect state information would be available MVP has 92% less intrusions for the high traffic density and 48% less for the low traffic density compared with the swarming method.

Using ADS-B based state information or perfect state information results in similar values for the MVP method as shown in Figure 16a, supporting **(H-2)** regarding the MVP method. The biggest difference occurs at the lowest traffic density, resulting in 45% between the Realistic ADS-B model and perfect state information.

The difference between the ADS-B models and perfect state information for the swarming methods are larger. Perfect state information results in a larger number of intrusions than ADS-B based state information. This is not in line with **(H-3)**.

Intrusion severity results are shown in Figure 17. Figure 17a corresponds to the MVP method and Figure 17b to the swarming method.

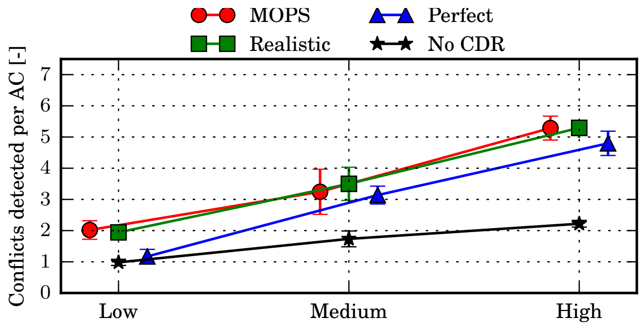

(a) MVP method.

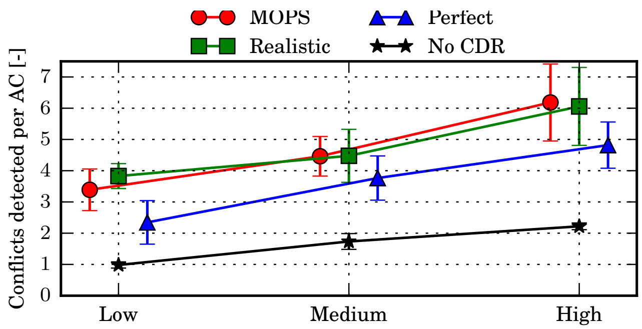

(b) Swarm method.

Figure 15: Detected number of conflicts per aircraft. Experiment - I.

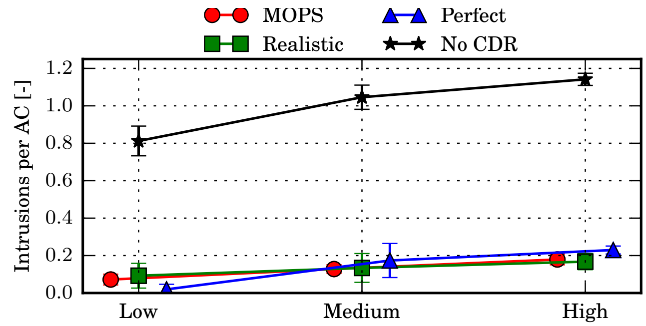

(a) MVP method.

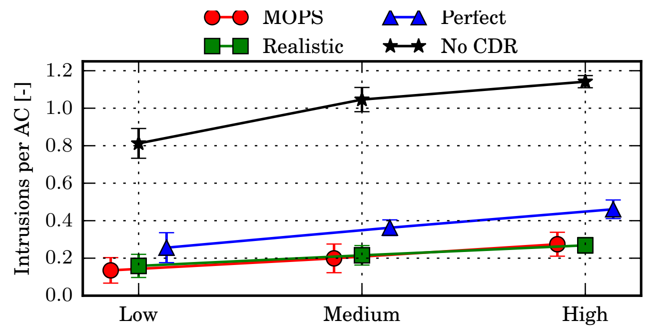

(b) Swarm method.

Figure 16: Average number of intrusions per aircraft. Experiment - I.

The MVP method results in a lower average intrusion severity than the swarming method for most cases. For perfect state information the average intrusion severity for MVP is between 40% and 60% lower than the swarming method. Again the difference between perfect state information and ADS-B based state information is small for both CD&R methods. The biggest difference occurs at the low traffic density, but here also the variance is high. At the higher densities the difference is $\pm$ 20%, but the confidence intervals show a large overlap. This observation supports **(H-1)** and **(H-2)**.

Again the MVP method improved performance when subjected to perfect state information, while the swarming method shows slightly worse results using perfect state information. Also this observation has the tendency to reject hypothesis **(H-3)**.

C. *Efficiency*

The route efficiency with respect to the great circle distance between initialization location and destination is shown in Figure 18. In the experiment some aircraft left the experiment area prematurely; while solving a conflict or swarming, an aircraft could be forced out of the experiment region. This results in the specific aircraft not able to reach its original destination. For these aircraft the remaining distance towards the original destination is added to calculate its efficiency. The MVP method, shown in Figure 18a shows an decreasing trend with traffic density as expected; an increase in traffic results in an increase in number of conflicts, resolution maneuvers and covered distance.

Subsequently the swarming method shows an opposite trend regarding route efficiency, shown in Figure 18b. This can be the result of the distance correction discussed above. Aircraft are swarming more at a higher traffic density and leave the experiment area prematurely. The additional distance to be covered is simply the direct distance between the point of deletion and the destination.

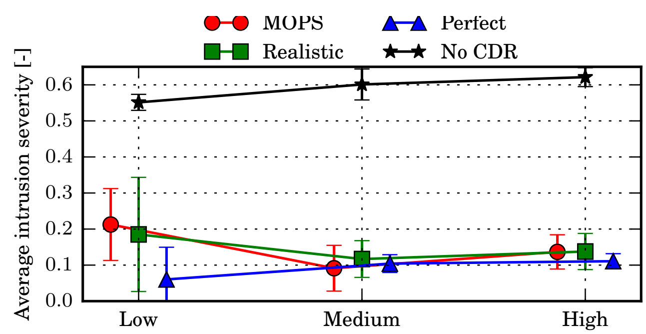

(a) MVP method.

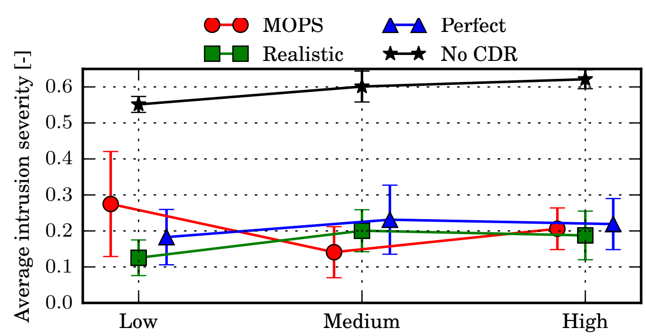

(b) Swarm method.

Figure 17: Average intrusion severity. Experiment - I.

In reality it is likely additional resolution maneuvers had to be performed, which are not taken into account due to the correction.

Additionally the difference in efficiency for the different ADS-

B models is small for the both CR methods. For each CD&R and density setting the 95% confidence intervals overlap. This observation supports hypothesis **(H-1)**. Also no large differences are observed between the ADS-B based case and perfect information case. This observation supports **(H-2)**.

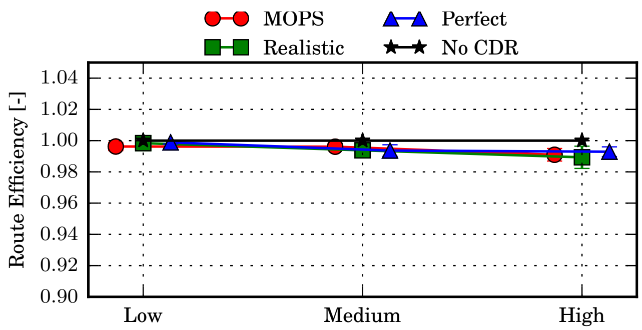

(a) MVP method.

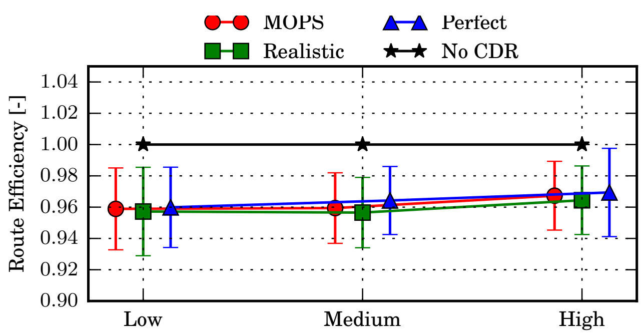

(b) Swarm method.

Figure 18: Route efficiency results. Experiment - I.

D. Stability

The DEPs for both CDR methods are shown in Figure 19. The results regarding DEP are similar for both ADS-B models regarding the MVP methods, as shown in Figure 19a. It should be noted that for the calculation of the DEP the ADS-B based conflicts are used in the nominator and the denominator (CDR on and CDR off).

The DEP for the swarming method is relatively large with a large variance. This is expected, since aircraft are grouped together, resulting in situations where more conflicts are likely to occur. No real trend can be observed for the swarming method. This can be caused by aircraft leaving the experiment region prematurely.

No real differences are observed between both ADS-B models, and the perfect state information case. These results support **(H-1)** and **(H-2)**.

VI. Results Experiment - II

The goal of this experiment was to identify the impact of the two main contributing situation related factors: range and interference. As benchmark the MOPS situation, discussed in Section III, is used. The results are shown Section VI-A to Section VI-C.

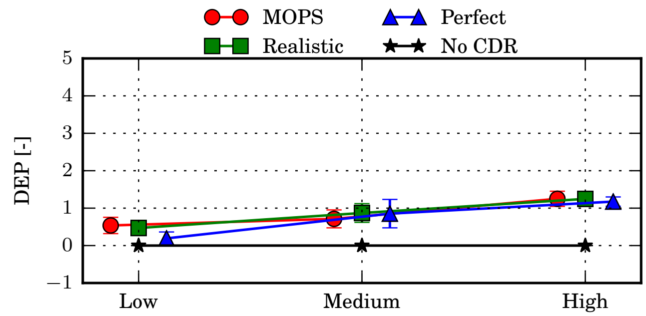

(a) MVP method.

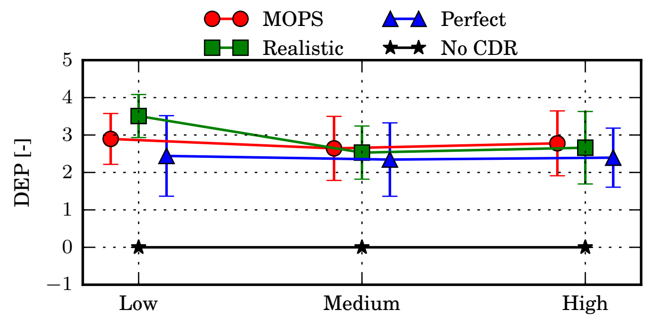

(b) Swarm method.

Figure 19: Domino effect parameter. Experiment - I.

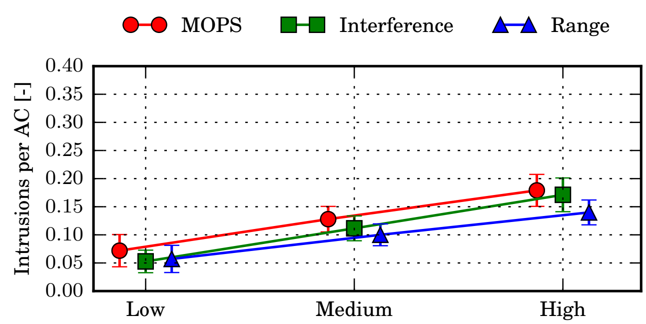

(a) MVP method.

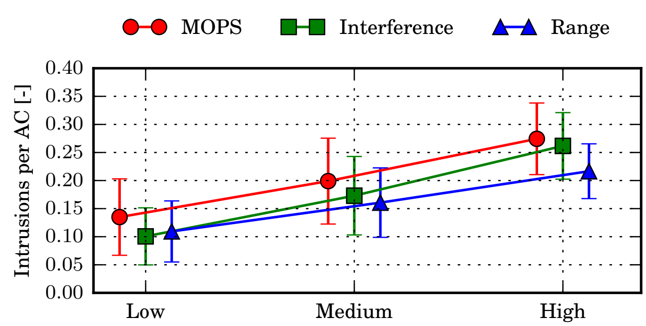

(b) Swarm method.

Figure 20: Number of intrusions per aircraft. Experiment - II.

A. Safety

Figure 20 shows the number of intrusions per aircraft for the MVP and swarming method.

The number of intrusions, while subjected to the interference model, are higher than the range model for the high traffic density. Here the number of intrusions is almost similar for the MOPS model and the interference only model. The effect of the range only model is about 50% smaller than the MOPS and interference only model. This is expected since a larger traffic density results in a more dominant interference effect.

Figure 21 shows the mean intrusion severity per aircraft for the MVP and swarming method. Again the intrusion severity is smaller

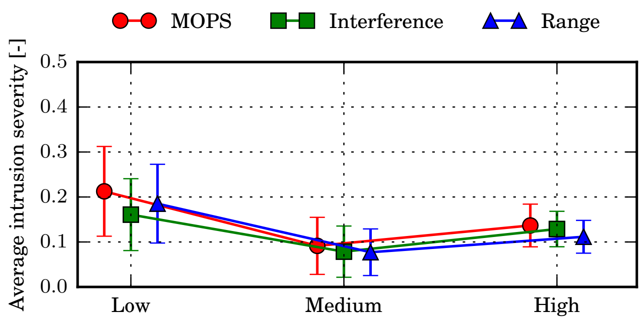

(a) MVP method.

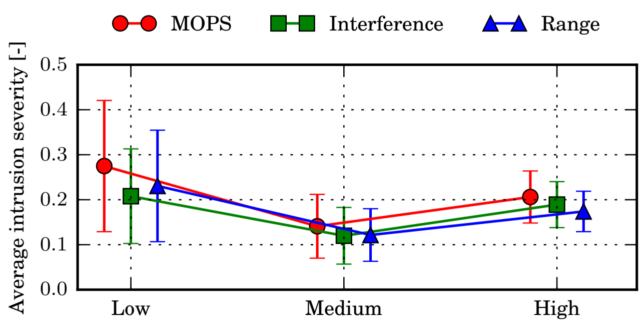

(b) Swarm method.

Figure 21: Mean intrusion severity per aircraft. Experiment - II

than the MOPS ADS-B case. The interference effect has a more negative impact than the range effect, especially at the High traffic density. The interference model has a similar average intrusion severity as the MOPS case, while the range case has a slightly lower average intrusion severity. The interference effect has a more severe impact on the safety related metrics than the range effect.

B. Efficiency

Figure 22 shows the route efficiency for the MVP and swarming method. For the interference model the route efficiency shows similar results as the MOPS models for both the MVP and swarming method.

C. Stability

Figure 23 shows the DEP values for the MVP and swarming method.

The DEP values for the range and interference model are both lower than the MOPS model. The interference model and range model show similar performance as the MOPS model regarding airspace stability.

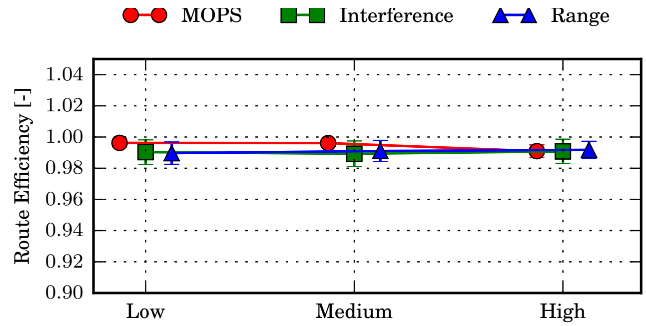

(a) MVP method.

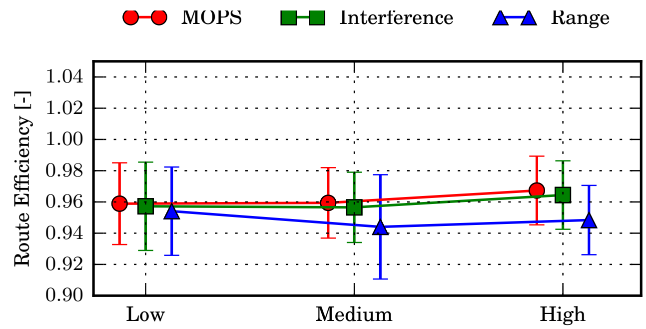

(b) Swarm method.

Figure 22: Mean route efficiency. Experiment - II.

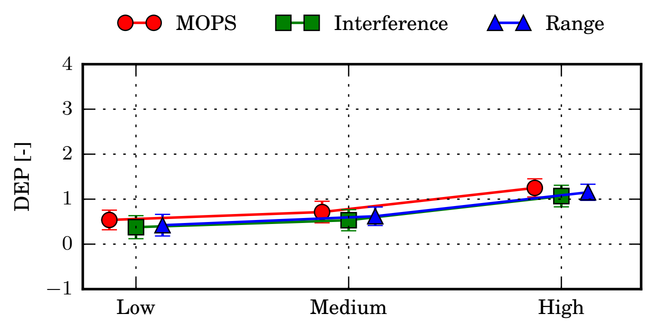

(a) MVP method.

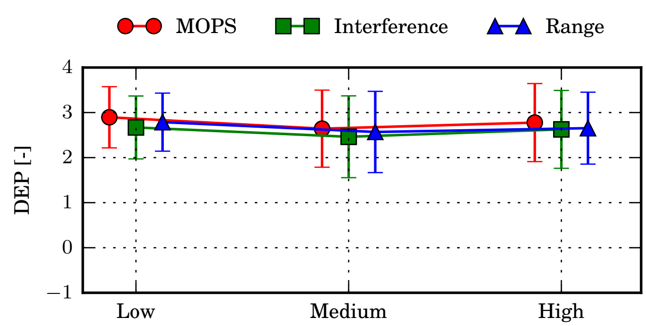

(b) Swarm method.

Figure 23: Domino effect parameter. Experiment - II.

From the sensitivity analysis it can be concluded that the interference effect contributions has more impact than the range effect. This observation becomes more evident during the high traffic density simulations.

VII. Results Experiment - III

In addition to the simulations, described in Section IV and Section VI, a range analysis is performed for the MVP method. This method is selected over the swarming method since it shows more promising results and is more suitable for a pure free flight situation. In the previous section it was found that interference degrades detect and decode probability. Therefore it can be concluded that an infinite range is not beneficial; causing additional interference. The goal of this analysis is to assess the effect of an increase in range, which also results in an increasing interference effect. The results are presented in the following subsections. The legend indicates the ADS-B model as fraction of the MOPS range.

A. Safety

Figure 25 shows the number of intrusions and Figure 26 the mean maximum intrusion severity. Large differences start to occur between $\frac{1}{8}^{th}$ and $\frac{1}{4}^{th}$ of the range of the MOPS performance (12 NM and 24 NM). At 25% of the MOPS range the number of intrusions show about a 50% increase, while at 12.5% of the MOPS range the number of intrusions increases with 250% for the highest traffic density.

The intrusion severity is similar for all cases. The Low traffic density shows a larger variance due to the smaller sample size. From Figure 24 it is obtained the percentage of head-on conflicts starts increasing at $\frac{1}{8}^{th}$ of the MOPS range. This can be explained by the fact that for these type of traffic situations the relative velocity between the two aircraft is the highest.

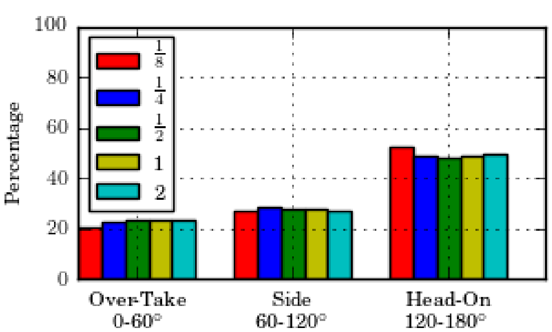

Figure 24: Percentage intrusion angle for the different ADS-B MOPS based settings(in legend). Δ heading angle of involved aircraft on the x-axis. Experiment - III

B. Efficiency

The double MOPS range shows the best results regarding efficiency and the $\frac{1}{8}^{th}$ MOPS range the worst. The single and double MOPS range don't show much differences. The larger range enables earlier conflict resolution, improving the efficiency.

C. Stability

In Figure 28 it can be observed that number of conflict detected increases with ADS-B range. Again the ("1") and double ("2") MOPS ranges show similar results. The number of detected conflicts

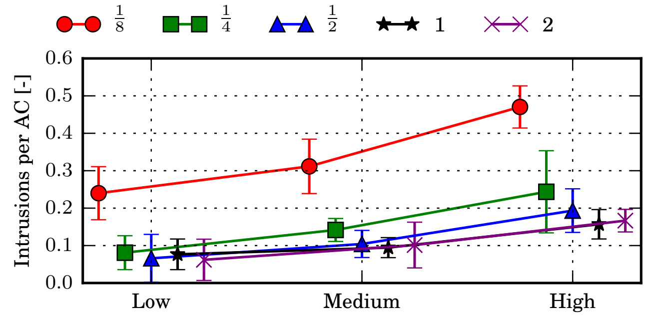

Figure 25: Number of intrusions per AC. Experiment - III

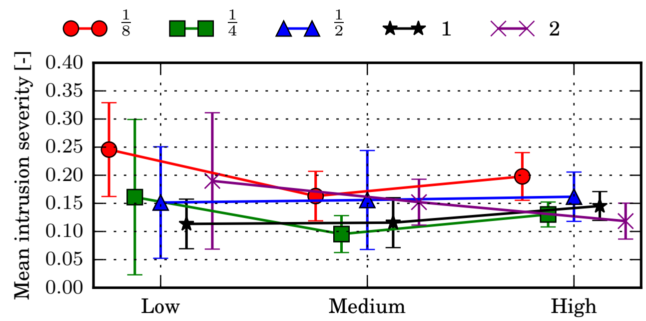

Figure 26: Mean intrusion severity per aircraft. Experiment - III.

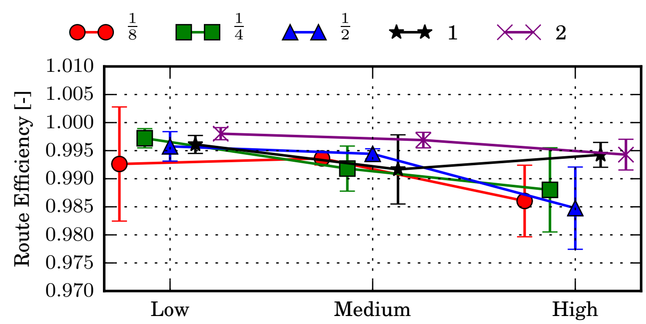

Figure 27: Mean route efficiency. Experiment - III

is larger for the MOPS range than the double MOPS range, as shown in Figure 28. This is caused by the interference effect, which is larger for the double MOPS ADS-B range and has more effect for the High traffic density.

The DEP values, shown in Figure 29, indicate a similar trend as the number of detected conflicts.

D. Interference

From the metrics discussed above it is found that the performance difference for the single MOPS model, with a range of 96 NM ("1") is slightly better than the model with double the MOPS model, with a range of 190 NM ("2") regarding conflicts detected and number of intrusions. With the 5 minutes look-ahead time, for both ADS-B models, the range dependent detect and decode probabilities are in the linear region, close to 1. However, the effect of interference increases. This is clearly shown in Figure 30; where the detect and

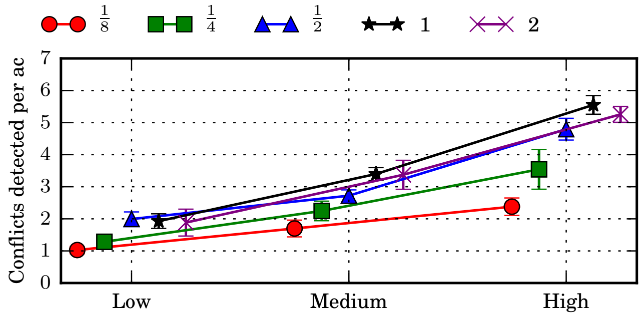

Figure 28: Conflicts detected per aircraft.
Experiment - III.

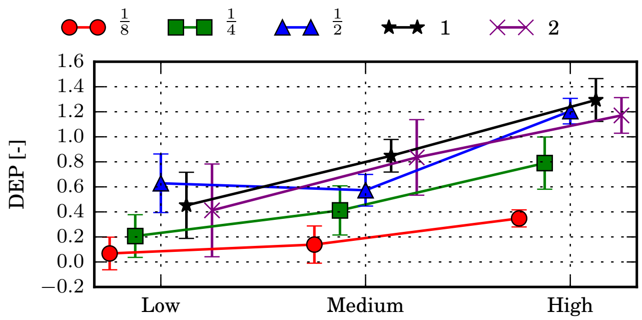

Figure 29: Domino effect parameter.
Experiment - III.

decode probability caused by interference is shown. The increased range results in a decrease of detect and decode probability due to additional interference. Therefore it can be concluded that the interference effect should be taken into account in extremely high traffic density situations.

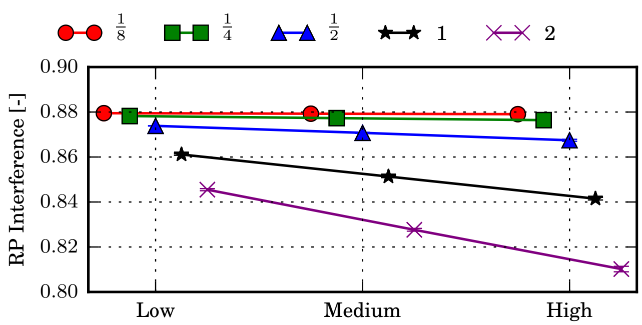

Figure 30: Mean interference reception probability.
Experiment - III.

VIII. Discussion

In this section the results presented in the previous sections are further discussed. Each individual hypotheses, stated in Section IV-H, are reflected with respect to the results in Section VIII-A. A general discussion is stated in Section VIII-B. This section is concluded with recommendations in Section VIII-C.

A. Reflection on hypotheses

H-1: The difference between the two ADS-B models is small regarding all metrics.

The percentage of false conflicts between the two ADS-B models is in the order of 10% for MOPS, and 5% for the Realistic ADS-B model with respect to the total number of detected conflicts. The MOPS based ADS-B model results in more false positives and false negatives. This can be caused by the difference in state information between the two models, the state accuracy of the MOPS based model is lower. The obtained results support this hypothesis, since the differences between the two ADS-B models are small, especially for the MVP method.

H-2: The negative effect of ADS-B based state information will be small, compared with perfect state information, regarding efficiency and safety for both CD&R methods.

Hypothesis 2 holds for the MVP, and partly for the swarming method; the efficiency and to a smaller extent, number of intrusions, are similar between ADS-B based state information and perfect state information. The number of intrusions for the swarming method show a different trend. Using ADS-B based state information results in 45 to 62% less intrusions compared with using perfect state information, which is an unexpected result.

It should be noted the efficiency is larger at the High traffic density situation for the swarming method. This is explained by the correction of aircraft leaving the experiment region to early due to swarming and conflict resolution. It was found a lot more aircraft left the experiment area premature during the High density swarming simulation. The reason of aircraft leaving the experiment area too early for the swarming method is caused by the combination of the swarming elements and the trajectory recover algorithm. As explained in Section II-B, the CPA location is used as reference for trajectory recovery. The swarming elements (velocity alignment component) cause very shallow conflict angles with the CPA location far away (Figure 31). This results in a large portion of CPA locations outside of the experiment area. Aircraft are being deleted and are not able to fly to the original destination. The grouping of aircraft also results in some aircraft being constantly in conflict with others in the swarm. The aircraft is not able to obtain a track to its original destination. Therefore no relevant conclusions can be drawn regarding the efficiency of the swarming method at the high traffic density simulation. **(H-2)** can be accepted for the MVP method. No solid conclusions can be drawn for the swarming method.

H-3: Using ADS-B based state information for CD&R has a more negative effect on swarming than MVP regarding number of intrusions and intrusion severity.

The swarming method shows an increase in intrusions with an increase in state information quality. Using ADS-B based state information results in 45 to 62% less intrusions compared to using perfect state information. Therefore hypothesis **(H-3)** is rejected, since it was expected more intrusions would occur when the state information quality decreases, especially for swarming, since this method required close and precise coordination for aircraft flying in groups. From the simulations it was observed aircraft show more swarm behavior using perfect state information. The grouping of aircraft, caused by the swarming elements, has a de-stabilizing effect regarding safety as it is currently implemented in the BlueSky simulator. The MVP method has the tendency to spread aircraft equally over the available airspace, resulting in better performance for all ADS-B cases with respect to swarming. The rejection of hypothesis 3 is also supported by Figure 31.

From this figure it can be concluded more than ±85% of the

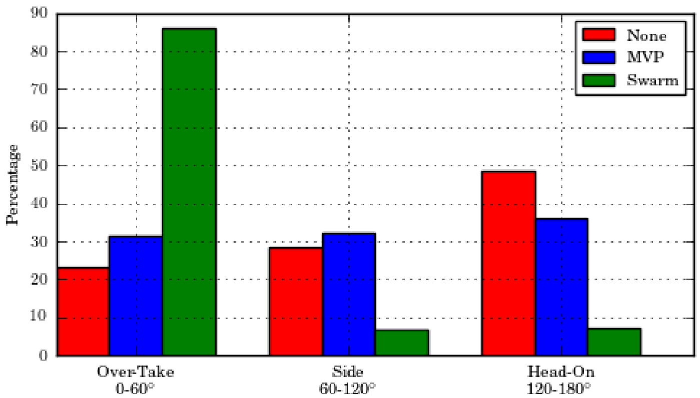

Figure 31: Percentage intrusion angle for the three different CDR methods on y-axis. Δ heading angle of involved aircraft on x-axis.

intrusions of swarming are shallow conflict intrusions. These shallow conflict intrusion are caused by the velocity alignment component of the swarming method, as discussed in Section II.

B. General discussion

It can be concluded that the effect of ADS-B based state information is small on both CD&R methods for the assessed traffic densities, compared to using perfect state information. This is partly due to the look-ahead time of 5 minutes, resulting in a detect and decode probability close to one. Subsequently the interference effect is not strong enough for the assessed traffic densities to have a significant impact. Also the position accuracy is high with respect to the dimensions of the IPZ. Only small differences were found for the two assessed CD&R methods regarding safety, efficiency and stability when comparing the results between ADS-B based and perfect state information. Based on the results from this experiments it can be concluded the assumption of perfect state information availability is valid for airborne CD&R research for relative low traffic densities. Also the ADS-B system shouldn't be considered as a limiting factor for a free flight airspace system. But in the sensitivity analysis (Experiment - III) the effect of interference became larger at higher traffic densities. The interference effect has a more dominant effect at extreme traffic densities. The detect and decode probability decreases with increasing number of aircraft according to the Poisson distribution. Additionally an increase in maximum reception range (i.e. transmit power) decreases this probability even further. A larger transmit power increases the number of aircraft within range causing interference. Additionally, the impact of each aircraft increases, due to the higher received power level. Current ATM research aims to increase air traffic capacity. Therefore the interference result is a valuable observation and could be incorporated in future research.

Use of perfect state information resulted in a small increase in performance with respect to ADS-B based state information for the MVP method. This is intuitive, since more accurate state information is available. The same outcome was hypothesized for the swarming method. But for the swarming method this was the other way around. Perfect state information resulted in more swarming behavior and worse performance than using ADS-B based state information. During the simulations it was observed that the swarming elements have a negative effect on CD&R performance. The swarming method results in more shallow intrusion angles ($\pm 85\%$). For all metrics the MVP method performed better than swarming, also when subjected to ADS-B based state information. During the third experiment it was obtained that the MVP method is very robust. A tipping point between $\frac{1}{8}^{th}$ and $\frac{1}{4}^{th}$ of the MOPS range resulted in a large increase in number of intrusions.

However, a different swarming implementation in the BlueSky simulator can result in different outcomes. Additionally the nature of the experiment plays a role. The current experiment is based on an extreme "Free Flight" concept, where aircraft have a randomly distributed destination and no destinations in common. This is advantageous for the MVP method since this method is based on evenly spreading aircraft over the available airspace. This experiment structure had drawbacks for the swarming method. The swarming method can have a more positive effect when a different experiment structure is defined. With only a limited amount of destinations, aircraft sharing their destination will swarm together.

C. Recommendations

Several additional factors are not taken into account in this research. No weather related disturbances are present in this simulation. Wind, causing drifting, can have a degrading effect on the trajectory prediction. It should be noted aggressive control inputs are required in some cases to prevent conflicts (especially in Experiment - III). These maneuvers are not assessed against passenger comfort and aircrew workload. Subsequently it could be worthwhile to further analyze the swarming method. This CD&R method can have potential positive effects under a different type of experiment structure, such as a limited number of destinations where it would be more beneficial to create swarms of aircraft. Also the human machine interface and pilot acceptance level can be researched further. Additional topics to study could be to what extend does an aircrew allow machine intervention, and what is a good way to present the pilot CD&R information. Finally the security issues related to the ADS-B system should be addressed. The simplicity of the ADS-B message modulation allows it to easily be jammed or spoofed.

IX. Conclusion

In this research an ADS-B model, based on state related and system related limitations and inaccuracies, is created. Different CD&R methods, MVP and Swarming, are assessed in a free flight environment subjected to these limitations and inaccuracies. An additional sensitivity analysis and range analysis for the MVP method are performed. The goal of this research is to study the effect of these ADS-B limitations and the robustness off the two CD&R methods. The following conclusions are drawn:

- The differences between the two assessed ADS-B models, and use of perfect state information, are small for both CD&R methods. MVP performance slightly deteriorated when subjected to ADS-B based information, while for Swarming it was the other way around. It was obtained that this is caused by the negative effect of the swarming method; aircraft showed less swarming behavior when subjected to ADS-B based state information.
- The sensitivity analysis showed that the interference effect becomes more dominant during high traffic densities. It is likely to play a more severe effect at extremely high traffic densities. Additionally increase in transmit power increases interference.

- The MVP methods showed better results in a pure free flight setting than the swarming method. Also when subjected to ADS-B limitations and inaccuracies the MVP method showed better results.
- The range analysis showed that MVP is a very robust method. Even for a reception range of $\frac{1}{4}^{th}$ of the ADS-B MOPS range (24 NM). The most affected metric at this range is found to be the number of intrusions.
- The ADS-B system should not be considered as a limiting factor in Free Flight experiments. However, the interference effect at high traffic densities should be taken into account. The use of a single carrier frequency, increase in transmit power and high traffic density increase the interference effect.

References

[1] European Organisation for the Safety of Air Navigation (EUROCONTROL), "Challenges of Growth 2013," Tech. Rep., 2013.

[2] J. How, "Increasing autonomy of UAVs," *Magazine, Automation and Engineers, Electronics*, 2012.

[3] NextGen, "NextGen Update: 2014," no. August, 2014.

[4] SESAR Consortium, "European ATM Master Plan - Edition 2," *The Roadmap for Sustainable Air Traffic Management*, no. October, pp. 1–100, 2012.

[5] J. Tadema, E. Theunissen, and K. M. Kirk, "Self Separation Support for UAS," *AIAA Infotech@ Aerospace Conference*, no. April, pp. 1–15, 2010.

[6] J. Krozel, M. Peters, K. Bilimoria, C. Lee, and J. S. B. Mitchell, "System performance characteristics of centralized and decentralized air traffic separation strategies," in *4th USA Europe Air Traffic Management RR Seminar*, Santa Fe, Dec. 2001.

[7] M. S. Eby, "A Self-Organizational Approach for resolving Air Traffic Conflicts," *The Lincoln Laboratory Journal*, vol. 7, no. 2, pp. 239–253, 1994.

[8] K. Bilimoria, K. Sheth, H. Lee, and S. Grabbe, "Performance evaluation of airborne separation assurance for free flight," in *18th Applied Aerodynamics Conference*. American Institute of Aeronautics and Astronautics, 2000.

[9] R. Barhydt, M. T. Palmer, and N. Langley, "Ads-b within a multi-aircraft simulation for distributed air-ground traffic management," *AIAA Digital Avionics Systems Conference*, 2004.

[10] M. Prandini, J. Hu, J. Lygeros, and S. Sastry, "A Probabilistic Approach to Aircraft Conflict Detection," *IEEE Transactions on Intelligent Transportation Systems*, vol. 1, no. 4, pp. 199–219, 2000.

[11] B. S. Y. D. Ali, W. Schuster, W. Ochieng, A. Majumdar, and T. K. Chiew, "Framework for ADS-B Performance Assessment : the London TMA Case Study," *AIAA*, pp. 39–52, 2013.

[12] RTCA Special Committee 186, "Minimum Aviation System Performance Standards for Automatic Dependent Surveillance Broadcast (ADS-B)," *Rtca/Do-242a*, 2002.

[13] D. J. Bernays, S. D. Thompson, and W. H. Harman, "Measurements of ADS-B Extended Squitter performance in the Los Angeles basin region," in *Digital Avionics Systems Conference, 2000. Proceedings. DASC The 19th*, vol. 2, 2000, pp. 7B1/1—-7B1/8 vol.2.

[14] J. Maas, "A Quantitative Comparison of Conflict Resolution Strategies for Free Flight," 2015.

[15] J. Hoekstra and R. Ruigrok, "Conceptual Design of Free Flight With Airbrone Separation Assurance," 1998.

[16] J. K. Kuchar and L. C. Yang, "A Review of Conflict Detection and Resolution Modeling Methods," *IEEE Transactions on Intelligent Transportation Systems*, vol. 1, pp. 179–189, 2000.

[17] J. Ellerbroek, *Airborne Conflict Resolution In Three Dimensions*, 2013.

[18] R. C. J. Ruigrok, R. Van Gent, and J. M. Hoekstra, "The transition towards free flight: A human factors evaluation of mixed equipage, integrated air-ground, free flight ATM scenarios," *SAE Technical Papers*, 1999.

[19] J. Hoekstra, R. van Gent, and R. Ruigrok, *Designing for safety: the free flight air traffic management concept*, 2002, no. November.

[20] M.-J. T. Chang-Su Park and H. Bang, "Multiple aerial vehicle formation using swarm intelligence," *AIAA 2003-5729*, no. August, 2003.

[21] J. Maas, E. Sunil, J. Ellerbroek, and J. Hoekstra, "The effect of swarming on a voltage potential-based conflict resolution algorithm," *ICRAT*, 2016.

[22] J. Hoekstra, R. V. Gent, and J. Groeneweg, "Airborne separation assurance validation with multiple humans-in-the-loop," *5th USA/Europe air traffic management R&D seminar*, vol. 251, pp. 1–10, 2003.

[23] (2008) Global positioning system standard positioning service performance standard. [Online]. Available: http://www.gps.gov/technical/ps/2008-SPS-performance-standard.pdf

[24] W. Chung and R. Staab, "A 1090 Extended Squitter Automatic Dependent Surveillance - Broadcast (ADS-B) Reception Model for Air-Traffic-Management Simulations," *AIAA 2006-6614, Modeling and Simulation Technologies Conference and Exhibit, August*, no. August, pp. 1–11, 2006.

[25] J. M. Hoekstra and J. Ellerbroek, "BlueSky ATC Simulator Project : an Open Data and Open Source Approach," *ICRAT 2016*.

[26] M. Jardin, "Air Traffic Conflict Models," in *AIAA 4th Aviation Technology, Integration and Operations (ATIO) Forum*. American Institute of Aeronautics and Astronautics, 2004.

[27] D. Delahaye, A. Vidosavljevic, and E. Sunil, "Metropolis urban airspace design," 2015.

Part II

Preliminary Report

Chapter 1

Introduction

Recent and on-going developments in aviation require a modernization of current airspace design. First of all; due to the steady and continuous growth of air traffic the current Air Traffic Control (ATC) system is reaching its capacity limits. A steady growth is predicted for Europe in the number of IFR flights, even for the most pessimistic economic scenario, as shown in figure 1-1 (European Organisation for the Safety of Air Navigation (EUROCONTROL), 2013). A restructuring of airspace and a novel Air Traffic Management (ATM) system are identified as main solutions to fulfill future airspace capacity demand. The current use of predefined airways prevents pilots from flying their preferred routes. Therefore, a transition to the "Free Flight" concept, where the aircrew is allowed to fly its preferred route, is researched and identified as a promising concept for future airspace. Besides the capacity increase of the airspace, Free Flight (Valenti Clari, Ruigrok, & Hoekstra, 2000) will result in economical and environmental gains (M. S. Eby, 1994; Bilimoria, Sheth, Lee, & Grabbe, 2000). A fundamental element of Free Flight is airborne self separation; instead of a ground-based controller the aircrew is responsible for maintaining the defined separation distance with respect to other aircraft. Studies are done to assess the performance of Conflict Detection & Resolution (CD&R) methods and to quantify the realities and uncertainties in the ADS-B system. However, the effect of the realities on CD&R performance has not been investigated. The research objectives goal is to fill the gap between two ongoing research areas and developments.

Secondly, recent developments in the Unmanned Aircraft System (UAS) area require a novel approach to ATC. Current technologies rely on communication with the pilot and a ground-based controller, both actively involved to prevent conflicts. A trend in the UAV area is observed from pilot guided UAV to a higher level of autonomy (Magazine & Engineers, 2012). UAVs in a future airspace system must be kept in mind for a safe integration. Airborne self separation might be a promising concept to integrate UAVs in a safe manner with conventional air traffic (Tadema, Theunissen, & Kirk, 2010). Airborne self separation can be achieved using so-called CD&R methods. A key-enabling technology of airborne self separation using CD&R methods is the ADS-B system. Both these concept are introduced in the following section.

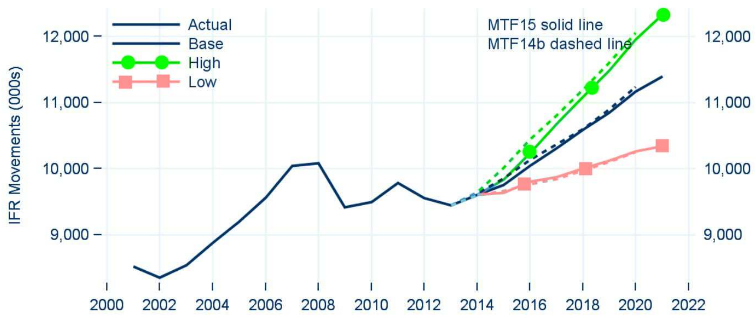

Figure 1-1: Forecast IFR movements three different scenarios, depending on economic growth in Europe. Figure from(European Organisation for the Safety of Air Navigation (EUROCONTROL), 2013).

1-1 The ADS-B system and CDR methods

The goal of CD&R is to predict when and if a conflict is going to occur, subsequently communicate a detected conflict to a human operator, guide in resolving the conflict or automatically solve the conflict. However, different techniques can be used for conflict detection and resolution. CD&R consists of two parts; detection and resolution. A good definition is given in (Kuchar & Yang, 2000):

Conflict detection can be thought of as the process of deciding when action should be taken and conflict resolution involves determining how or what action should be performed.

The two steps involved in CD&R are introduced in the following two paragraphs.

The first part is **conflict detection**. To detect a conflict, state information of surrounding aircraft needs to be known. These states (location, velocity, heading) provide an estimation of the current air traffic situation. With the states of the aircraft, a dynamic trajectory can be created to predict future conflicts. In general two methods are used in literature: state based and intent based trajectory prediction (Kuchar & Yang, 2000; Prandini, Hu, Lygeros, & Sastry, 2000). In (Kuchar & Yang, 2000) both methods are discussed. State-based trajectory planing consists of extrapolation of the most recent speed vector of the aircraft. Intent-based trajectory planning uses, for example, the flight plan to incorporate the intent of a specific aircraft in the trajectory planning.

The second part of CD&R is **conflict resolution**. A good base for the discussion of several CD&R algorithms is (Kuchar & Yang, 2000), in which 68 CD&R modeling methods, focused at non-human-centered issues, are discussed and compared. The CD&R methods can be divided in four categories; prescribed methods, optimization methods, force field methods and manual methods. CD&R methods are discussed in more detail in section 2-1-2.

It should be noted that for both the conflict detection and the resolution part, state information of neighboring aircraft has to be known. A recent, developing technology, called ADS-B, enables direct state information exchange between aircraft through a digital datalink. ADS-B is a cooperative surveillance technology, where each aircraft is equipped with an ADS-B transmitter (ADS-B-OUT) and a receiver (ADS-B-IN). In this research, when referred to the ADS-B system, both the transmitting and receiving airborne part is meant (shown in fig. 1-2). One of the benefits using the ADS-B system is that using technologies such as satellite based navigation and on-board equipment an aircraft can determine its state (location, velocity, heading etc.) more accurately than a secondary radar (Ali, Schuster, Ochieng, Majumdar, & Chiew, 2013). Aircraft transmit an ADS-B message, containing state and identity information, in an omnidirectional manner with an interval time of seconds. A general overview of the ADS-B system is shown in fig. 1-2.

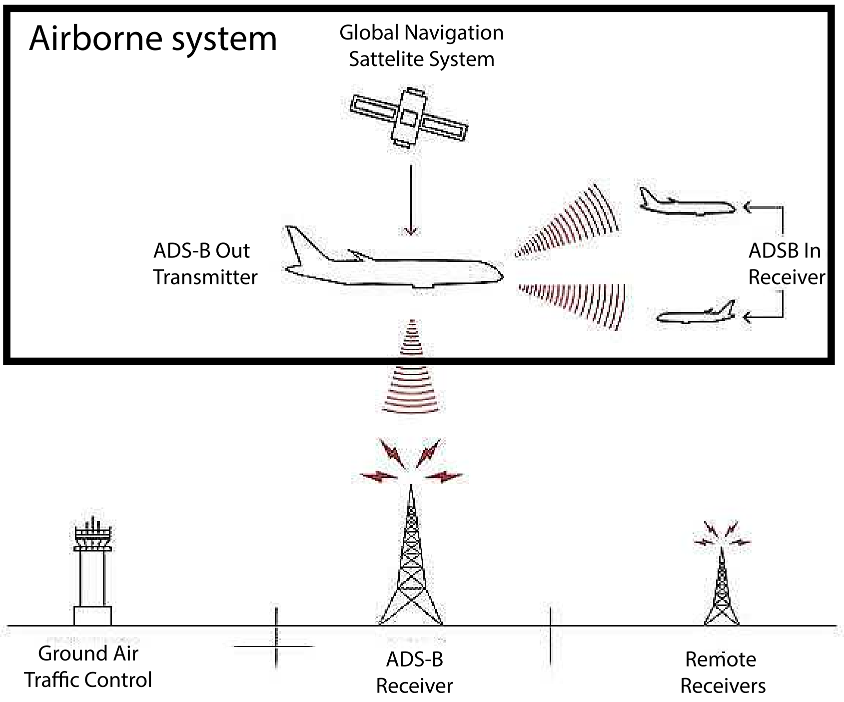

Figure 1-2: Overview of the ADS-B system. Figure from (Barhydt et al., n.d.).

Aircraft equipped with ADS-B-IN are able to receive the ADS-B signal. This last functionality enables airborne separation assurance. In this research the focus is on the data link between aircraft communicating state information using the 1090 MHz frequency, the airborne system in fig. 1-2. Further applications of ADS-B are described in (RTCA Special Committee 186, 2002). ADS-B is in several prominent studies identified as the enabling technology of airborne self separation (Barhydt et al., n.d.; M. Eby & Kelly, 1999).The following ADS-B message reports are send, including the transmission rate (Eurocontrol, n.d.):

- Airborne positions squitter (2/sec)
- Surface position squitter (1/sec)
- Airborne velocity squitter (2/sec)
- Aircraft identification squitter (0.2/sec)

- Operational Status (0.4/sec)
- Target state (0.8/sec)

The ADS-B signal transmission is subjected to uncertainties and realities. First of all the location of the aircraft needs to be determined on-board. Therefore the Global Navigation Surveillance System (GNSS) and inertial systems are being used. Since inertial sensors drift with time, satellite based navigation such as Global Positioning System (GPS) is considered the most important source for position determination (Ali et al., 2013). The range of the ADS-B broadcast message is limited due to several factors. Extensive measurements to the performance of the ADS-B extended squitter signal have been done in (Bernays, Thompson, & Harman, 2000) and (Ali et al., 2013). In these studies the main focus is on accuracy and latency of the ADS-B message. In (Bernays et al., 2000) a quantitative assessment of the air-to-air range of ADS-B equipment is researched. A decreasing reception probability is observed for an increasing distance between aircraft. Besides distance, aircraft message interference has to be considered since all ADS-B mode S communication is performed on the same 1090 MHz frequency. It is found in (Barhydt, Palmer, & Langley, 2004) that the message interference resulting from overlapping messages at the receiver side can be modeled as the sum of multiple Poisson distributions. Additional effects are more system related. Since only a limited number of bits are available, the state information can be transmitted up to a certain accuracy; the truncation effect (Eurocontrol, n.d.). As discussed above aircraft don't transmit their state continuously. Finally the aircraft need some time to generate a message, transmit the data and process the ADS-B message causing, some latency. These properties are further discussed in chapter 3.

1-2 Thesis Objective and Research Questions

The research objective is aimed at filling the gap between two ongoing researcher areas and developments. On one side, the research associated with enabling a Free Flight environment using CD&R methods, and on the other side, the developments in the ADS-B system. The goal of this research is to study the effects of ADS-B system characteristics on CD&R performance. The research objective is stated as follows:

Study and analyze the effect of ADS-B realities and uncertainties on the performance of different CD&R algorithms.

Several aspects are involved in this research objective. Therefore, not one but multiple research questions are defined, each containing sub-questions. These are the sub-questions:

1. What affects proper reception by aircraft of an ADS-B signal?
    (a) How can the quality of an ADS-B message be assessed?
    (b) How do the consequences of ADS-B system specifications affect the ADS-B signal reception?

   (c) How do external factors affect the ADS-B signal reception?

2. What ADS-B related variables influence the performance of a CD&R method and to what extend?
   (a) What are suitable metrics to asses the performance of the CD&R method related to:
      i. Safety?
      ii. Efficiency?
      iii. Airspace stability?
   (b) Which elements of the ADS-B system affect the CD&R performance?
3. How can the effect of ADS-B signal realities and uncertainties on CD&R performance be evaluated in an experiment/simulation?
   (a) What should be the dependent and independent variable in the experiment and simulation?
   (b) Which test environments are suitable for assessing the performance of CD&R method?

During the preliminary phase some of these research questions were answered. Therefore the following additional research questions were defined, to be investigated in the main phase:

1. What is the relation between different CD&R methods subjected to ADS-B uncertainties and realities and the following CD&R performance indicators:
   (a) Safety, measured using $LOS_{severity}$, number of LOS and LOS duration?
   (b) Stability, measured using the Domino Effect Parameter?
   (c) Efficiency, measured as route efficiency?
2. Which CD&R parameters has the largest effect on CD&R performance?
3. Is the ADS-B system a limiting factor for a free flight airspace?

1-3 Research Approach

This section will discuss the steps to be taken to answer the research questions and research objective stated in section 1-2.

First of all an analysis of different ADS-B specifications is performed. Subsequently several studies regarding the ADS-B system and CD&R methods are analyzed. Different papers are found discussing the realities and uncertainties in the ADS-B system (Barhydt et al., 2004; Chung & Staab, 2006). This research is a good base for developing an ADS-B system model. Additionally, knowledge about CD&R methods needs to be obtained. In (Kuchar & Yang, 2000) a comparison between multiple methods is performed. In that research, several categories of CD&R methods are discussed and gives a good general overview of suitable CD&R

applications for airborne separation assurance. The effect of different ADS-B uncertainties and realities on CD&R performance can be assessed by developing an ADS-B model. Subsequently this ADS-B model can be implemented in the BleuSky simulator. In this simulator fast-time simulations can be performed and data will be logged. From this logged data the effect of the ADS-B limitations on CD&R performance can be determined.

From the knowledge obtained during the literature study an ADS-B model can be developed. Since these need to be implemented and tested in the BlueSky simulator, knowledge regarding the Python programming language and the BlueSky Simulator is required. Subsequently an air traffic scenario needs to be designed in which all the aspects regarding CD&R performance are evaluated. Before the experiments, an hypothesis is discussed. It is assumed the performance of CD&R methods degrades with increasing ADS-B uncertainty and reality effects. However, this should be confirmed by experiments. Also the extend to which the ADS-B uncertainties and realities affect the CD&R methods can be concluded from these experiments.

This research will use the BlueSky open air traffic simulator as discussed in section section 4-1. In the BlueSky simulator air traffic scenarios can be loaded and analyzed. Different types of airborne separation assurance systems using CD&R methods will be assessed. Subsequently the performance of these methods can be analyzed. Since no ADS-B model is available and the current use of CD&R methods doesnt allow the use of ADS-B data, adaption to the BlueSky simulator need to be made. Different CD&R methods will be evaluated with a range of ADS-B settings. Subsequently data regarding the performance of these CD&R methods will be logged. The performance can be assessed in different ways, focusing on safety and efficiency.

1-4 Research Scope

This research focuses on the airborne separation aspect during the Free Flight part for en-route air traffic. En-route flight mostly occurs at high altitudes and with a constant airspeed. Subsequently during en-route and the free flight concpet, aircraft are mostly travelling in a straight line without sudden maneuvers such as cornering and speed deviations.

This research focuses on simulation using the BlueSky Simulator. The resources allow only simulated flight, so no humans are involved in the loop. Using the BlueSky Simulator makes it possible to create and implement an ADS-B model. This model only takes several variables in account; in reality shielding of the ADS-B signal by the aircraft, (some level of) multipath effects, degrading performance due to weather etc. may be present. These variables are not modeled in the ADS-B model. Subsequently the CD&R methods tested are the Modified Voltage Potential (MVP) and Swarming method, since these are available in the BlueSky Simulator.

1-5 Preliminary Thesis Outline

The thesis consists of two parts; a preliminary phase and the main phase. This part describes the findings of the preliminary phase.

This preliminary report starts with the literature study in chapter 2. Different research areas are discussed. CD&R is discussed in section 2-1 and subsequently the ADS-B system is discussed in section 2-2. From the literature review, more research is performed to the ADS-B system by creating an ADS-B reception model, discussed in chapter 3. First the different properties affecting the quality of an ADS-B report are discussed in section 3-1. Subsequently the general software implementation of an ADS-B model into software is discussed in section 3-2-1, and the implementation in the BlueSky open ATM simulator in section 3-2-2. The chapter is concluded with verification of the implementation of the ADS-B model in the BlueSky Simulator in section 3-2-3. The experiment design in discussed in chapter 4, by defining the independent and dependent variables in section 4-2-1 and section 4-2-2 respectively. The report is concluded with the conclusion in chapter 5.

Chapter 2

Literature review

This chapter contains the literature review associated with this research. In the early stage of the research orientation two major research fields were identified; CD&R and ADS-B. Therefore this literature study is also divided in two parts. section 2-1, elaborates on different CD&R methods, with conflict detection discussed in section 2-1-1 and conflict resolution in section 2-1-2. The next section, section 2-2, discusses the airborne ADS-B system and its limitations.

2-1 Conflict Detection and Resolution

In this section literature related to CD&R is discussed. Conflict detection is discussed in section 2-1-1, followed by conflict resolution in section 2-1-2.

2-1-1 Conflict Detection

The first part is conflict detection. However, first the definition of a conflict needs to be known. In Free Flight concepts constraints are defined to ensure safe flight. Defined by the RTCA for en-route flight are 5 nautical miles separation in the horizontal plane and 1000 feet separation in the vertical plane. This results in a disk-shaped volume with a thickness of 2000 feet and a radius of 5 nautical miles, shown in fig. 2-2. This zone is in literature defined as the protected zone or intruder protected zone (Ellerbroek, 2013; Krozel & Peters, 1997). Intrusion of other aircraft within this zone results in a Loss Of Separation (LOS).

Several methods are found to predict a conflict. In (Krozel & Peters, 1997) an alert zone is defined. If the alert zones of two aircraft overlap a LOS will occur in the future. Therefore a conflict resolution maneuver should be performed to prevent LOS. In (J.M. Hoekstra, 1998) a look-ahead time is defined of five minutes. The future location of aircraft is calculated by extrapolation of state information of surrounding aircraft.

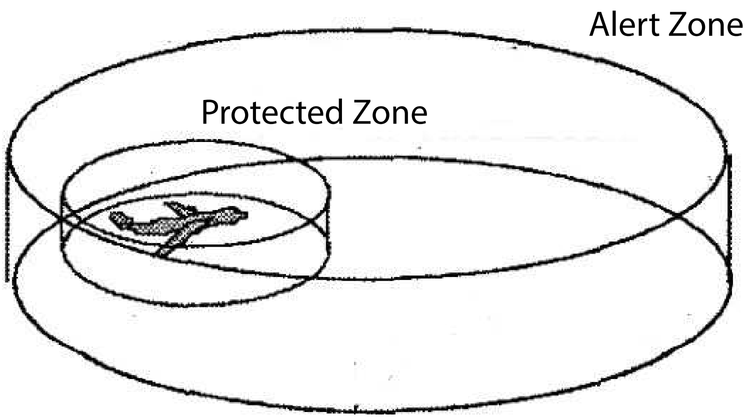

Figure 2-1: Aircraft Protected Zone and Alert Zone definition. Figure obtained from (Krozel & Peters, 1997).

To detect a conflict, state information (velocity, location, heading) of surrounding aircraft needs to be known. With the states of the aircraft a dynamic trajectory can be created to predict future conflicts. In general two methods are used in literature: state based and intent based trajectory planning(Kuchar & Yang, 2000; Prandini et al., 2000). In (Kuchar & Yang, 2000) both methods are discussed.

Intent-based trajectory planning uses for example the flight plan to incorporate the intent of a specific aircraft in the trajectory planning. However, these prediction methods have some level of inaccuracy, increasing with look-ahead time and time interval of the state update (Kuchar & Yang, 2000; Prandini et al., 2000). It was found in (J.M. Hoekstra, 1998) that when using a look-ahead time of five minutes the level of intent hardly improves the quality of the predictions compared with state extrapolation during en-route flight. The main reason is that most of the times the intended route is the current track when flying direct routes.

State-based trajectory planing consists of extrapolation of the most recent speed vector of the aircraft. Several studies have been performed on predicting the future state of aircraft. In (Kuchar & Yang, 2000) three different state-based trajectory prediction methods are discussed. First the nominal projection methods are described as extrapolating the current speed vector in a straight line. The second method is the worst-case projection. All possible future locations of the aircraft (assuming a wide range of possible maneuvers inside the flight envelope) are considered as possible aircraft locations. This results in a large area where a conflict might occur. This method is very conservative and will therefore also have a high false-alarm rate. Finally the probabilistic method is discussed. In this method different future trajectories are assigned a probability of the aircraft following this trajectory. This method can be considered as a balance of the two earlier described methods. These three state propagation methods are visualized in fig. 2-2. From (J.M. Hoekstra, 1998) it was concluded a state based method results in a similar to better prediction for en-route flight with respect to an intent-based approach. In (Kuchar & Yang, 2000) it was found a nominal-projection method will result in good estimation results for en-route flight, since an aircraft is mostly flying a straight line during this flight phase. Therefore a state-based, nominal projection method will be used in this research.

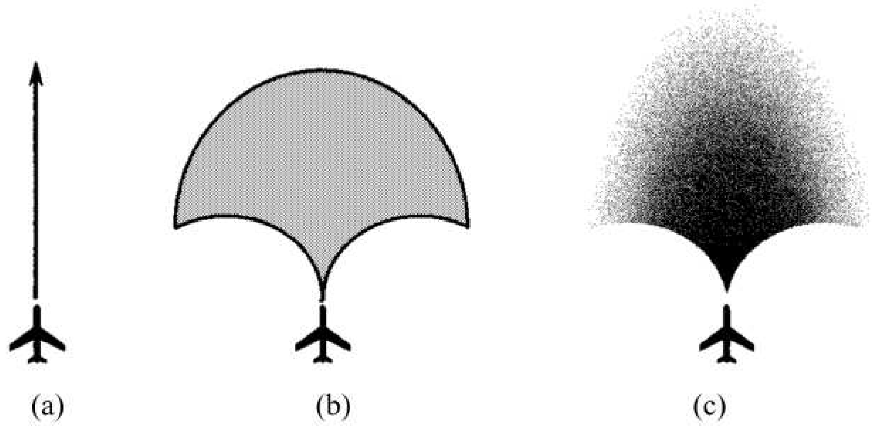

Figure 2-2: State based trajectory planning methods: A: Nominal Projection, B: Worst-case Projection, C: Probabilistic Projection. Figure obtained from(Kuchar & Yang, 2000).

2-1-2 Conflict Resolution

The second part of CD&R is conflict resolution. A suitable starting point for the discussion of several CD&R algorithms is (Kuchar & Yang, 2000), in which 68 CD&R modeling methods focused at non-human-centered issues, are discussed and compared. Several conflict detection methods are already discussed above. Four categories are identified with respect to conflict resolution methods in (Kuchar & Yang, 2000) .

1. **Prescribed method:** A fixed maneuver is performed in case of a predicted conflict. An example is (Kuchar & Carpenter, 1997). This method however is mostly suitable for terrain and runway related conflicts.

2. **Optimization method:** In general a kinematic model is combined with a set of cost metrics. Subsequently an optimal resolution strategy is determined based on the cost metric. The cost metric can be for example fuel, time, workload or separation distance. Techniques such as genetic algorithms and fuzzy control are being used. (Lachner, 1997)

3. **Force field method:** These methods model the aircraft as similar charged particles and will generate a repulsive force between two aircraft. Examples are (Duong, Hoffman, & Nicolaon, 1997) and (M. S. Eby, 1994)

4. **Manual method:** A human operator selects the most suitable resolution method. This method is more flexible and human intuition is involved. Additional information, such as weather, can be incorporated by the decision making. An example is (J.M. Hoekstra, 1998) which uses the force field method in combination with human decision.

It should be noted that the methods in (Kuchar & Yang, 2000) were evaluated by separate authors, under different conditions. The CD&R methods were individually evaluated in a qualitve manner, under different circumstances. (Maas, 2015) compared three different CD&R methods, MVP, swarming method and differential game, in a quantitative way, with similar experiment conditions. It was concluded MVP was the most promising CD&R method to ensure safe flight. However, this might be different when ADS-B uncertainties and realities are implemented in the simulation. The MVP and swarming method are selected to further evaluate, described below.

MVP

The MVP method is based on modeling aircraft as identical charged particles as described in (J. Hoekstra, Gent, & Ruigrok, 2002). These particles have a repellent force with respect to each other, increasing with decreasing distance. This method is based on the voltage potential method described in (M. Eby & Kelly, 1999), where the aircraft and destination are modeled as positive and negative charged particles respectively. The geometrical relation to resolve a conflict using the MVP method is shown in figure 2-3. In figure 2-3 two conflicting aircraft are shown, A and B. The protected zone of aircraft A is indicated with a circle.

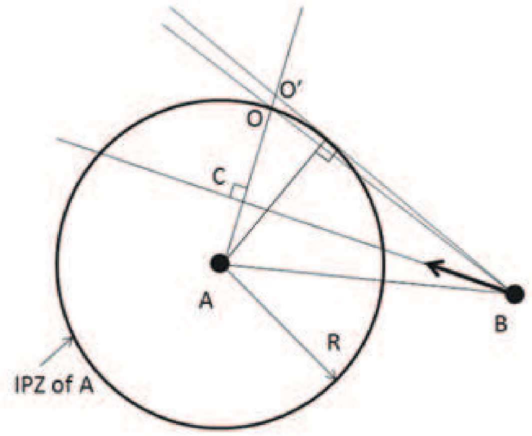

Figure 2-3: Geometrical relation of two conflicting aircraft for MVP. Figure obtained from (Maas, 2015)

First the relative velocity (black arrow) vector and Closest Point of Approach (CPA) (point C) will be calculated. Subsequently the time to closest point of approach, t_{CPA} can be determined. It is assumed the location and velocities of both aircraft are known. The location of point C can be determined using geometric relations. Subsequently the distance vector CO can be obtained. However, this will still result in a LOS. Therefore the tangent line BO' accent need to be obtained. CO' can be calculated using equation 2-1 (J. Hoekstra et al., 2002).

$$\frac{|CO'|}{|CO|} = \frac{1}{|cos(arcsin(\frac{R}{AB}) - arcsin(\frac{AC}{AB}))} \tag{2-1}$$

Swarming method

Swarming intelligence, described in (Aerial, Formation, & Swarm, 2003), is a bio-inspired interaction between animals in large groups, such as a school of fish and a flock of birds. In this research the goal was to apply the swarming method to Unmanned Aerial Vehicle (UAV)s. The behavior of each individual object consists of three elements and can be applied to air traffic situations, as shown in (Maas, 2015):

- **Collision Avoidance (CA)**: Sum up the vectors of surrounding aircraft and define the vector pushing away from the center of the group.
- **Velocity Matching (VM)**: Match the velocity of surrounding aircraft and thereby lowering the possibility of collisions. Velocity matching is a dynamic way of collision avoidance.
- **Flock Centering (FC)**: Obtain the graphical center of surrounding aircraft and steer in that direction.

These elements are respectively shown in figure 2-4

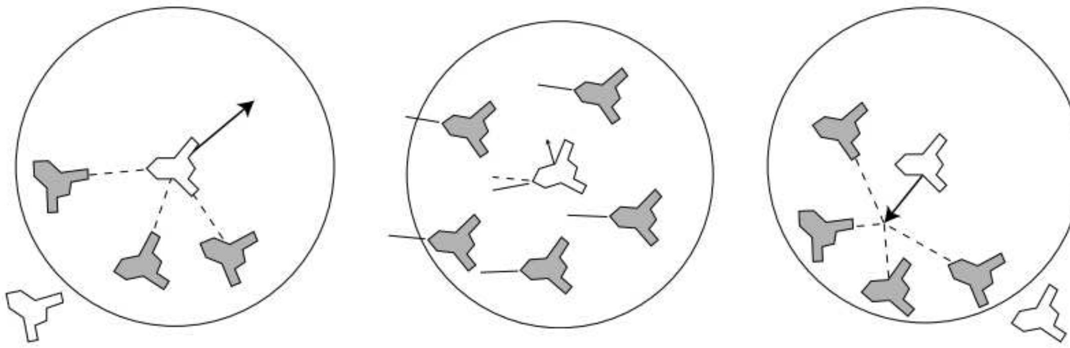

Figure 2-4: Three elements of swarming method. From left to right: Collision Avoidance, Velocity Matching and Flock Centering. Image obtained from (Aerial et al., 2003).

In essence the swarming method is a weighted combination of the three actions described above. This equation is shown in 2-2 with the different vectors indicated with $\vec{V}$ and the weights with W. The corresponding Swarming element is shown in the subscript.

$$\vec{V}_{SW} = \frac{W_{CA} \times \vec{V}_{CA} + W_{VA} \times \vec{V}_{VA} + W_{FC} \times \vec{V}_{FC}}{W_{CA} + W_{VA} + W_{FC}} \tag{2-2}$$

2-2 Automatic Dependent Surveillance-Broadcast

A developing technology called ADS-B enables direct state information exchange between aircraft through a digital data-link. Aircraft transmit an ADS-B message, containing state information, in an omnidirectional manner with an interval time of seconds. Aircraft equipped with ADS-B IN are able to receive this signal. Besides state data also weather related data can be received from a ground station. An overview is shown in figure 1-2.

In this research the focus is on the data link between aircraft communicating state information using the 1090 MHz frequency, the airborne system in figure 1-2. Further applications of ADS-B are described in (RTCA Special Committee 186, 2002). ADS-B is in several prominent studies identified as the enabling technology of airborne self separation (Barhydt et al., n.d.; M. Eby & Kelly, 1999; J. Hoekstra, Gent, & Groeneweg, 2003).The following ADS-B message reports are send, including the transmission rate (Eurocontrol, n.d.):

- Airborne positions squitter (2/sec)
- Surface position squitter (1/sec)
- Airborne velocity squitter (2/sec)
- Aircraft identification squitter (0.2/sec)
- Operational Status (0.4/sec)
- Target state (0.8/sec)

2-2-1 ADS-B message characteristics

The ADS-B message is transmitted using a 1090 MHz carrier frequency using PPM. One transmission message consists of a preamble of 8 μs and a data block of 112 μs with a bit duration of 1 μs resulting in a data rate of 1 Mbps. A bit is divided in two parts; a pulse in the 1st half of the bit indicates a 1 and a pulse in the second half of the bit a 0. A schematic overview is shown in fig. 2-5, with the bit indicating a 0. The content of an actual ADS-B message, bit-wise, is shown in table 2-1 (Harman, Gertz, & Kaminsky, 1998) (Eurocontrol, n.d.).

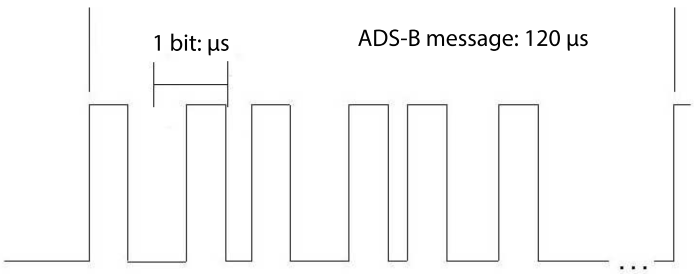

Figure 2-5: ADS-B message using PPM. ADS-B message duration of 120μs, containing 120 bits and bit length of 1 μs.

A detailed description about the content of each part of the ADS-B message is given by (Eurocontrol, n.d.). The preamble is used to synchronize the receiver to decode the signal. The down link format indicates the data format, DF17 in case of an ADS-B ES signal indicated with the binary code 10001. The third part of the message is the capability; this indicates the number of sub-type of the ADS-B message. The main focus on this research is related to the state exchange between aircraft using the ADS-B system.

Table 2-1: Bit-wise content of ADS-B extended squiter message. Information obtained from (Eurocontrol, n.d.; Harman et al., 1998)

Number of Bits	Name	Function
8	Preamble	Used for synchronization of reception
5	Down link Format	Used to specify down link format
3	Capability	Sub type of down link format
24	Aircraft ACAO dress	Unique identification code of aircraft
56	ADS-B data	Send ADS-B related data
24	Parity check	Error detection/integrity check usign CRC method

2-2-2 ADS-B Realities and Uncertainties

The ADS-B system is not a perfect system, but subjected to realities and uncertainties. During the literature study several key elements are identified. The realities and uncertainties can be divided in two main groups; system related an situation related. The situation related elements mostly affect the reception probability of an ADS-B message. The system related elements affect the accuracy of the state information within the ADS-B report and the time of reception of the report. A general overview is shown in fig. 2-6. These effects are discussed in the following paragraphs.

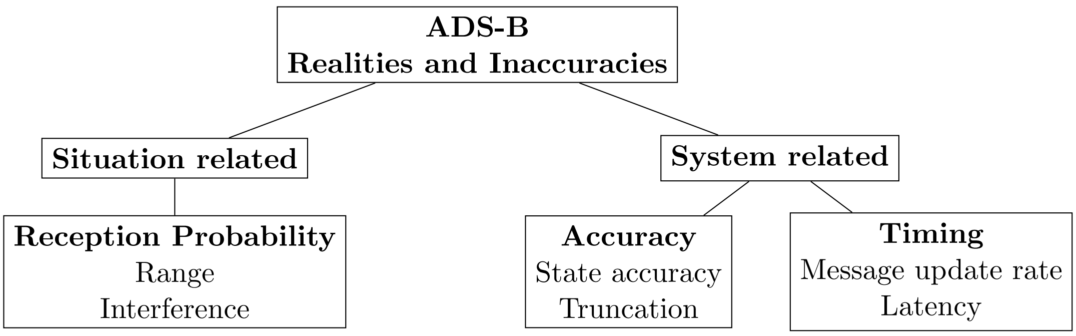

Figure 2-6: Schematic overview ADS-B realities and uncertainties.

Accuracy

First of all the location of the aircraft needs to be determined on-board. Therefore the GNSS and inertial systems are being used. Since inertial sensors drift with time, satellite based navigation such as GPS is considered the most important source for position determination. In (Ali et al., 2013) it is concluded ADS-B combined with GPS provide a significantly more accurate method to determine positions than radar. Only a specific amount of bits are reserved for a specific state in the ADS-B message. Therefore the accuracy of a state can not be described with infinite accuracy. The truncation effect should be considered (Eurocontrol, n.d.).

Timing

Aircraft don't send their ADS-B report continuously. In (Barhydt et al., 2004; Chung & Staab, 2006) it is analyzed how the message update rate affects the message reception probability due to interference. Due to a specific transmit rate of an ADS-B message the aircraft is not aware of the aircraft state for a certain time interval. Therefore the message transmit rate is a trade-off between an allowable message reception probability caused by interference and a sufficient update rate of state information. This has also the result aircraft don't receive each others state at the same time; aircraft A might be aware of aircraft B, but not the other way around.

Latency
It should be noted that the receiving aircraft does not have the real-time state information of the other aircraft. Aircraft A generates a position report and sends this to Aircraft B. However, Aircraft A needs some time to send the ADS-B message and aircraft B needs some time to process the ADS-B message. Therefore some latency can affect the performance of the CDR method. In (Ali et al., 2013) it is found the latency due to processing is less than a second.

Range effect
The range of the ADS-B broadcast message is limited due to several factors. Extensive measurements to the performance of the ADS-B extended squitter signal have been done in (Bernays et al., 2000) and (Ali et al., 2013). In these studies the main focus is on accuracy and latency of the ADS-B message. In (Bernays et al., 2000) a quantitative assessment of the air-to-air range of ADS-B equipment is researched. A decreasing reception probability is observed for an increasing distance between aircraft.This relation is shown in fig. 2-7.

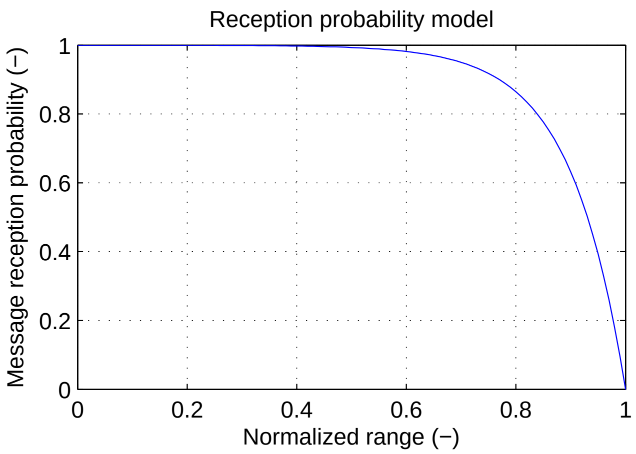

Figure 2-7: Reception probability with respect to normalized range (max range). Model obtained from (Chung & Staab, 2006)

Interference effect
Besides distance, aircraft message interference has to be considered since all ADS-B mode S communication is performed on the same 1090 MHz frequency. It is found in (Barhydt et al., 2004) the message interference resulting from overlapping messages at the receiver side can be modeled as the sum of multiple Poisson distributions.

It can be concluded that the ADS-B system is subjected to different types of realities and uncertainties, shown in fig. 2-6. In general these types can be divided in system related and situation related parameters. The situation related parameters are mainly affecting the reception probability of an ADS-B message. The system related parameters affect the update interval (due to latency and transmission rate) and state accuracy (due to measurement accuracy, GPS accuracy and truncation). These elements form the base for the generation of the physical ADS-B model discussed in section 3-1.

Chapter 3

ADS-B model

In this chapter the ADS-B model is discussed in more detail. The different properties affecting the reception performance and accuracy of an ADS-B report are discussed in section 3-1. Subsequently, the translation from the analytical ADS-B model into software is discussed in section 3-2.

3-1 Physical model of the ADS-B system

In this section the properties affecting the reception performance and accuracy of an ADS-B report is discussed. It is found these properties can be divided in two main groups; system related properties, discussed in section 3-1-1 and situation related properties, discussed in section 3-1-2. It is found the first one mainly influences the accuracy of the state-information, while the latter mostly influences the reception probability of the ADS-B report.

3-1-1 System related properties

Several system-related properties are found. These properties are discussed in the following paragraphs.

Truncation
Since only a limited number of bits are available the states cannot be transmitted with infinite accuracy. Therefore the truncation affect has to be considered. Since the location is expressed in latitude and longitude, this state is considered to be the most sensitive for truncation. The position is described using Compact Position Reporting (CPR) format; an efficient way which uses less bits to encode position information. This method requires two position reports, an odd and an even frame. The last report is used to determine the position of the aircraft. The details of this method are further discussed in (Soediono, 1989). The latitude an longitude are both transmitted using 6 significant digits; therefore the accuracy based on truncation is the distance between two locations where the 6th digit is changed. The Haversine function,

shown in eq. (3-1), is used to calculate the great-circle distance between two points in meters, expressed in latitude and longitude. In this equation ϕ is latitude (rad), λ is longitude (rad), and R (m) is the earth radius.

$$a = sin(\frac{\delta \cdot \phi}{2}) + cos(\phi_1) \cdot cos(\phi_2) \cdot sin^2(\frac{\delta \cdot \lambda}{2}) \quad (3\text{-}1a)$$

$$c = atan2(\sqrt{a}, \sqrt{1-a}) \quad (3\text{-}1b)$$

$$d = R \cdot c \quad (3\text{-}1c)$$

Using the Haversine function and a position described in longitude and latitude with a six digit significance level results in a accuracy ranging from 9 to 17 m, depending on the location on the earth.

Accuracy
Additional to the truncation effect the state accuracy of the on-board measurement equipment affects the location precision. Location determination is done using the GNSS system and altitude and airspeed using an on-board barometer and airspeed sensor respectively. Of these states, position is the state depending on an external system, such as GNSS or Wide Area Augmentation System (WAAS). Therefore the accuracy of this state is further discussed. In (DoD, 2016) it is found an GPS measurement has an accuracy of $\leq$7.8 meter with a 95% confidence interval.

Both the truncation effect and the accuracy of a state, position for example, can be modeled as a normal distribution. It was found the truncation effect results in a accuracy ranging from 9 to 17 meters and the GPS accuracy a 95% confidence interval of $\leq$ 7.8 meters. The value in the ADS-B report can be modeled as a normal distribution with the positions being the expected value and a standard deviation of 15 meters. When location at position 0, this results and the probability of corresponding deviation shown in fig. 3-1. The same procedure can be used for other states.

ADS-B message update rate
ADS-B messages are not transmitted continuously; they are transmitted with a specific update rate. Therefore an aircraft only knows the "old" location of other aircraft. This is depending on the transmission rate of the ADS-B report. As discussed in (Eurocontrol, n.d.) an update rate of 1-2 Hz per message is proposed for state information reports. An asynchronous update also results in a difference in state information; aircraft A might be aware of aircraft B, while not the other way around. Also the probability of reception affects the timing of an ADS-B report. These factors are discussed in section 3-1-2.

3-1-2 Situation related properties

Besides the system related properties the situational related properties have an effect on the ADS-B system performance. The main factors to be considered are the range effect and

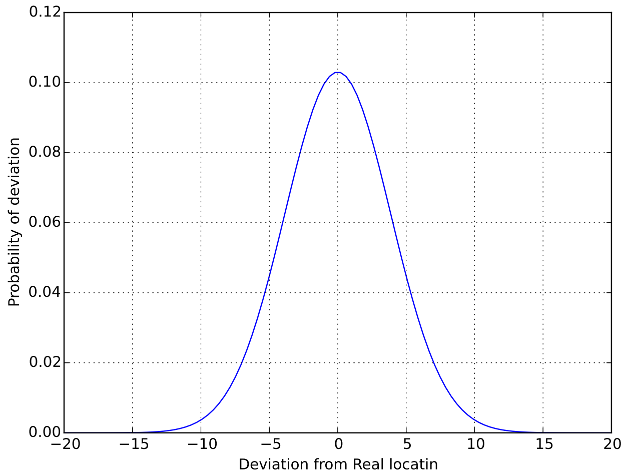

Figure 3-1: Normal distribution used for position modeling $\mu = 0$ and $\sigma = 15$.

interference effect, both influencing the reception probability of an ADS-B message. These two properties are discussed below.

Range effect
First of all the reception of an ADS-B message is limited by the range between the two aircraft. The reception probability with respect to the range of a transmitting and receiving aircraft can be modeled. This model is based on the specification stated in 1090 ES MOPS (RTCA Special Committee 186, 2002) and the model in (Barhydt et al., 2004; Chung & Staab, 2006) . In this derivation the following steps are taken.

1. **Step 1:** Free Space Path Loss (FSPL) per mile calculated
2. **Step 2:** Rewrite received power as function of range
3. **Step 3:** Reception probability exponential modeled with respect to received power
4. **Step 4:** Received power substituted by range
5. **Step 5:** Parameters for specific transmit power and minimum triggering level derived based on (RTCA Special Committee 186, 2002)

The following assumptions are made:

1. Omni-directional antenna used on transmitting and receiving aircraft
2. No multi-path effects
3. No shielding of ADS-B transmitter/receiver antenna

Table 3-1: Definition of variables

Name	**Symbol**	**Value**	**unit**
Speed of light	c	2.997910^8	m/s
Carrier frequency	f_{ES}	-	Hz
Extended Squitter (ES) frequency	f_{ES}	$1090 \cdot 10^6$	Hz
FSPL	FSPL	-	dBi
Minimum triggering level	S_{MTL}	-	dBm
Distance	d	-	m
Distance	r	-	NM
Transmit Power	Strans	-	dBm
Received Power	Srec	-	dBm
Received Power at 1 NM	Srec1NM	-	dBm
Received Power with 0 reception probability	Srec0	-	dBm
Reception probability	p	-	-

The variables and constants are defined in table 3-1.

The model is based on the link budget between a transmitting and receiving aircraft. The decrease in power level due to the FSPL is shown in equation eq. (3-2) and rewritten to dB.

Step 1:

$$FSPL = (\frac{4\pi df}{c})^2 \tag{3-2a}$$

$$FSPL(dB) = 10 \cdot log_{10}\big((\frac{4\pi df}{c})^2\big) \tag{3-2b}$$

$$FSPL(dB) = 20 \cdot log_{10}\big(\frac{4\pi df}{c}\big) \tag{3-2c}$$

The FSPL with respect to distance (in Nautical Mile (NM)) can be obtained from eq. (3-2), resulting in eq. (3-3).

$$FSPL_{1NM} = 20 \cdot log_{10}\frac{f4\pi r}{c} \tag{3-3a}$$

$$FSPL_{1NM} = 20 \cdot log_{10}\frac{1090 \cdot 10^6 \cdot 4 \cdot \pi \cdot 1852 \times r}{2.997910^8} \tag{3-3b}$$

$$FSPL_{1NM} = 95.55 + 20 \cdot log_{10}(r)[\frac{dB}{NM}] \tag{3-3c}$$

Using eq. (3-2) the received power (S_{rec}) for a specific transmit power (S_{trans}) can be obtained for a distance (d), shown in eq. (3-4).

The received power with the corresponding FSPL at a distance of 1 NM for the 1090 MHz frequency can now be calculated, shown in eq. (3-4). This results in an inverse quadratic relation of range with respect to received power; if the range increases by a factor of 2 the received power decreases with a factor of 4.

Step 2:

$$S_{rec} = S_{trans} - FSPL_{1NM} - 20 \times log(r) = S_{rec\_1NM} - 20 \times log(r) \tag{3-4a}$$

$$S_{rec} = S_{rec\_1NM} - 20 \times log(r) \tag{3-4b}$$

In eq. (3-4) ($S_{trans} - FSPL_{NM}$) is equal to the received power at a distance of 1 NM, called S_{rec_1NM} with a transmitted power of S_{trans}. Rewriting this equation, a relation between distance and received power can be obtained, shown in eq. (3-5).

$$r = 10^{\frac{-(S_{rec} - S_{rec\_1NM})}{20}} \tag{3-5a}$$

$$r = e^{-(S_{rec} - S_{rec\_1NM})(\frac{ln(10)}{20})} \tag{3-5b}$$

Step 3:

The detect and decode probability of an ADS-B report without interference is modeled as an exponential function of received signal power (S_{rec}). From (RTCA Special Committee 186, 2002) it can be obtained that there is a specific signal power (S_{rec0}) where the reception probability is 0 (due to background noise and sensor sensitivity), corresponding with a distance r_0. The variable k is introduced to scale the curve of the probability function resulting in eq. (3-6). This equation is later used for substitution.

$$p(S_{rec}) = 1 - e^{-k(S_{rec} - S_{rec0})(\frac{ln(10)}{20})}, S_{rec} \geq S_{rec0} \tag{3-6a}$$

$$p(S_{rec}) = 1 - 10^{-k\frac{(S_{rec} - S_{rec0})}{20}}, S_{rec} \geq S_{rec0} \tag{3-6b}$$

Substitute eq. (3-5) in eq. (3-6) where r_0 is the distance where the received power is S_0 resulting in a 0 reception probability, so r_0 is where S_{rec0} is reached. Now eq. (3-7) is obtained.

Step 4:

$$p(r) = 1 - (r \times e^{-(S_{rec\_1NM} - S_{rec0})(\frac{ln(10)}{20})})^k, r \geq r_0 \tag{3-7a}$$

$$p(r) = 1 - (r \times 10^{-\frac{(S_{rec\_1NM} - S_{rec0})}{20}})^k, r \geq r_0 \tag{3-7b}$$

$$p(r) = 1 - (\frac{r}{r_0})^k, r \geq r_0 \tag{3-7c}$$

Subsequently, eq. (3-7c) can be used to determine the no-interference reception probability as a function of received signal power.

Step 5:

The detect and decode probability without interference is modeled as a function of received signal power (S_{rec}). It is assumed there is a specific signal power (S_{rec0}) where the reception probability is 0 (due to background noise), corresponding with a distance r_0. The variable k is introduced to scale the curve of the probability equation. In (RTCA Special Committee 186, 2002) a minimum triggering level (S_{MTL}) of -90 dBm for Class A3 equipped commercial transport is defined with the following requirements

1. If link margin ($S_{rec} - S_{MTL}$) = 3dB the minimum reception probability should be $\geq$ 0.99.
2. If link margin ($S_{rec} - S_{MTL}$) = -3dB the minimum reception probability should be $\geq$ 0.15.

Using these values different reception probability curves can be generated for a range of transmit powers (P_{trans}). The values are substituted in eq. (3-7c) to determine the corresponding parameter k and r_0. From these equations figure fig. 3-2 can be generated, showing the relation between reception probability (y-axis) and distance between two aircraft (x-axis) for an ADS-B report. In this figure different output powers are plotted, indicated in the legend.

It should be noted this derivation is based on the system properties from (Barhydt et al., 2004; Chung & Staab, 2006). Several companies provide a much more sensitive ADS-B receiver, resulting in a lower Minimum Triggering Level (MTL) and thus better reception performance. Also different transmit powers are considered. Subsequently (RTCA Special Committee 186, 2002) is used to determine the relation between reception probability and signal power. However, this document is based on *Minimum* performance. Therefore it is expected the reception probabilities shown in fig. 3-2 are reached at a larger distance. The different settings used in the simulations are discussed in section 4-2-1.

Interference effect
To model the effect of interference on reception probability the Poisson distribution, shown in eq. (3-8) has been used. This probability distribution is generally used to calculate the number off occurrences during a specified time interval.

$$P[X = k] = (\lambda t)^k \frac{e^{-\lambda t}}{k!}, k = 0, 1, 2, ... \tag{3-8}$$

With the following variables:

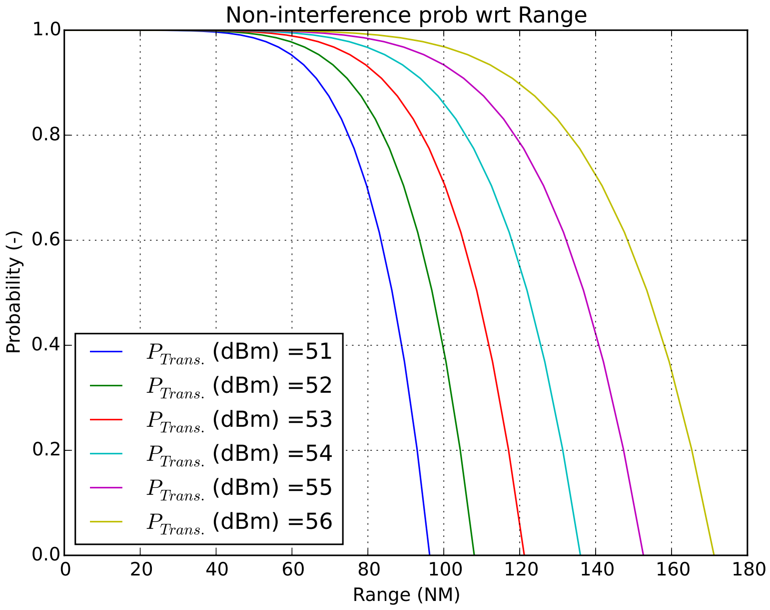

Figure 3-2: Non-interference reception probability with respect to distance for different transmitting powers.

- λ = Expected number of events occurring in 1 unit length of time.
- X = number of events occurring in an interval of length t.
- t = interval length.
- P = probability of X occurrences happening in an interval of length t.

An ADS-B extended squitter signal has the following properties, each with a message duration of $120\mu s$ seconds, (Eurocontrol, n.d.; Chung & Staab, 2006):

- Airborne positions squitter (2/sec)
- Surface position squitter (1/sec)
- Airborne velocity squitter (2/sec)
- Aircraft identification squitter (0.2/sec)
- Operational Status (0.4/sec)
- Target state (0.8/sec)

Only the Airborne position squitter, Airborne velocity squitter and Aircraft identification squiter are used by the Airborne Separation Assurance System (ASAS) system. However, also the other messages do cause interference on the 1090 MHz frequency and have to be taken into account when modeling the interference effect. This results in a total ADS-B transmission frequency of 6.4 Hz causing interference. Additional to the different type of ADS-B messages, an aircraft also transmits a Traffic Collision Avoidance System (TCAS) signal on the 1090 MHz frequency. A TCAS signal has a duration of $54\mu s$ and is transmitted with a frequency of 4 Hz. Using the characteristics stated above the probability of a message collision can be determined using the Poisson distribution from eq. (3-8). The following assumptions are made when modeling the interference:

1. Effect of distance of interfering aircraft is not been taken into account
2. No de-garbling is used
3. ADS-B message is modeled as 1 message, containing all the state information, instead of several different messages.
4. Aircraft at different distances have the same interference effect on degrading the reception probability.

λ can be calculated by the sum of the message update frequencies (F_{update}) multiplied by the number of aircraft within range(N_{ac}), shown in equation eq. (3-9b). This represents the expected number of instances (ADS-B messages received) in a specified time interval (1 s). The number of aircraft within range is the number of aircraft with a distance smaller than the maximum reception range, as discussed in the previous section.

$$\lambda = N_{ac} \cdot \sum F(Hz) = N_{ac} \cdot F \tag{3-9a}$$

$$\lambda = N_{ac} \cdot F_{update} \tag{3-9b}$$

Now assume a message is sent at t=0. The duration of an ADS-B message (τ) is $120\mu s$, equal to the time variable in eq. (3-8).

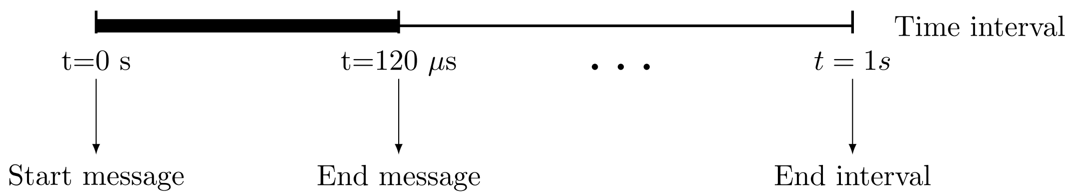

Figure 3-3: Schematic interference modeling overview.

To obtain the probability no other messages are sent in this time interval the X variable in eq. (3-8) is set equal to 0, resulting in eq. (3-10b). This is visualized in section 3-1-2. The same principle holds for a TCAS message, with a duration of $56\mu s$.

Since $x^0 = 1$ and $0! = 1$ the final equation to determine the probability of no message collision for N_{ac} within range and a message duration of τ seconds is shown in eq. (3-10b)

$$P[X = 0] = (\lambda t)^0 \frac{e^{-\lambda t}}{0!} = 1 \cdot \frac{e^{-N_{ac}(\cdot F_{ADS-B} \cdot \tau_{ADS-B} + F_{TCAS} \cdot \tau_{TCAS})}}{1} \tag{3-10a}$$

$$P[X=0] = e^{-N_{ac}(\cdot F_{ADS-B}\cdot\tau_{ADS-B}+F_{TCAS}\cdot\tau_{TCAS})} = e^{-N_{ac}\cdot(F_{ADS-B}\cdot 120\cdot 10^{-6}+F_{TCAS}\cdot 56\cdot 10^{-6})} \tag{3-10b}$$

This model is visualized in fig. 3-4, with a TCAS update frequency of 4 Hz and an ADS-B update frequency of 6.4 Hz and a corresponding message duration of 56 and 120 μs respectively.

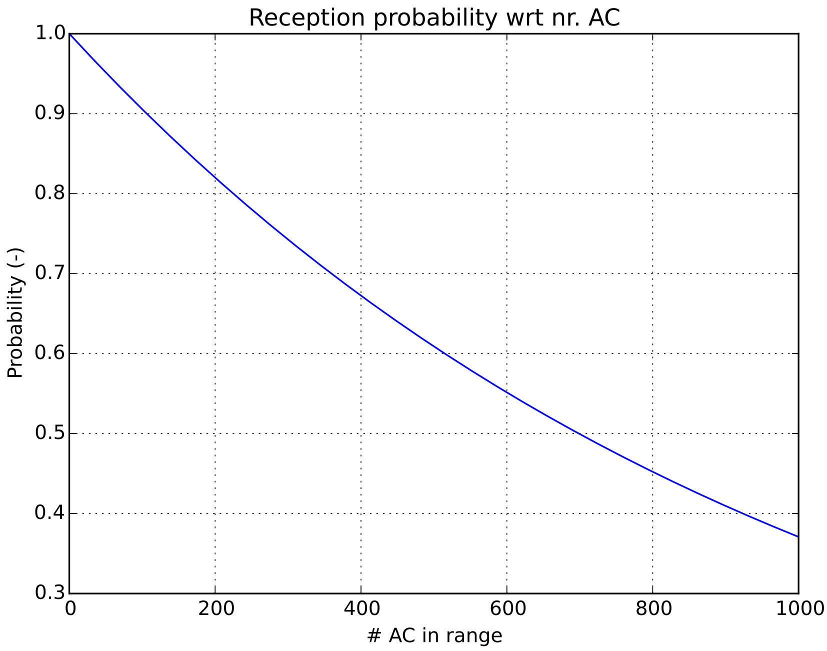

Figure 3-4: Interference probability as function of aircraft within range. Number of aircraft in range is defined as the number of aircraft within a distance from which the ADS-B message can still be received and decoded (see section 3-1-1).

It can be concluded that two major situation related factors affect the reception probability; the range between two aircraft and the number of surrounding aircraft. A model is generated, based on the link budget and Poisson distribution. The reception probability of an ADS-B message is modeled as a function of range in NM between two aircraft and the number of interfering aircraft as independent variables. The total reception probability is calculated using eq. (3-11). The total model is shown in fig. 3-5.

$$P_{total} = P_{range} \cdot P_{interference} \tag{3-11}$$

Now an ADS-B model is generated, the effect on CD&R should be assessed. Therefore the BlueSky software environment will be used, introduced in section 4-1. How the ADS-B model is implemented in the BlueSky simulator is discussed next in section 3-2.

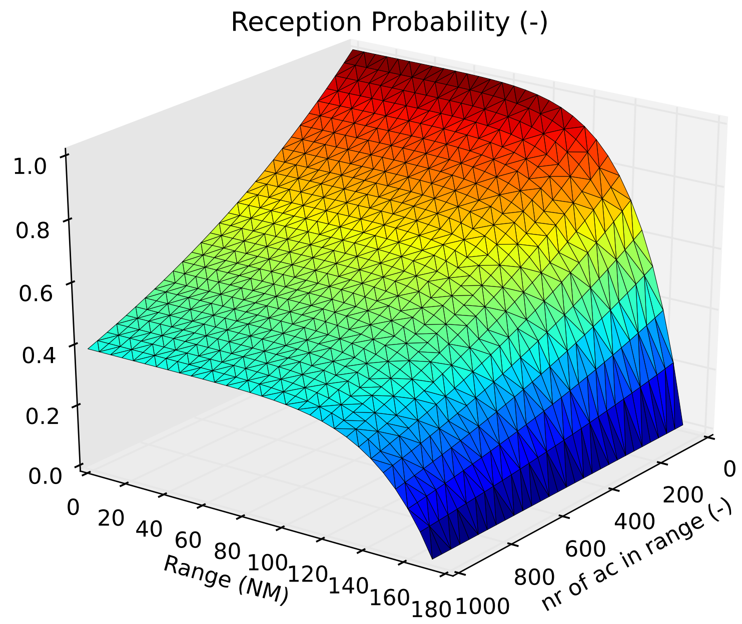

Figure 3-5: ADS-B message reception probability model. X-axis indicates range between two aircraft, Y-axis number of interfering aircraft. The corresponding reception probability is shown on the Z-axis.

3-2 Implementation in BlueSky simulator

The translation of the physical ADS-B model discussed in section 3-1 is translated in software. The general implementation is discussed in section 3-2-1. The implementation in the BlueSky ATM simulator is discussed in section 3-2-2.

3-2-1 General implementation ADS-B model

The different limitations and uncertainties affecting the ADS-B system performance are discussed in section 3-1. Two categories are defined; system related properties and situation related properties discussed in section 3-1-1 and section 3-1-2 respectively. The properties discussed in section 3-1 are translated into a software model. A schematic overview is shown in fig. 3-6.

Figure 3-6 shows a schematic overview of how to translate the ADS-B properties discussed in section 3-1 into software. Different loops are indicated; running on the simulation and the ASAS update rate to have optimal computational performance.

Each iteration starts at the top left, with $[N]$ number of aircraft. Each aircraft has a specific real state. This state is used to calculate a relative reception probability based on range

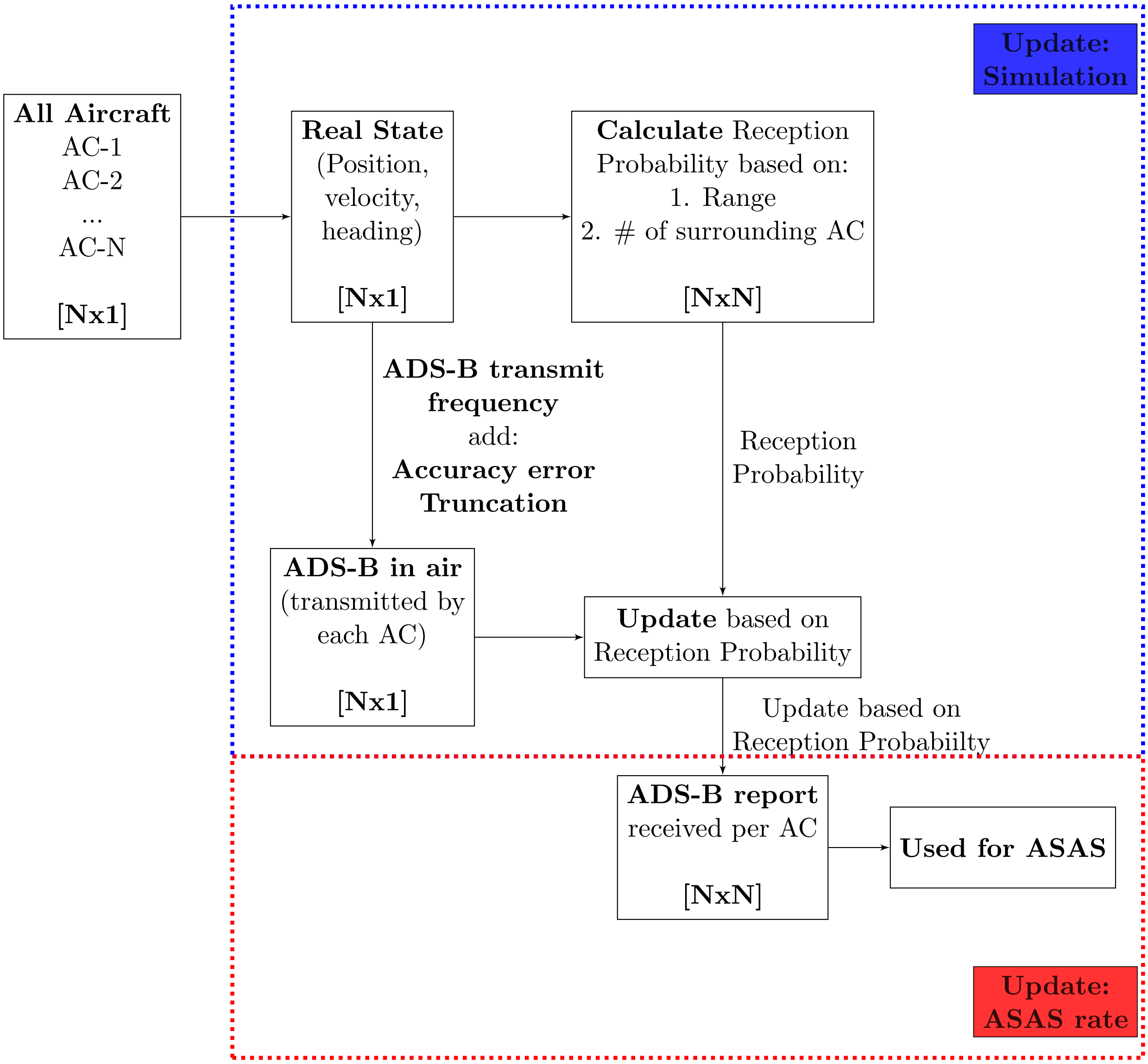

Figure 3-6: Schematic overview of how to implement ADS-B model in software for N aircraft. Start at left top and end at right bottom. Two different update rates are indicated with red and blue respectively; simulation update rate dt and ASAS update rate to optimize computation time. Size of the elements are indicated between brackets

between each aircraft and interference caused by the number of aircraft within range. This results in $[NxN]$ relative reception probabilities. It should be noted aircraft A has a different reception probability of an ADS-B report with respect to aircraft B than aircraft B for aircraft A due to the interference effect. When only taking the range effect in to account both aircraft have the same reception probability. However, the number of surrounding aircraft is different. Therefore the reception probability is not a triangular matrix but a matrix containing $[NxN]$ elements.
From the real state $[Nx1]$ "ADS-B messages in the air" are generated with a rate corresponding with the ADS-B transmit frequency. However, not the real location is transmitted, some

error due to truncation and state accuracy is added. In the update block it is decided, based on the reception probability, if each aircraft receives and update of another aircraft resulting in $[NxN]$ ADS-B messages. These messages are used in the ASAS system for CD&R. It should be noted different recommended update rates are shown in fig. 3-6; simulation update rate in blue and ASAS frequency in red. The reception probability changes based on range, which changes every simulation step. The received ADS-B message however is only required when an ASAS iteration is performed. Therefore this can run on a lower frequency. In case the ASAS frequency and simulation frequency are identical the same frequency should be used for the both systems.

3-2-2 Implementation ADS-B model in BlueSky simulator

A general overview of how the the ADS-B model can be translated to a simulation environment is discussed in section 3-2-1. For this research the BlueSky simulator is used. In this subsection it is discussed how the ADS-B model is implemented in the BlueSky simulator. The BlueSky ATM is discussed in more detail in section 4-1 and (J. Hoekstra, 2015). The following modules are modified and used to implement the ADS-B model.

- **traffic.py** Module where aircraft are created, deleted and processed. Aircraft kinematics are modeled as a point-mass. Systems such as autopilot and Flight Management System (FMS) are simulated. Also performance data of aircraft is included. In the traffic module the **traf** instance is created, containing (real) state information about each aircraft. This module is the source for state information to generate ADS-B reports and calculate ADS-B reception probabilities.
- **cstack.py** In the command stack the input in the command window is processed. Different type of commands are possible, ranging from generating traffic, define logging data to switching specific modules on or off. This module is adapted so the user is able to change different aspects of the ADS-B model and logging settings. Four type of ADS-B settings can be used; 1) perfect reception, 2)interference and range effect, 3) only range effect and 4) only interference effec.t
- **ASAS.py** In this module the CD&R part is performed. Conflicts are detected and, depending on the resolution setting, resolved. The input for this module has a $[Nx1]$ dimension. However, as explained in section 3-2 this needs to be converted to a $[NxN]$ input.
- **adsbmodel.py** The **adsbmodel.py** module is generated, containing the **ADSB-Model** class. This class contains ADS-B related parameters in different attributes, defined in the constructor. The class also inherits all attributes from the traffic class for easy access to calculate reception probabilities. Subsequently different ADS-B related methods are defined. This module is further discussed below.

The **ADS-B module** consists of different parts, discussed below.

Instances Different instances are created in the constructor of the **ADSBModel** class. In general three groups can be defined:

1. **ADS-B model settings**: Different parameters of the ADS-B model are defined, such as maximum range, message update rate, message duration and position accuracy in the ADS-B report. Also settings are implemented; the interference effect or range effect can be switched on or off. These variables can be changed through the BlueSky command window using the **cstack.py** module.
2. **ADS-B situation related parameters**: Variables for the different reception probabilities (range and interference) are stored. Also instances to store the different reception probabilites are created.
3. **ADS-B reports** A database is created to store the most up to date ADS-B message in the air and the most up to date ADS-B message received for each aircraft.

Methods Besides different variables also different methods are defined in the **ADSBModel** class. These are divided in three groups and discussed below.

1. **Reception probability calculation** Two main methods are created to determine the reception probability. The derivation of these functions is discussed in section 3-1-1. The first method calculates the reception probability of two aircraft with range as independent variable, based on eq. (3-7c). The second function is based on the Poisson distribution and calculates the reception probability due to interference, based on eq. (3-10b).
2. **Situation related parameters calculation** Different methods are defined to calculate situation related parameters. The two most important functions are the calculation for the relative distances between all aircraft and the relative number of surrounding aircraft for each aircraft. The obtained values are stored as a variable and used in functions to calculate the reception probability.
3. **ADS-B signal related methods** As discussed in section 3-1-1 different system related uncertainties are present in the ADS-B system. The three main factors are ADS-B report update rate, truncation and accuracy.
   (a) **Accuracy** The on-board navigation system uses GNSS to determine its location, so the position determination depends on the accuracy of the GNSS system. Subsequently states as altitude and heading are determined using on-board equipment. All these states have some level of accuracy. This inaccuracy is modeled as a normal distribution. It was found that for example GPS has an accuracy of 7.8 meter with an 95% confidence interval (DoD, 2016).
   (b) **Truncation** The truncation effect is discussed in section 3-1-1. The worst case scenario is assumed; a distance, caused by the truncation effect is added to the real location of the aircraft. It is found this is depending on the location on the earth and ranging from 12-17 m max. The truncation effect can, like the accuracy, be modeled as a normal distribution.
   (c) **Update rate** As discussed in 2-2 aircraft don't send their ADS-B report continuously, but they have a specific update rate. This is modeled by assigning each aircraft an initial random time variable. Subsequently a timer is started. If the specific ADS-B update rate for an aircraft has passed a new "in air" ADS-B signal is created and the $[Nx1]$ "in air" database is updated.

3-2-3 Verification situation related effects

The situation related reception probabilities are implemented in the BlueSky simulator. Two different verification scenarios are generated to check the implementation of the range-effect and the interference effect and check the implementation for inconsistencies such as errors and singularities . These scenarios and the results are discussed below. For both verification scenarios the ADS-B settings described by the optimistic model in section 4-2-1 are used, corresponding with a maximum range of 300 NM.

Range effect To verify the implementation of the range-effect as discussed in section 3-1-2 a simple air traffic scenario is generated. Two aircraft are generated with an initial distance of 300 NM shown in fig. 3-7. During this scenario the aircraft are flying towards each other, reducing the distance. The distance between the two aircraft and the range-related reception probability are logged.

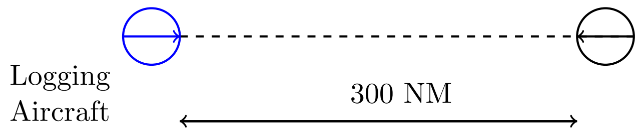

Figure 3-7: Range verification BlueSky Scenario. Two aircraft flying towards each other. For the blue aircraft the reception probability based on range and distance with respect to the other aircraft is logged.

A maximum reception range of 300 NM has been used, based on (Barhydt et al., 2004) for verification purposes. This results in an analytical reception model, shown in fig. 3-8. Subsequently reception probability based on range and distance between the two aircraft is logged in the air traffic scenario. These are also shown in fig. 3-8.

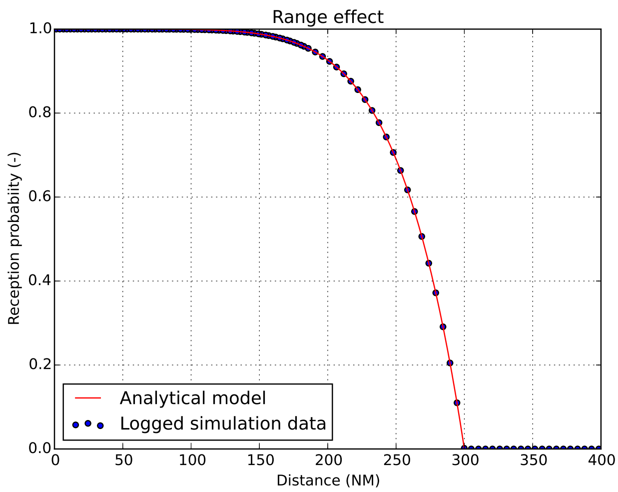

Figure 3-8: X-axis showing distance between two aircraft and y-axis reception probability due to range. Red solid line is the analytical model, discussed in section 3-1-2. The blue dots are logged simulation data using the BlueSky simulator.

From the comparison between the analytical model and the logged simulation data it can be obtained the range effect probability is correctly implemented in the BlueSky ATM simulator.

Interference effect Subsequently the interference effect, as discussed in section 3-1-2, is verified. An air traffic scenario of one aircraft, flying towards a string of 600 aircraft with a distance of 1 NM between each aircraft is generated. The initial distance between the string and single aircraft is 300 NM This scenario ensures a wide range of number of interfering aircraft,ranging from 0 to 600 aircraft within interferring range. An overview of the scenario is shown in fig. 3-9.

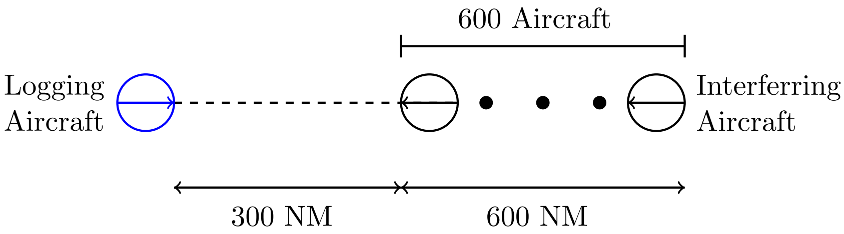

Figure 3-9: Interference verification BlueSky Scenario. One aircraft (blue) flying towards a string of 600 aircraft (black) to verify the Interference reception probability.Two aircraft flying towards each other. For the blue aircraft the reception probability based on interference and number of interferring aircraft within range (300NM) is logged.

The interference-related reception probability and number of surrounding aircraft (within 300 NM) are logged. The data is shown in fig. 3-10.

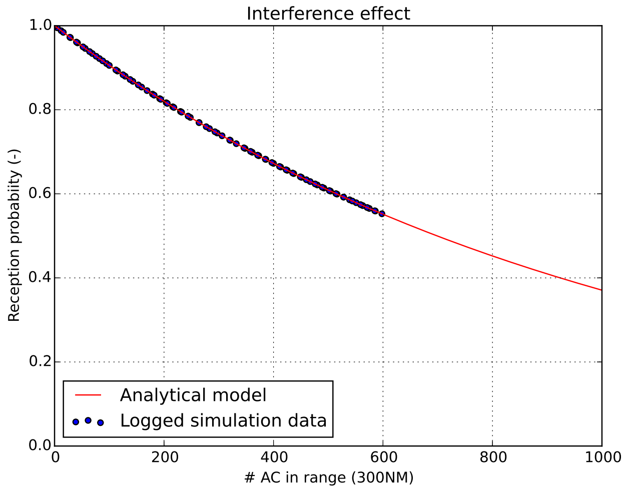

Figure 3-10: X-axis showing number of aircraft in range (300 NM) and y-axis reception probability due to interference. Red solid line is the analytical model, discussed in section 3-1-2. The blue dots are logged simulation data using the BlueSky simulator.

From the comparison between the analytical model and the logged simulation data it can be obtained the interference effect probability is correctly implemented in the BlueSky ATM simulator.

Chapter 4

Experiment design

To assess the effect of ADS-B properties on CD&R performance an experiment will be designed. The effects are investigated by three-dimensional flight simulations through an airspace. Conflicts are tried to be resolved using state information obtained from the modelled ADS-B system. First the experiment platform, the BlueSky open ATM simulator, is discussed in section 4-1. Subsequently the variable selection is discussed in section 4-2 by elaborating on the independent variables in section 4-2-1 and the dependent variables in section 4-2-2. The experiment area is discussed in section 4-3. This chapter is concluded with an hypothesis in section 4-6.

4-1 BlueSky open air traffic simulator

An air traffic simulation environment has been developed at the Aerospace Engineering faculty of Delft Technical University, called BlueSky. The goal of BlueSky is to provide everybody who wants to visualize, analyze or simulate air traffic with a tool to do so without any restrictions, licenses or limitations. It can be copied, modified, cited, etc. without any limitations (J. Hoekstra, 2015).The BlueSky simulator is written in the Python(2.xx) programming language and uses pygame for visualization. An overview is shown in fig. A-1.

The BlueSky simulation environment has many build-in features like airborne separation assurance, different conflict detection and resolution methods, data-log options and much more (J. Hoekstra, 2015). Due to it's open-source character it is possible to implement new features, such as an ADS-B reception model.
For creating an aircraft and its flight plan, the parameters shown in table 4-1 need to be defined.

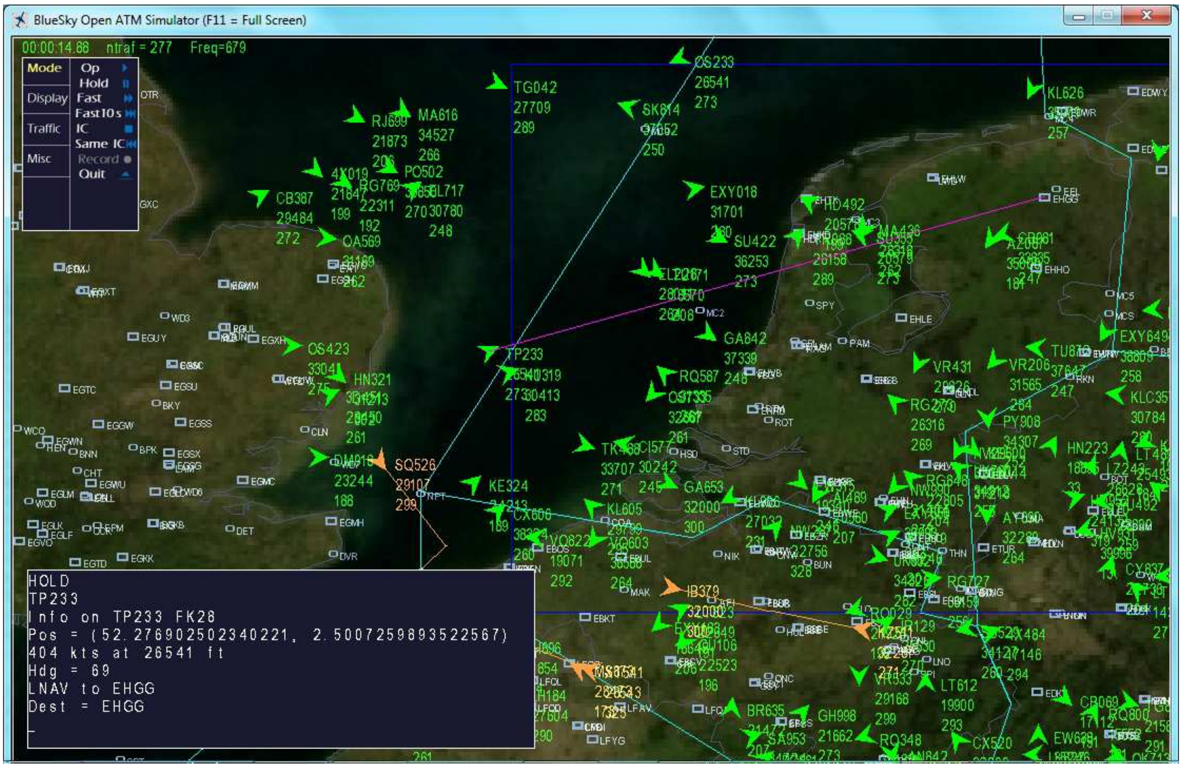

Figure 4-1: BlueSky Simulator environment (J. Hoekstra, 2015)

Table 4-1: BlueSky Aircraft initialization variables.

Parameter	**Unit**
Aircraft ID	[string]
Initialization position	[lat,long]
Heading	[deg]
Altitude	[feet]
True Airspeed	[kts]

4-2 Variable selection

In this section the variable selection is discussed. First the independent variables are discussed in section 4-2-1. Three main categories; Conflict Detection (CD) method, air traffic density and ADS-B settings are identified. Subsequently the dependent variables are discussed in section 4-2-2.

4-2-1 Independent variables

For the experiment different independent variables are selected. These can be divided in three categories, each discussed in the following paragraphs.

CD&R method

The first dependent variable is the CD method. In section 2-1-1 different CD methods are discussed. Subsequently different Conflict Resolution (CR) methods are introduced in section 2-1-2, being the MVP and swarming method. In (M. Eby & Kelly, 1999; J. Hoekstra et al., 2002) and (Aerial et al., 2003) it is discussed both these methods are suitable techniques that can be incorporated in a future ASAS system. These methods are quantitatively assessed in (Maas, 2015), where it was found the MVP method performance was better than the swarming methods. Some error is introduced to assess the performance of the CD methods, but not a realistic ADS-B model has been implemented. Since the general conclusion is that these methods are suitable for airborne separation assurance, these methods are selected.

From the literature review it is found in (J.M. Hoekstra, 1998) that using a look-ahead time of five minutes the level of intent hardly improves the quality of predictions, compared for en-route flight.In (Kuchar & Yang, 2000) it is found the nominal projection method results in a small error rate for en-route flight, since aircraft are mainly flying in a straight line. Since en-route flight is identified as the most suitable option for applying Free Flight using ASAS, nominal projection using a look-ahead time is selected as most suitableCD method. Therefore a single CR method has been used and is not a variable. Since the CD is closely related to CR, it is discussed in this section.

ADS-B performance

The different ADS-B limitations and uncertainties are discussed in detail in chapter 3. A general outline of the ADS-B system properties are stated in (Eurocontrol, n.d.). Several researchers have modelled the situation related effect in (Barhydt et al., 2004; Chung & Staab, 2006), based on the **Minimum** Operation Performance Specifications (RTCA Special Committee 186, 2002). It should be noted a worst-case scenario viewpoint is considered and therefore not representing a realistic model. For example; in (RTCA Special Committee 186, 2002) a maximum reception range of 90 NM is defined while during experiments a range of 200+ NM has been reached.
It is decided four types of ADS-B performance models are created, based on (Barhydt et al., 2004; Chung & Staab, 2006; Eurocontrol, n.d.) and:

1. Pessimistic model, based on (RTCA Special Committee 186, 2002).
2. Realistic model, based on field experiments.
3. Optimistic model.
4. Perfect model.

The ADS-B state accuracy is based on the analysis in section 3-1-1. In general the message duration of an ADS-B message is fixed, however to change the behavior of reception probability due to interference a different message duration is selected. The different model variables are shown in table 4-2

It should be noted different ADS-B and TCAS message durations are used, influencing the interference reception probability. In reality this message duration is fixed, following the values for the realistic model ($120\mu s$). However, de-garbling algorithms can be used to differentiate

Table 4-2: Different ADS-B model parameter settings

Parameter/Model	Pessimistic	Realistic	Optimistic	Perfect	Unit
Maximum reception range	90	200	300	∞	NM
ADS-B Message duration	240	120	80	0	μs
ADS-B Update rate	3	1	0.5	∞	Hz
TCAS Message duration	112	56	28	0	μs
Position standard deviation	150	15	1.5	0	m
Heading standard deviation	5	3	1	0	deg
Speed standard deviation	10	5	3	0	knts

between two overlapping messages. On the other hand; messages can cause additional interference due to multipath effects. Additionally aircraft out of interference range can also still have a (minor) interference effect. Therefore half and double the message duration is used for the pessimistic and optimistic scenario respectively.

As discussed in chapter 3 the state information in the ADS-B report do have some inaccuracies. The three states used for CD&R are position, heading and velocity. It was found in section 3-1-1 that due to sensor inaccuracies and using the Haversine equation the position can be modeled as a Gaussian distribution with a standard deviation (σ) of 15 meters. For the pessimistic and optimistic model a factor of 10 is applied. It is assumed also the speed and heading sensor-accuracy can be modeled according to a Gaussian distribution with the corresponding standard deviation shown in table 4-2 and the real value as mean(μ).

Traffic density
Increasing traffic density has a negative effect on the CD&R performance. First of all the interference effect as discussed in section 3-1-1 degrades the reception probability of an ADS-B message. Additionally a larger traffic density results in more complex conflict situations. To study the effect of traffic density, different densities are used in the simulation. In (Aviation, 2008) two capacity limits are defined for Schiphol airport during the summer, an arrival peak and a departure peak. The flights are spread evenly over 20 minute blocks. The values are shown in table 4-3. It gives a good indication of the amount Instrument Flight Rules (IFR) flights in the area around Schiphol as independent variable.

Table 4-3: Capacity limit for Schiphol airport, obtained form (Aviation, 2008).

Parameter/Model	Number of IFR flights per hour
Movements Arrival peak	106
Of which arrivals	68
Of which departures	38
Movements Departure peak	110
Of which arrivals	36
Of which departures	74

In fig. 1-1 the predicted growth of air traffic is shown. From this figure it can be seen an increase ranging between 10 and 20 % is predicted in 2022, depending on the economic growth. However, to observe a relation of air traffic density with CD&R performance doubling and halve of the number of IFR flights is chosen.

Table 4-4: Air traffic movements per hour. Independet variables in simulation environment, based on fig. 1-1 and table 4-3

Scenario	IFR movements	% difference
Half	50	50%
Current	$+-100$	0
Double	200	+100 %

As discussed above two different CD&R methods are discussed; the MVP and Swarm method. As a benchmark, also the same scenarios are assessed without applying CD&R as benchmark, resulting in a total of **three** variables. Subsequently **3** different ADS-B models are evaluated; a pessimistic, realistic, and perfect model. Finally **three** different air traffic densities are tested; based on current air traffic. Therefore it can be concluded in total **36** different scenarios are assessed. Each scenario will be repeated 5 times to obtain a consistent result. The experiment design is further discussed in section 4-3.

4-2-2 Dependent variables

As discussed in section 1-2 the performance of a CD&R method can be assessed with respect to different metrics; safety ,efficiency and stability. Metrics related to these two categories are selected as dependent variables and discussed below.

Safety
The safety aspect performance can be measured in different ways. First of all, the number of LOS can be logged. The definition of LOS is discussed in section 2-1-1. Subsequently the duration of each LOS is determined. Finally also the severity of the LOS can be determined.

Besides the number of LOS the severity can be identified. In (Delahaye et al., n.d.) a metric has been developed, based on the path flown by an intruding aircraft through the protected zone of another aircraft, shown infig. 4-2.

In this figure a path traveled of an intruding aircraft is shown. The $LOS_{severity}$ can be calculated using eq. (4-1) (Delahaye et al., n.d.).

$$LOS_{severity} = max[min(I_H, I_V)] \tag{4-1}$$

In fig. 4-2 for example, this results at a $LOS_{severity}$ value of around 0.8, reached on the most right point on the x-axis. Using the $LOS_{severity}$ a trend might be observed, showing a relation between CD&R method or ADS-B model and $LOS_{severity}$ location.

Efficiency
Besides the safety also the efficiency of a CD&R method should analyzed. First of all the distance traveled for each aircraft is logged. Also the amount of thrust is logged. Using this date the work-done, shown in eq. (4-2), can be calculated post-simulation and compared for different experiment settings. In this formula t=0 and t=end is the time when the aircraft

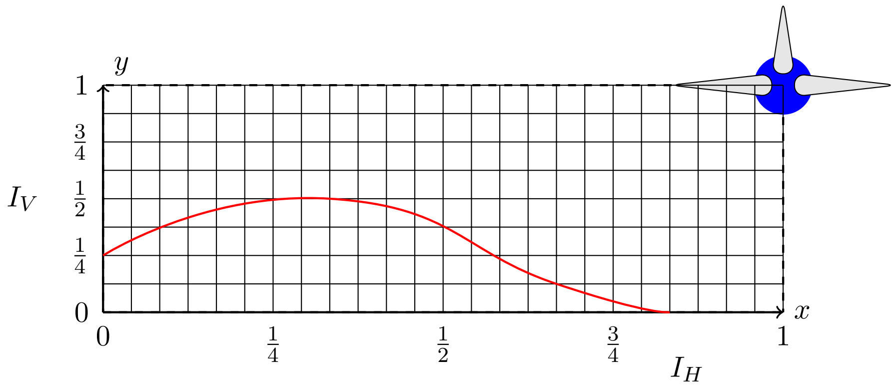

Figure 4-2: Figure showing path of intruding aircraft through IPZ of other aircraft (IPZ). Back view with $\frac{1}{4}^{th}$ of the IPZ shown. Vertical and horizontal $LOS_{severity}$ component indicated by I_V and I_H respectively. X and Y axes show the normalized IPZ dimensions.

enters and leaves the test volume respectively. Thrust is the trust and s the distance traveled. When integrating these variables over the total flight path inside the Test Volume the total work done is calculated.

$$W = \int_{s(t=0)}^{s(t=end)} T \, \mathrm{d}s. \tag{4-2}$$

Stability
As a final metric the airspace stability is tested, using the Domino Effect Parameter (DEP) (Krozel, Peters, Bilimoria, Lee, & Mitchell, 2001). Resolving a conflict using CD&R might result in creating one or multiple different conflicts. Conflicts can be divided in two groups; S_1 and S_3. S_1 represents the number of conflicts with resolution on and S_3 the number of conflicts with resolution. These groups have a set of common conflicts (shown in red), conflicts that occurred in both situations S_2, and a separate part. The separate part of S_3 is the number of conflicts caused by resolution maneuvers, creating a de-stabilizing effect. An overview is shown in fig. 4-3.

The DEP can be calculated using eq. (4-3).

$$DEP = \frac{S_3 - S_1}{S_1} = \frac{S_3}{S_1} - 1 \tag{4-3}$$

In this equation S_3 is the number of conflicts when CD&R is on and S_1 when CD&R is off. A negative implies a de-stabilizing effect using CD&R and a positive value a stabilizing effect of using CD&R.

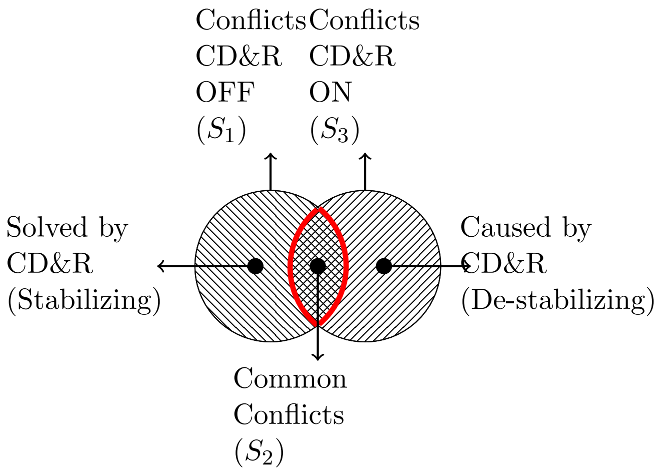

Figure 4-3: Domino Effect Parameter.

All dependent variables are shown in table 4-5. To compare different air traffic densities the values shown in table table 4-5 can be normalized or averaged to compare different traffic rate scenarios.

Table 4-5: Dependent variables

Type	Variable	Calculation	Unit
Safety	Normalized number of LOS	$\frac{\sum(LOS)}{Ntotal}$	$[\frac{LOS}{AC}]$
Safety	Normalized LOS duration	$\frac{\sum Time_{LOS}}{NLOS}$	$[\frac{s}{AC}]$
Safety	$LOS_{severity}$	eq. (4-1)	[-]
Efficiency	Work done	eq. (4-2)	[J]
Stability	DEP	eq. (4-3)	[-]

4-3 Experiment Area

With the variables defined in section 4-2, a scenario can be generated. First the experiment requirements and the limitations are stated in section 4-3-1. The shape and dimensions of the experiment area is discussed in section 4-3-2. The general shaping and flight levels are discussed in this subsection.

4-3-1 Experiment Area Requirements

To assess the performance of a CD&R algorithm, an experiment area needs to be defined. The experiment area needs to fulfill several requirements and is limited due to several factors.

Number of aircraft in simulation
The ADS-B reception probability calculations are computational expensive and grow quadratically with the number of aircraft in the simulation (N); for each aircraft a relative reception probability is calculated with each other aircraft resulting in N^2 calculations. Results from simulations shown in table 4-6 show the duration of all ADS-B calculations with respect to the number of aircraft, which confirms the quadratic relation of number of calculations (i.e. time) with number of aircraft in the simulation.

Table 4-6: Duration of ADS-B calculation loop in BlueSky ATM simulator for different number of aircraft.

# of AC in simulation	ADS-B loop duration (s)
150	0.075
300	0.3
600	1.15

Since it is desired to run the simulation at real-time (or a little slower) the instantaneous number of aircraft in the simulation should be ≤ 600 aircraft. It should be noted aircraft can be deleted an created to maintain a certain traffic density.

Experiment Area
A discussed above the number of aircraft in the simulation is limited. In section 4-2-1 typical IFR movement in the area around Schiphol were discussed. Therefore an experiment area is defined. Difficulties occur at the edges of the experiment area. At the edges of the experiment area aircraft are affected less by the interference effect than aircraft located at the center of the experiment area. Aircraft entering and leaving the experiment area, while keeping the number of aircraft in the simulation relatively low, can be simulated by creating aircraft on the edges of the area an deleting aircraft when leaving the area. It should be made sure aircraft are not created and cause an immediate conflict with an already existing aircraft. Subsequently conflicts can be resolved by steering an aircraft outside the experiment area, resulting in deleting the aircraft. These factors should be considered in the experiment design.

Horizontal and Vertical plane
To study the effect in three dimensions several flight levels need to be implemented. When creating the aircraft in 1 vertical plane only horizontal resolution is assessed. Therefore aircraft need to be created on multiple flight levels, and some portion of the aircraft need to have a vertical velocity; moving from one flight level to another.

4-3-2 Experiment Area Definition

Due to the limitations of number aircraft a finite experiment area has to be used. Different type of scenarios are considered; an circular area and a square experiment area. The smaller the experiment area the larger the effect of the corners in case of a square experiment area. Therefore a circular (which has an equal shape) experiment area is selected as used in literature (Bilimoria et al., 2000; M. S. Eby, 1994; Maas, 2015). The main advantage of using an circular experiment area over an square experiment area is the equal shape; no corners exist which can cause a quick, artificial deleting of aircraft. Since also the 3D effect needs to be taken into account, a cylindrical shaped test volume is selected, shown in fig. 4-4.

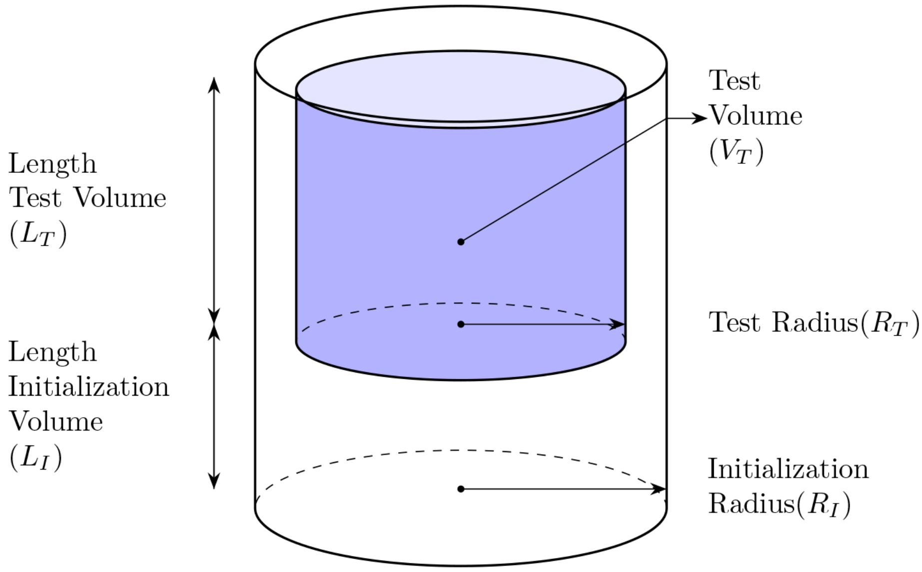

Figure 4-4: Isometric overview of the research field.

Two volumes can be seen; a Test Volume(V_T) surrounded by an Initialization Volume(V_I). Aircraft are generated on the edges of the initialization volume with a specific altitude, airspeed and heading crossing the Test Volume. The aircraft are not immediately logged; since by creating an aircraft an instant conflict can be created, skewing the results. Only aircraft inside the Test Volume are logged. It should be noted this has an additional advantage: Aircraft outside the Test Volume still cause interference. Therefore aircraft at the boundaries of the Test Volume don't experience an (artificially) lower interference effect but a realistic interference level when inside the Test Volume.

The aircraft are logged for performance indicators, discussed in table table 4-5, when entering the Test Volume. Subsequently the aircraft are deleted when crossing the Initialization Volume again. The distance between the edges of the Test Volume and Initialization Volume should be at least as large as the time traveled by an aircraft during the look-ahead time. ($R_I - R_T \geq S_{Look-Ahead}$). This case no artificial conflicts are created. Subsequently the interference effects of aircraft that just entered the Test Volume should be realistic. This can be achieved by making sure enough aircraft are initialized (but still outisde the Test Volume) causing interference for the aircraft at the edges of the Test Volume. Finally the effect of climbing and descending aircraft should be included. Therefore three different flight levels are defined, as shown in figure fig. 4-5.

In fig. 4-5 it can be seen three different flight levels are created. In total three types of aircraft can be created, schematically indicated by black, red and green arrows. Black aircraft are en-route aircraft keeping the same altitude and start at a specific flight level. Subsequently ascending and descending aircraft are created; indicated by a red and green arrow respectively. These aircraft start at a flight level and will, at a specific time, travel to another flight level.

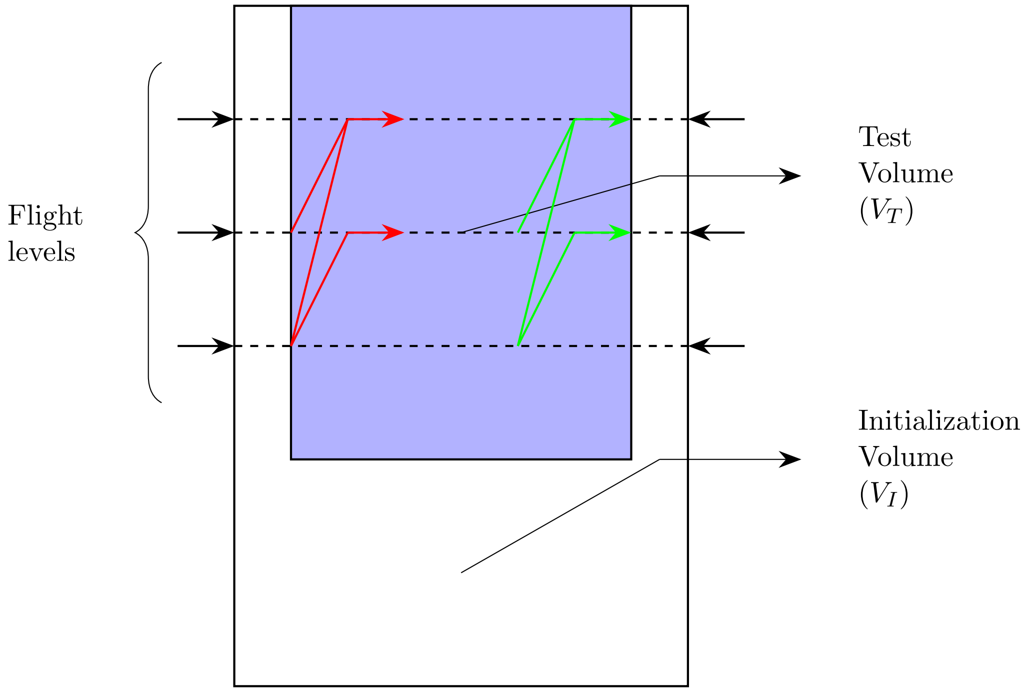

Figure 4-5: Experiment Area side-view

By having three flight levels all type of maneuvers will be tested; horizontal conflicts and vertical conflicts.

4-4 Experiment area dimensions

In this section the dimensions of the experiment area are discussed. An overview of the dimensions is shown in table table 4-7. Typical airspeed for en-route air traffic is in the order of 150 m/s, as discussed further in section 4-5. To have proper measurements it is expected an aircraft should be on average in the experiment volume 30 minutes. However, aircraft will also have to perform resolutions and some will have to climb or descend to a different flight level, estimated to take around 5 minutes. Therefore a crossing time of 25 minutes is used as basis for the experiment dimensions. This results in an experiment area diameter of 225 km. As discussed in section 4-2, the minimum time the aircraft should be in the initialization region should be equal to the look-ahead time of 5 minutes. As discussed in section 4-5, the maximum airspeed in the simulation will be 200 m/s. Therefore an minimum distance between Test Volume and Initialization Volume is 60 km. The variables discussed above results in an Test Radius of 112.5 km and an Initialization Radius of 132.5 km.

To assess the behavior with respect to intruding aircraft in the vertical dimension, three flight levels were defined. Since the vertical separation minimum is 1000 feet, these flight levels should be at least 2000 feet apart. An extra margin of 1000 feet is selected, resulting in a distance of 3000 feet between the flight levels. The lower airspace in the area around Schiphol, controlled by Lucht Verkeersleiding Nederland (LVNL), ranges from FL095 to

FL245. Therefore in this experiment the intermediate, FL170 is chosen, corresponding with an altitude of 17000 feet, or 5 km.

Table 4-7: Experiment dimensions.

Name	Symbol	Value	unit
Test Radius	R_T	112.5	[km]
Initialization Radius	R_I	132.5	[km]
Flight Level interval	-	3000	[ft]
Number of Flight Levels	-	3	[-]
Altitude middle Flight Level	-	50000	[ft]

4-5 Experiment scenario design

An experiment area is defined, containing of an Test Volume and a Initialization Volume. Aircraft are created at the edge of the Initialization Volume with an uniform distribution. In this section the actual aircraft scenario variables are explained. In section 4-2-1 different IFR movements per hour scenarios are defined. To create a scenario aircraft can be created at random location, with an uniform distribution, on the edge of the Initialization Volume. The aircraft will have a heading directing at the other half side of the Initialization Volume, shown in fig. 4-6.

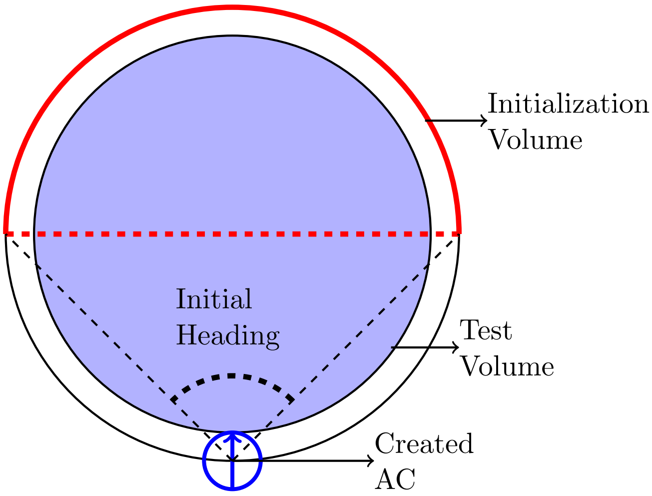

Figure 4-6: Experiment Area side-view top view. Showing initial heading range of created aircraft.

Besides the heading and location, the airspeed (TAS) needs to be defined. The aircraft a assigned a random airspeed based on an uniform distribution between 100 and 200 $\frac{m}{s}$. Three different flight levels were defined, over which the aircraft are also uniformly distributed. As discussed in section 4-3, also a mix of climbing and descending aircraft is required to assess the 3 dimensional aspect. Therefore also an uniform distribution of aircraft moving to the other flight level or staying at their current flight level is used. The location where the aircraft will start its ascend or descend is chosen randomly. The climb or descend rate follows a normal distribution with a mean of 1500 $\frac{ft}{min}$ and a standard deviation of 10 $\frac{ft}{min}$. The variables are summarized in table table 4-8.

As discussed in section 4-2 a specific aircraft rate ($\frac{ac}{hr}$) is assessed. It was assumed it takes on average 25 minutes to enter and exit the Test Volume. Since a constant traffic rate is assumed, an pre-logging phase is required to have the specific amount of aircraft in the simulation. Subsequently aircraft generated during the test-period need to be able to finish their flight. During this phase aircraft still need to be generated to sustain the required number of aircraft in the simulation, called the run-out phase. After the experiment the logged data is analyzed. This is schematically shown in figure fig. 4-7.

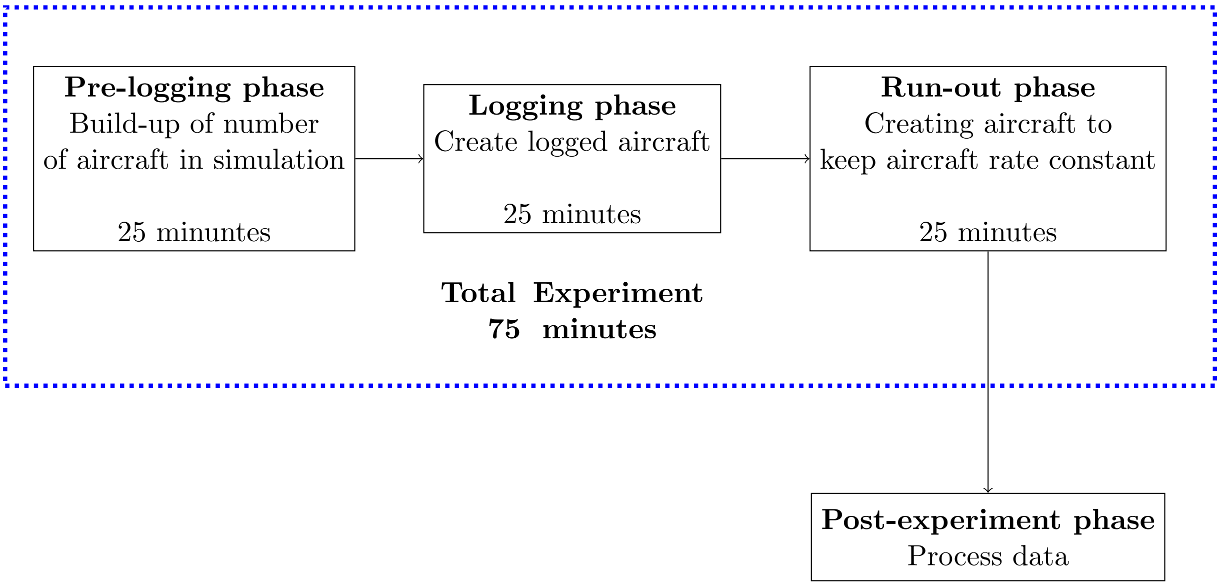

Figure 4-7: Schematic Phases experiment.

Table 4-8: Experiment design, aircraft initialization variables.

Parameter	Distribution	Range	Unit
Location	Uniform	0-360 degrees on initialization boundary	$[^0]$
True Air Speed	Uniform	100-200	$[\frac{m}{s}]$
Heading	Uniform	-45 to +45 wrt straight crossing	$[^0]$
Flight level	Uniform	first, second or third FL	$[-]$
Vertical movement	Uniform	to first, second or third FL	$[-]$
Vertical rate	Normal	$\mu = 150, \sigma = 1$	$\frac{ft}{min}$

These variables should result in an experiment with a good mix of airspeed, conflict angles, horizontal conflicts and spread of conflicts through the experiment area. However, this should be verified later. This covers all the initialization variables of a newly created aircraft in the BlueSky simulator, as discussed in section 4-1.

4-6 Hypothesis

In this section a hypothesis is stated with, reflecting back to some of the research questions and the research goal:

Study and analyze the effect of ADS-B limitations and uncertainties on the performance of different CD&R algorithms by implementing an ADS-B model and perform simulations in the BlueSky simulator

Different type of ADS-B limitations and uncertainties are identified, which can be grouped in situation related and system related properties. These properties affect the quality of the ADS-B signal in accuracy and reception probability. It is expected an decrease in ADS-B accuracy or a decrease in reception probability will result in more conflicts. However, the severity of decrease in CD&R with respect to a degrading quality of ADS-B system performance is difficult to predict. This will follow from experiments logging the metrics discussed in table 4-5. It is expected the reception probability and update rate have the largest effect on ADS-B performance; a not received signal results in an offset from the real location in the order of several hundreds of meters, while the accuracy of the GNSS is in the order of dozens of meters (For example: an Boeing 747 has a cruise speed of $\pm 200\frac{m}{s}$, resulting in a large error and increasing with time when using out-dated information).

Similarly an increase in traffic density will likely degrade the CD&R performance in two ways. First of all an increase in traffic density will result in an increase in interference effect; decreasing the reception probability of surrounding aircraft. Secondly a larger air traffic density will result in more complex air traffic scenarios and likely result in an increase in conflicts.

The working principles of the CD&R algorithms(swarming and MVP) differentiates and is complex. Therefore it is difficult to make a hypothesis with respect to the performance of both CD&R methods with respect to ADS-B performance. During experiments the performance of both CD&R methods with similar ADS-B model performance will be evaluated. However, it is expected that the effect of ADS-B limitations will be larger on the swarming method, since this method requires close coordination between aircraft.

Chapter 5

Conclusion

It is observed two recent and ongoing developments require a modernization of the airspace structure and management. First of all; due to current and predicted future growth of air traffic, a novel ATC system is required to fulfill the (future) capacity demands. A key-element for free flight and (autonomous) UAV integration in the current airspace system is ASAS; a shift from a ground-based controller to an airborne controller. An important aspect in the ASAS system is Conflict Detection and Resolution, CD&R. Different type of CD&R methods exist and can be used for ASAS. In this research the MVP and swarming method are researched. It should be noted that for all CD&R method state information of surrounding aircraft is required. An enabling technology to obtain airborne state information is the ADS-B system, where each aircraft transmits its state information in an omni-directional manner to surrounding aircraft. However; the ADS-B system is subjected to realities and uncertainties. Al tough some research is done to the ADS-B realities and uncertainties and CD&R algorithms, **the effects** of these ADS-B system properties on CD&R methods has not been investigated. This research aims to combine and relate these two research fields. Therefore the following research objective is stated:

Study and analyze the effect of ADS-B realities and uncertainties on the performance of different CD&R algorithms by implementing an ADS-B model and perform simulations in the BlueSky simulator.

To answer this research objective several research questions are stated. First of all the different ADS-B realities and uncertainties are identified. These can be divided in two main categories; system related properties and situation related properties. The situation related properties affect the reception probability of an ADS-B message by an aircraft, caused by a decreasing power level with distance and interference caused by surrounding aircraft. The system related parameters result in a decrease in accuracy of state information. The situation related parameters can be modeled using the FSPL and Poisson distribution. The system related parameters can be modeled according to a Gaussian distribution. And ADS-B model has been implemented and tested in the BlueSky simulator. An experiment design has been performed to assess the effect of the ADS-B system properties on the two CD&R methods (MVP and swarming). The performance of the CD&R methods can be measured according to efficiency, safety and airspace stability.

It is expected the performance of both CD&R methods degrades with decreasing ADS-B message level quality (i.e.: lower reception probability and accuracy). The increase in traffic density results in a generally lower reception probability; likely to also decrease the CD&R performance. However, it is not possible to predict which CD&R methods is more sensitive to the effect of ADS-B properties. Also the severity of the decrease in ADS-B performance needs to be tested using stability, efficiency and safety metrics.

The research performed in this thesis can provide a basement for further research in the application of free flight using CD&R methods and the ADS-B system. This research can help solving the problem of air traffic capacity demand and the integration of (autonomous) UAV in the current airspace system while maintaining, or even improving, safety and efficiency.

Appendix A

Project Plan

The aim of the project related to this project proposal and plan is to identify the different factors influencing the quality of the ADS-B signal and study its effect of the CD&R performance. Therefore the characteristics of the ADS-B data link are studied. Subsequently different characteristics of CD&R algorithms and their applicability to the unmanaged airspace concept are assessed. It is found that the ADS-B data performance is degraded by interference of surrounding aircraft and range between two aircraft. Elaborate research studying the effect of ADS-B effects on CD&R performance has not been found. This research will fill this gap by evaluating the effect of ADS-B realities on different CD&R methods by modeling the ADS-B data link and simulate several unmanaged airspace scenarios.

A-1 Introduction

To process the increasing demand of air traffic in a safe and economic way a modernization of the current air traffic management system is required (SESAR Consortium, 2012; Francisco & Louisville, 2014). The current system consists of specified air routes, so called 'highways-in-the-sky', along which air traffic is directed by air traffic controllers. The pilot must follow instructions from the Air Traffic Controller (ATCo) and ask permission for route changes. The ATCo is therefore responsible of maintaining a safe distance between aircraft and sustain an efficient flow of traffic.

However, the increase in air traffic (Ballin, Wing, Hughes, & Conway, 1999; Valenti Clari et al., 2000) and developments in UAV technology require a new approach of air traffic control (Conde, Alejo, Cobano, Viguria, & Ollero, 2012). Current development in ATM strategies show a responsibility shift from the ground-based ATCo to the pilot in the cockpit to maintain a safe separation between aircraft (Ellerbroek, 2013; Barhydt et al., 2004). The aircrew can be guided in solving conflicts by using Conflict Detection and

Resolution (CD&R) methods (M. Eby & Kelly, 1999; Duong et al., 1997). These algorithms detect a conflict and provide possible solutions to resolve a conflict. Different levels of autonomy are researched in literature; ranging from human in the loop to fully autonomous conflict resolution(Duong et al., 1997), (J.M. Hoekstra, 1998). CD&R methods require state information of neighboring aircraft. A new technology, Automatic Dependent Surveillance - Broadcast (ADS-B) enables state exchange between aircraft (Eurocontrol, n.d.). ADS-B is considered in several studies the key-technology used for airborne separation assurance (Valenti Clari et al., 2000; M. Eby & Kelly, 1999). The performance of the ADS-B signal is limited (Barhydt et al., 2004; Bernays et al., 2000). Studies are performed to assess the performance of CD&R methods, but the effect of ADS-B uncertainties and realities has not been evaluated. Therefore the research goal is to study the effect of ADS-B realities and uncertainties on the performance of different airborne CD&R algorithms.

The aim of this report is to provide a structured basis for the steps to be performed research on this topic. First the relevant research areas and current understanding of these areas are discussed in appendix B-2. Subsequently the research questions, aims and objective are stated and evaluated in appendix B-3. In appendix A-4 the theory associated with this research is discussed. The steps to be taken to answer the research questions are stated. The different dependent and independent variables are discussed in appendix A-6. A Gantt-Chart is created and explained in appendix A-7. This project plan is concluded in appendix B-4 with a summary of discussed content in this report.

A-2 State of the art / Literature review

Different aspects are involved in this project plan report. As stated in appendix B-1, important aspects related with this research are the ADS-B system and CD&R methods. Additionally a software environment is required to evaluate the performance of CD&R methods and analyze the effect of ADS-B realities and uncertainties. Therefore this section is divided in several sub-sections. CD&R methods and the ADS-B system are discussed in appendix B-2-2 and appendix B-2-3 respectively. The software-environment is discussed in appendix A-5-1.

A-2-1 Conflict Detection and Resolution

The goal of the CD&R system is to predict the occurance of a conflict, subsequently communicate the detected conflict to a human operator and guide in resolving the conflict (Kuchar & Yang, 2000). Other ways of resolving are also proposed; such as fully automatic decision making (Introduction, 2006). Conflict detection and resolution can be divided in two parts. A good definition is stated in by (Kuchar, 2000) (Kuchar & Yang, 2000):

"conflict detection can be thought of as the process of deciding when action should be taken and conflict resolution involves determining how or what action should be performed".

However, different techniques can be used for conflict detection and resolution. These are discussed in the following two paragraphs.

The first part is conflict detection. To detect a conflict, state information of surrounding aircraft needs to be known. These states (location, velocity, heading) provide an estimate of the current air traffic situation. With the states of the aircraft, a dynamic trajectory can be created to predict future conflicts. In general two methods are used in literature: state based and intent based trajectory planning (Kuchar & Yang, 2000; Prandini et al., 2000). In (Kuchar, 2000) both methods are discussed (Kuchar & Yang, 2000). State-based trajectory planing consists of extrapolation of the most recent speed vector of the aircraft. Intent-based trajectory planning uses for example the flight plan to incorporate the intend of a specific aircraft in the trajectory planning. However, these prediction methods have some level of inaccuracy, increasing with look-ahead time and time interval of the state update (Kuchar & Yang, 2000; Prandini et al., 2000). Several studies are performed on predicting the future state of aircraft. In (Kuchar, 2000) three different state-based trajectory planning methods are discussed (Kuchar & Yang, 2000). First the nominal projection methods is described as extrapolating the current speed vector. The second method is the worst-case projection. All possible locations of the aircraft (assuming a wide range of possible maneuvers inside the flight envelope) are considered as possible aircraft locations. This results in a large area where a conflict might occur. This method is very conservative but will have a high false-alarm rate. Finally the probabilistic method is discussed. In this method different future trajectories are assigned a probability of the aircraft following this trajectory. This method can be considered as a balance of the two earlier described methods.

The second part of conflict detection and resolution is resolution. A good base for the discussion of several CD&R algorithms is performed by (Kuchar, 2000) (Kuchar & Yang, 2000), in which 68 CD&R modeling methods, focused at non-human-centered issues, are discussed and compared. Several conflict detection methods are already discussed above. Four categories are created with respect to conflict resolution methods.

1. Prescribed method: a fixed maneuver is performed in case of conflict. An example is described in (Kuchar, 1997) (Kuchar & Carpenter, 1997). This method however is mostly suitable for terrain and runway related conflicts.

2. Optimization method: In general, a kinematic model is combined with a set of cost metrics. Subsequently an optimal resolution strategy is determined based on the cost metric. The cost metric can be for example fuel, time, workload or separation distance. Techniques such as genetic algorithms and fuzzy control are being used (Kuchar & Yang, 2000; Prandini et al., 2000).

3. Force field method: These methods model the aircraft as similar charged particles and will generate a repulsive force. Examples are (Duong et al., 1997) and (Eby, 1994) (Duong et al., 1997; M. S. Eby, 1994).

4. Manual method: A human operator selects the most suitable resolution method. This method is more flexible and human intuition is involved. Additional information, such as weather, can be incorporated by the decision making. An example is analyzed by (Hoekstra, 1998) which uses the force field method in combination with human decision (J.M. Hoekstra, 1998).

It is obtained that for all CD&R method state information of surrounding aircraft is required. In an signification amount of studies to CD&R methods,the ADS-B system is identified as the key system to obtain and transmit state information between aircraft(Duong et al., 1997; J.M. Hoekstra, 1998; M. S. Eby, 1994) . However, the ADS-B system is subjected to uncertainties and realities(Bernays et al., 2000; Ali et al., 2013), discussed in the next section.

A-2-2 ADS-B realities and uncertainties

Automatic Dependence Surveillance - Broadcast is a system in which an aircraft automatically transmits its state information and is able to receive traffic information from surrounding aircraft. Aircraft equipped with ADS-B IN are able to receive this signal. In this literature survey the focus is on the data link between aircraft communicating state information using the 1090 MHz frequency (Eurocontrol, n.d.). Further applications of ADS-B are described in the ADS-B Minimum Aviation System Performance Standards (MASPS) (RTCA Special Committee 186, 2002) . ADS-B is in several prominent studies identified as the enabling technology of airborne self separation using CD&R methods (Valenti Clari et al., 2000; M. Eby & Kelly, 1999).
The following ADS-B message reports are send, including the transmission rate(Eurocontrol, n.d.):

- Airborne positions squitter (2/sec)
- Surface position squitter (1/sec)
- Airborne velocity squitter (2/sec)
- Aircraft identification squitter (0.2/sec)
- Operational Status (0.4/sec)
- Target state (0.8/sec)

The ADS-B signal transmission is subjected to uncertainties and realities. First of all the location of the aircraft needs to be determined on-board. Therefore the Global Navigation Surveillance System (GNSS) and inertial systems are being used (Eurocontrol, n.d.). Since inertial sensors drift with time, satellite based navigation such as GPS is considered the most important source for position determination. By (Ali, 2013) it is concluded that ADS-B is a significant more accurate method to determine positions than radar with horizontal position error smaller than 150m for 66.7% of the aircraft (Ali et al., 2013).

The range of the ADS-B broadcast message is limited due to several factors. Extensive measurements to the performance of the ADS-B extended squitter signal have been done by (Beryans, 2000) and (Ali, 2013) (Bernays et al., 2000; Ali et al., 2013). In these studies was mainly focused on accuracy and latency of the ADS-B message. In (Beryans, 2000) a quantitative assessment of the air to air range of ADS-B equipment is researched (Bernays et al., 2000). A decreasing reception probability is observed for an increasing range of aircraft. Besides range, aircraft message interference has to be considered since all ADS-B mode S communication is performed on the same 1090 MHz frequency. It is found in (Barhydt, 2004) the message interference resulting from overlapping messages at the receiver side can be modeled as the sum of multiple Poisson distributions (Barhydt et al., 2004) . The Poisson distribution is depending the following properties:

- Message transmitting aircraft in range
- Message frequency
- Message duration

In both (Barhydt, 2004) and (Chung et al. 2006) an ADS-B model is created with reception probability as main output (Barhydt et al., 2004) (Chung & Staab, 2006) . The message reception probability is modeled as a function of two variables: range between aircraft and level of interference due to surrounding aircraft.

From the literature review it can be concluded research is done to CD&R methods and the ADS-B system. Both systems are required for airborne self separation. However, in current research these two areas are not combined. This research aims to help fill current gap in these two research areas and study the effect of ADS-B shortcomings on CD&R performance.

A-3 Research question, aims and objectives

The research objective is inspired to fill the gap between two ongoing researcher areas/developments. On one side the research associated with enabling an unmanaged airspace environment using CD&R methods and on the other side the the ADS-B system. The goal of the research associated with this literature review is to study the effects of ADS-B system characteristics on CD&R performance. The research objective is stated as follows:

Study and analyze the effect of ADS-B realities and uncertainties on the performance of different CD&R algorithms by implementing an ADS-B model and perform simulations in the BlueSky simulator.

Several aspects are involved in this research objective. Therefore multiple research question are defined, each containing sub-questions. The research questions are defined as follows:

1. How is proper reception by aircraft of an ADS-B signal affected?
   (a) How can the quality of and ADS-B message be assessed?
   (b) How do ADS-B system specifications affect the ADS-B signal reception?
   (c) How do external factors affect the ADS-B signal reception?
2. What ADS-B related variables determine the performance of a CD&R method?
   (a) What are suitable metrics to asses the performance of the CD&R method related to:

   i. Safety?
   ii. Efficiency?
   iii. Airspace stability?
 (b) Which elements of the ADS-B system affect the CD&R performance?

3. How can the effect of ADS-B signal realities and uncertainties on CD&R performance be evaluated in an experiment/simulation?
   (a) What should be the dependent and independent variable in the experiment/simulation?
   (b) Which test environments are suitable for assessing the performance of CD&R method?

The research questions are created, using the SMART method. The research questions are specific and will lead to measurable results. It is achievable and realistic to research these topics using the BlueSky simulator. Finally it is discussed with the supervisor if the work to be done is achievable in 9 months; it was concluded it is. In the literature study a gap was found linking CD&R performance and the realities and uncertainties in the ADS-B system. This research will identify suitable CD&R methods for airborne separation assurance and analyze the effect of ADS-B realities and uncertainties and by linking these two research fields. The use of the BlueSky ATM simulator will help performing experiments as discussed in appendix A-5-1.

A-4 Theoretical Content/Methodology

This section will discuss the theoretical basis of the work that will be undertaken to fulfill the research objective and answer the research questions stated in appendix B-3. From the research questions it can be concluded first some level of knowledge is required regarding the ADS-B system and CD&R methods. A good start for this research is to gain in-depth knowledge about these two topics. Different papers are found discussing the realities and uncertainties in the ADS-B system (Barhydt et al., 2004; Bernays et al., 2000). This research is a good base for developing and ADS-B system model. The state of the art resarch considering the ADS-B system has been discussed in more detail in appendix B-2-3. A software-model of the ADS-B system can be generated; linking a specific reception probability of a message to factors like range between two aircraft and number of interfering aircraft.

Additionally, knowledge about CD&R methods needs to be obtained. Research done by (Kuchar, 2000) is found where an comparison between multiple methods is performed (Kuchar & Yang, 2000). In this research several categories of CD&R methods are discussed and gives a good general overview of suitable CD&R applications for airborne separation assurance. CD&R methods have been further discussed in appendix B-2-2. Using this knowledge suitable CD&R methods can be evaluated to study the effect of the ADS-B realities and uncertainties. Since these need to be implemented and tested in the BlueSky simulator, knowledge regarding the Python programming language and the BlueSky Simulator is required. Subsequently an air traffic scenario needs to be designed in which all the aspects regarding CD&R performance are evaluated. Before the experiments an hypothesis is stated. It is assumed the performance of CD&R methods degrades with increasing ADS-B uncertainty and reality effects. However, this should be confirmed by experiments. Data will be logged and analyzed to study the effect of ADS-B realities and uncertainties on different CD&R methods. By analyzing the generated data in the experiments the goal is to quantify the performance of different CD&R methods in case an ADS-B model is implemented.

A-5 Experimental Set-up

This research will use the BlueSky open air traffic simulator as discussed in appendix A-5-1. In the BlueSky simulator air traffic scenarios can be loaded and analyzed. Different types of airborne separation assurance systems using CD&R methods will be assessed. Subsequently the performance of these methods can be analyzed. Since no ADS-B model is available and the current use of CD&R methods doesn't allow the use of ADS-B data, adaption to the BlueSky simulator need to be made. Different CD&R methods will be evaluated with a range of ADS-B settings using a specific air traffic scenario. Subsequently data regarding the performance of these CD&R methods will be logged. The performance can be assessed in different ways, focusing on safety and efficiency. Examples of safety related metrics are the number of separations losses and severity of a separation loss (duration of separation loss, crossing distance, etc.). Besides safety also the efficiency should be considered. Efficiency can be measured with respect to flight time and distance traveled. These metrics will answer the research questions relating the ADS-B system uncertainties and realities to the CD&R performance. Experimental variables are further discussed in appendix A-6. General, in research the results and mathematical model need to be validated wit a physical representation. However, with the resources available for this research this is not a feasible option. Therefore this research is limited to performing computational simulations only.

A-5-1 BlueSky open air traffic simulator

An air traffic simulation environment has been developed at the TU Delft, called BlueSky. The goal of BlueSky is to provide everybody who wants to visualize, analyze or simulate air traffic with a tool to do so without any restrictions, licenses or limitations. It can be copied, modified, cited, etc. without any limitations (J. Hoekstra, 2015). The BlueSky simulator is written in the Python(2.xx) programming language and uses pygame for visualization. A screen shot is shown in fig. A-1.

The BlueSky simulation environment has build-in features like airborne separation assurance, different conflict detection and resolution methods, data-log options and much more (J. Hoekstra, 2015). Due to it's open-source character it is possible to implement new features such as an ADS-B model.

A-6 Results, Outcome and Relevance

As stated in appendix A-5 suitable air traffic scenarios need to be generated, covering different aspects of conflict detection and resolution performance. An example of these variables are

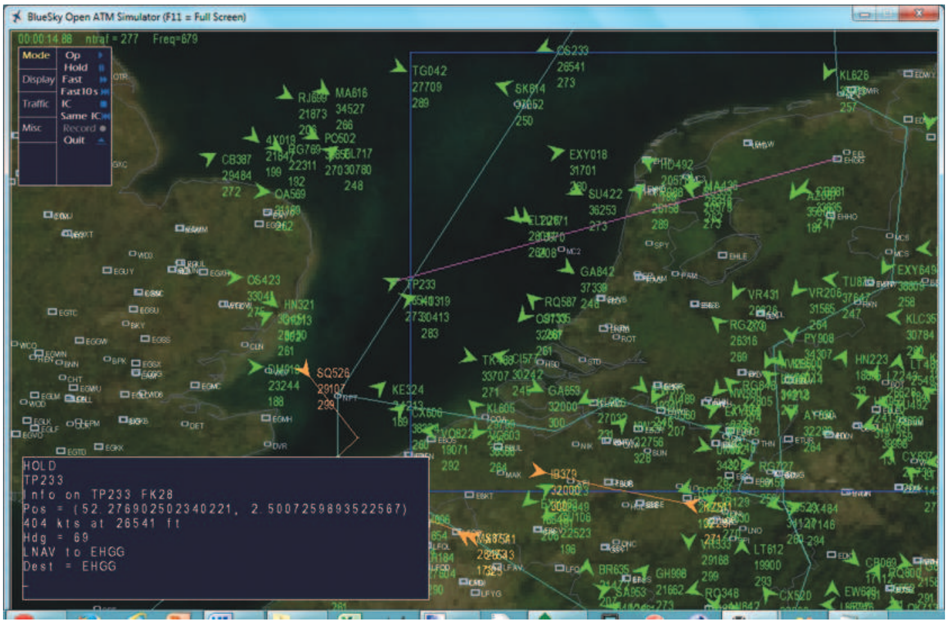

Figure A-1: BlueSky Simulator environment

the following:

- Air traffic density: number of aircraft per unit area.
- Conflict angle: the conflict angle can influence the performance of CD&R methods. Therefore a good mix of conflicts angles needs to be present in the test scenario.
- Aircraft states: the effect of a range in aircraft states needs to be evaluated.

Since the effect of the ADS-B system on CD&R performance will be evaluated, different settings of ADS-B system variables need to be tested. In (Barhydt, 2004) and (Chung et al., 2006) the ADS-B system is modeled with variables such as reception probability dependent on range and interference level (Barhydt et al., 2004; Chung & Staab, 2006). Other ADS-B related variables are latency and truncation effect. Therefore suitable independent variables in the experiment are sensitivity of reception probability and interference, latency duration and state accuracy of the ADS-B system. The metrics assessing the performance in terms of safety and efficiency of a CD&R method are the dependent variables. A lot of the dependent variables are related to Loss of Seperation (LOS); an occurnce where no safe separation between two aircraft is maintained. An overview of these variables is shown in table A-1.

From the performed experiments the relation between ADS-B signal quality and CD&R performance can be concluded. This research can help contributing to a framework for further selection of suitable airborne separation assurance methods in aviation.

Table A-1: Dependent and independent variables in experiment.

Type	Variable	Number of variables	Unit
Independent	ADS-B setting	3	[-]
Independent	Air Traffic density	3	$[\frac{AC}{NM^2}]$
Independent	CD&R method	3	[-]
Independent	Total	27	[-]
Dependent	Number of LOS	-	[LOS]
Dependent	Duration of LOS	-	[s]
Dependent	Distance traveled	-	[m]
Dependent	Time of flight	-	[s]

A-7 Project Planning and Gantt Chart

A Gantt chart is created to visualize and easily monitor the progress during the project. The project is divided in two parts; the preliminary phase and the main phase. The Gantt chart of the preliminary phase and the main phase are shown in fig. A-2 and fig. A-3 respectively. The preliminary phase consists of several parts with a duration of 4 months, starting with the orientation phase. First the kick-off meeting is held to discuss the research with the supervisors. Subsequently a literature study is performed in the orientation phase. Synchronously with the literature study familiarization with the Python programming language and the BlueSky simulator is performed. After the orientation phase the developed ADS-B model will be implemented in the BlueSky simulator and tested. Some preliminary simulations are performed and the findings so-far are documented. The preliminary phase is concluded with the preliminary presentation (mid-term review). In case an iteration is needed for completing the preliminary phase a delay of 1 or 2 weeks is taken into account.
After the preliminary phase the main phase is started with a planned duration of 5 months. The ADS-B model is further developed, implemented and tested in the BlueSky simulator. Experiment assessing the performance and effect of the ADS-B system on CD&R performance are generated. A month before the final thesis deadline the results so far are handed to the supervisors during the "Green light review". Any remarks or comments considering the result so far by the supervisors are implemented in an iterative manner. If sufficient, the final thesis phase is started. Finally the results are reported and presented to the public. Holiday and possible unforeseen delays are taken in consideration in the Gantt chart.

A-8 Conclusions

This project plan gives an outline of the aspects involved and an approach to research the effect of ADS-B uncertainties and realities on CD&R performance. Due to the growth of air traffic and new developments in the UAV area a modernization of current air space structure is required. The general consensus is a shift from ground-based controller to an airborne controller. Airborne self separation enables the concept of free flight; instead of following structured air-routes pilots can navigate from A to B themselves resulting in environmental, safety and economical gains. Developments in ADS-B technology provide state exchange between aircraft enabling airborne self separation using CD&R methods.

In the Literature study it was found the ADS-B system is subjected to uncertainties and realities. The link between the ADS-B system and its effect on CD&R methods has not been analyzed. Research investigating the effects of these limitations on the performance of CD&R algorithms should be performed and can be used to determine the feasibility of airborne self separation. In the literature review two key research areas were defined; ADS-B system performance and CD&R algorithms. Several properties of the ADS-B system, such as reception probability, accuracy and latency, are identified as factors influencing the performance of CD&R methods. Different categories of CD&R methods are discussed. Based on the literature study the research objective and multiple research questions are formulated based on SMART criteria. The theoretical content is discussed to answer these research questions and fulfill the research objective.

The experiment set-up, computational based modeling and simulation is discussed in more detail.The BlueSky simulator is introduced: A simulation environment suitable for evaluating air traffic scenarios, developed at the Delft University of Technology. The open-source character enables the implementation of an ADS-B system. Subsequently different metrics can be logged to relate the performance of ADS-B characteristics to CD&R performance. The results and outcome are discussed subsequently. Finally different work packages are created with an estimation of the amount of time involved. Also important milestones are identified and (possible) required iterations are taken into account. These work packages and milestones are used in creating Gantt chars.Two Gantt charts are created; one for the preliminary phase and one four the main thesis phase with an estimated duration of 4 and 5 month respectively.

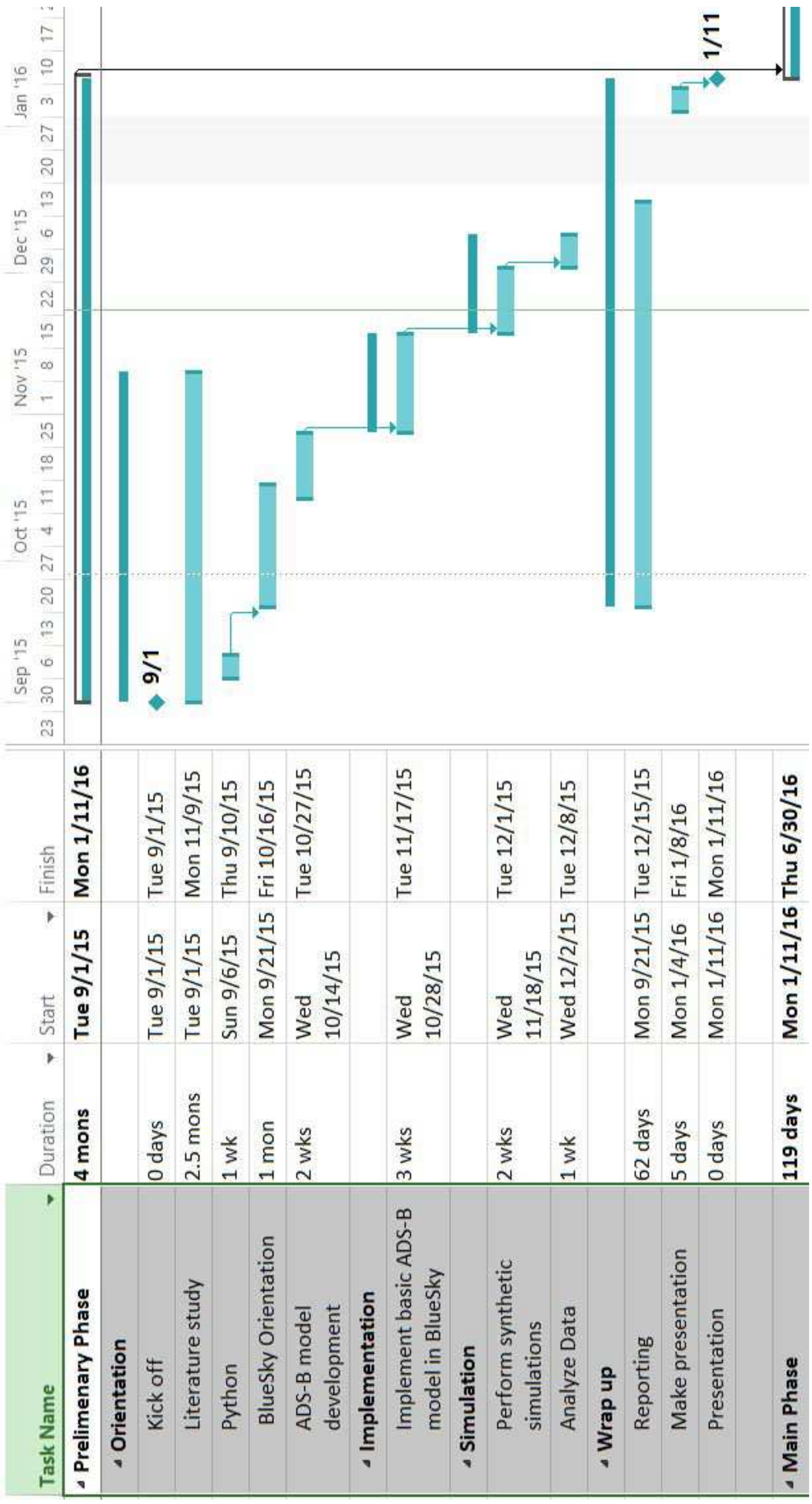

Figure A-2: Gantt Chart preliminary phase

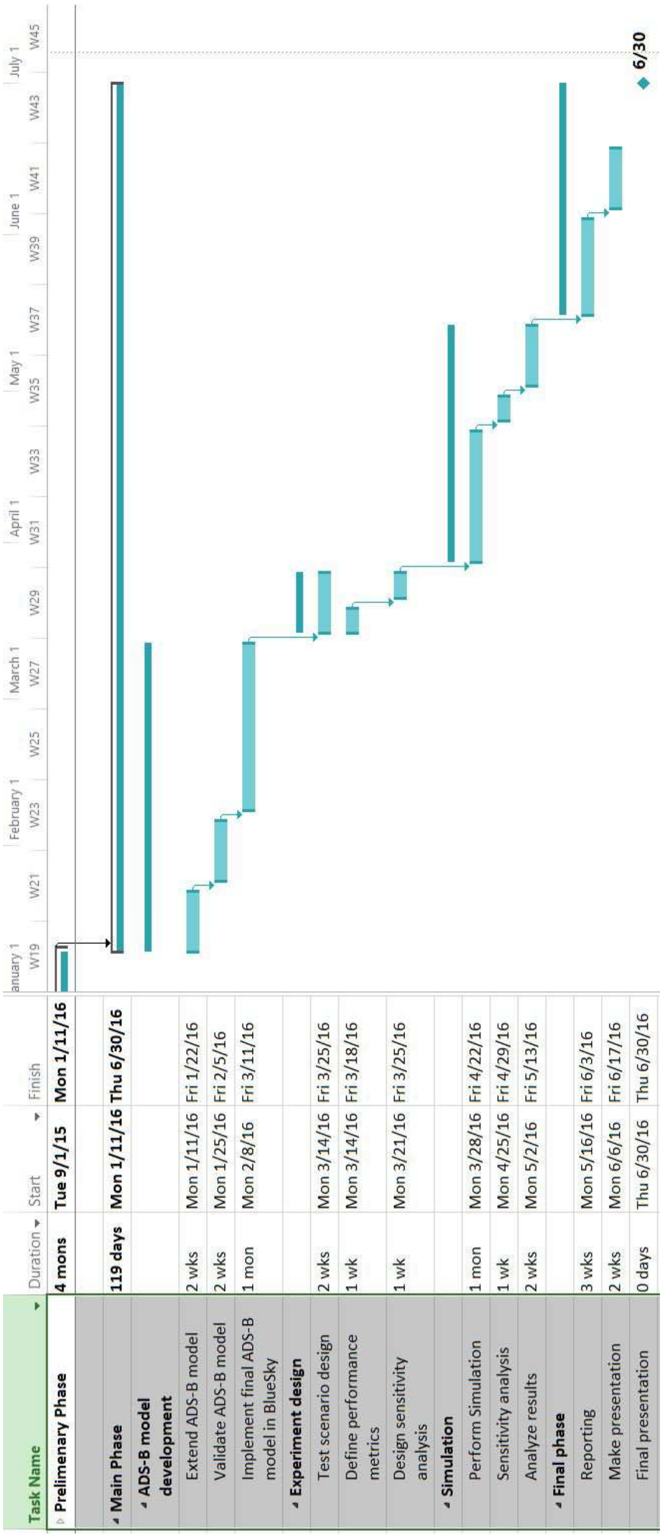

Figure A-3: Gantt Chart main phase

Appendix B

Literature Review

The aim of this literature review is to obtain an overview of performed research related to the research topic; unmanaged airspace, the ADS-B system and CD&R methods. Therefore literature related to the the ADS-B data link are studied. Subsequently different CD&R algorithms and their applicability to the unmanaged airspace concept are assessed using different scientific sources. It is found that the ADS-B data performance is degraded by interference of surrounding aircraft and range between two aircraft. Elaborate research studying the effect of ADS-B effects on CD&R performance has not been found. This research will fill this gap by evaluating the effect of ADS-B realities on different CD&R methods by modeling the ADS-B data link and simulate several unmanaged airspace scenarios.

B-1 Introduction

To process the increasing demand of air traffic in a safe and economic way a modernization of the current air traffic management system is required (SESAR Consortium, 2012; Francisco & Louisville, 2014). The current system consists of specified air routes, so called 'highways-in-the-sky', along which air traffic is directed by air traffic controllers. The pilot must follow instructions from the Air Traffic Controller (ATCo) and ask permission for route changes. The ATCo is therefore responsible of maintaining a safe distance between aircraft and sustain an efficient flow of traffic.

However, the increase in air traffic and developments in UAV technology require a new approach of Air Traffic Control (ATC) (Ballin et al., 1999; Valenti Clari et al., 2000; Conde et al., 2012). Current development in Air Traffic Management (ATM) strategies show a responsibility shift from the ground-based controller to the pilot in the cockpit to sustain separation standards between aircraft. The controller is responsible of maintaining a safe separation between aircraft and ensure a good traffic flow (Ellerbroek, 2013; Barhydt et al., 2004). An airborne controller will enable the concept of unmanaged airspace; instead of following specified air routes, pilots are able to plan their own route to their destination. In (Hoekstra, 2002) it is concluded that in an unmanaged airspace environment the subjective safety was equal or better than using a ground-based controller(J. M. Hoekstra et al., 2000). Besides safety other important aspects are studied, such as efficiency and airspace stability. Unmanaged airspace will enable the pilots to fly more efficient routes, resulting in time, environmental and financial gains (Valenti Clari et al., 2000). A crucial element is airborne separation assurance; the minimum separations standards of aircraft need to be maintained. Conflict detection and resolution methods can be used to aid air traffic controllers to maintain the minimum separation requirements, or can be used for fully automatic separation (Kuchar & Yang, 2000). ADS-B technology enables the application of new airborne separation assurance systems (Ellerbroek, 2013). ADS-B is a direct data-link between aircraft through which these transmit and receive state information like position, velocity and intend from surrounding aircraft (RTCA Special Committee 186, 2002). However, the performance of the ADS-B signal is limited (Barhydt et al., 2004; Bernays et al., 2000).

Several studies are performed to a distributed air ground traffic management system, with humans in the loop (Ballin et al., 1999; J. M. Hoekstra et al., 2000), and with an ADS-B model included (Barhydt et al., 2004). However, the **effect** of the ADS-B signal quality on the performance of CD&R algorithms has not been researched. Therefore the research goal is to study the effect of ADS-B realities and uncertainties on the performance of different airborne CD&R algorithms by implementing a ADS-B model in the BlueSky simulator. The corresponding research question is defined as:

"What is the quantitative effect of ADS-B uncertainties and realities on CD&R performance with respect to safety, efficiency and airspace stability?"

This literature review elaborates on the different CD&R methods and ADS-B signal characteristics. This report starts with a literature review in appendix B-2. The results and a analysis of this literature review is done in appendix B-3. Finally this literature review is concluded in appendix B-4 with a plan on how to fill this gap in current research.

B-2 State of the art / Literature review

Different aspects are involved in this research project. Therefore this section is divided in several subsections, each reviewing a relevant research area of the work carried out by other researchers. In appendix B-2-1 the unamanaged airspace concept is explained. In appendix B-2-2 conflict detection and resolution methods are analyzed. Subsequently the ADS-B signal is discussed in appendix B-2-3. Finally it is discussed in appendix B-2-4 how this research field fits in the current time framework.

B-2-1 Unmanaged airspace

As stated in several reports it is expected the air traffic demand will grow in the future (SESAR Consortium, 2012; Francisco & Louisville, 2014). To be able to process the air traffic flow in a safe, efficient en economical manner, a shift from ground controller to cockpit responsibility is proposed in several papers(Valenti Clari et al., 2000; J.M. Hoekstra, 1998; Ellerbroek, 2013). The main advantages are a decrease in controller workload, found in (Ellerbroek, 2013) (Ellerbroek, 2013) and a capacity increase (Hoekstra, 1998) (J.M. Hoekstra, 1998).

The definition of unamanged airspace is that all constraints of ATCo are lifted(M. Eby & Kelly, 1999; J.M. Hoekstra, 1998); a pilot is responsible for separation with respect to other aircraft and can plan his or her route freely. According to several studies the main advantages of free flight are: safety, robustness and environmental gains (M. Eby & Kelly, 1999; Duong et al., 1997). It is found that the effect on system stability by additional trajectory deviations was low (Bilimoria et al., 2000). The capacity of the airspace is increased by implementing the unmanaged airspace concept, that will otherwise be constrained by a centralized ground-based system (Ballin et al., 1999). Besides the performance gains also the acceptability of the users (aircrew) has been researched. In (Hoekstra, 2000) it is concluded that in a free-flight environment the subjective safety was equal or better than using a ground-based controller (J. M. Hoekstra et al., 2000). Many of the papers refer to Conflict Detect and Resolution (CD&R) techniques to predict the occurrence of future conflicts and determine possible resolutions. Therefore different CD&R techniques are discussed in the next subsection.

B-2-2 Conflict Detection and Resolution

The goal of the CD&R system is to predict the occurance of a conflict, subsequently communicate the detected conflict to a human operator and guide in resolving the conflict (Kuchar & Yang, 2000). Other ways of resolving are also proposed; such as fully automatic decision making (Introduction, 2006). Conflict detection and resolution can be divided in two parts. A good definition is stated in (Kuchar et al., 2000) (Kuchar & Yang, 2000):

"Conflict detection can be thought of as the process of deciding when action should be taken and conflict resolution involves determining how or what action should be performed".

However, different techniques can be used for conflict detection and resolution. These are discussed in the following two paragraphs.
The first part is conflict detection. To detect a conflict state information of surrounding aircraft needs to be known. These states (location, velocity, heading) provide an estimate of the current air traffic situation. With the states of the aircraft a dynamic trajectory can be created to predict future conflicts. In general two methods are used in literature: state based and intent based trajectory planning (Kuchar & Yang, 2000; Prandini et al., 2000). In (Kuchar et al., 2000) both methods are discussed (Kuchar & Yang, 2000). State-based trajectory planing consists of extrapolation of the most recent speed vector of the aircraft. Intent-based trajectory planning uses for example the flight plan to incorporate the intend of a specific aircraft in the trajectory planning. However, these prediction methods have some level of inaccuracy, increasing with look-ahead time and time interval of the state update (Kuchar & Yang, 2000; Prandini et al., 2000). For en-route air traffic, the scope of this research, state-based trajectory planning is considered the most suitable trajectory planning

method (Kuchar & Yang, 2000).

Several studies are performed on predicting the future state of aircraft. In (Kuchar et al., 2000) three different state-based trajectory planning methods are discussed (Kuchar & Yang, 2000). First the nominal projection methods is described as extrapolating the current speed vector. The second method is the worst-case projection. All possible locations of the aircraft (assuming a wide range of possible maneuvers inside the flight envelope) are considered as possible aircraft locations. This results in a large area where a conflict might occur. This method is very conservative but will have a high false-alarm rate. Finally the probabilistic method is discussed. In this method different future trajectories are assigned a probability of the aircraft following this trajectory. This method can be considered as a balance of the two earlier described methods. Al three state propagation methods are visualized in figure fig. B-1. For en-route flying most part of the aircraft path is a straight line between two points, for which nominal projection is the most suitable (J.M. Hoekstra, 1998). Therefore the main focus for this research should be on the nominal projection method.

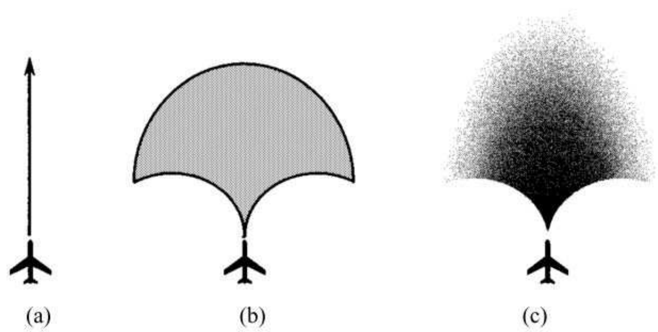

Figure B-1: From left to right: nominal projection, worst-case projection, probabilistic method. Figure from (Kuchar et al, 2000) (Kuchar & Yang, 2000).

The second part of conflict detection and resolution is resolution. A good base for the discussion of several CD&R algorithms done by (Kuchar et al., 2000) (Kuchar & Yang, 2000), in which 68 CD&R modeling methods, focused at non-human-centered issues, are discussed and compared. Several conflict detection methods are already discussed above. Four categories are created with respect to conflict resolution methods.

1. Prescribed method: a fixed maneuver is performed in case of conflict. An example is found in (Kuchar, 1997) (Kuchar & Carpenter, 1997). This method however is mostly suitable for terrain and runway related conflicts.

2. Optimization method: In general a kinematic model is combined with a set of cost metrics. Subsequently an optimal resolution strategy is determined based on the cost metric. The cost metric can be for example fuel, time, workload or separation distance. Techniques such as genetic algorithms and fuzzy control are being used (Kuchar & Yang, 2000).

3. Force field method: These methods model the aircraft as similar charged particles and

will generate a repulsive force. Examples are (Duong et al., 1997) and (Eby, 1994) (Duong et al., 1997; M. S. Eby, 1994).

4. Manual method: A human operator selects the most suitable resolution method. This method is more flexible and human intuition is involved. Additional information, such as weather, can be incorporated by the decision making. An example is found in (Hoekstra et al., 1998) which uses the force field method in combination with human decision(J.M. Hoekstra, 1998).

It should be noted that the developers of the CD&R algorithms in (Kuchar et al., 2000) (Kuchar & Yang, 2000) separately tested and evaluated the performance of their algorithm. In the paper only the basic working principles and capabilities are discussed and compared. To have a fair comparison, experiments of different CD&R algorithms using the same test scenario and same measuring performance metrics should be performed and analyzed.

B-2-3 ADS-B realities and uncertainties

Automatic Dependence Surveillance - Broadcast is a system in which an aircraft automatically transmits its state information and is able to receive information from other aircraft. A class of ADS-B is ADS-Broadcast (mode-S) Extended Squiter; the aircraft broadcasts its state with time intervals in the order of seconds in an omni-directional manner. Aircraft equipped with ADS-B IN are able to receive this signal. Besides state data also weather related data can be received. In this literature survey the focus is on the data link between aircraft communicating state information using the 1090 MHz frequency (Eurocontrol, n.d.). Further applications of ADS-B are described in the ADS-B Minimum Aviation System Performance Standards (MASPS) (RTCA Special Committee 186, 2002) . ADS-B is in several prominent studies identified as the enabling technology of airborne self separation (Barhydt et al., 2004; M. Eby & Kelly, 1999; J. Hoekstra et al., 2003).
The following ADS-B message reports are send, including the transmission rate(Eurocontrol, n.d.):

- Airborne positions squitter (2/sec)
- Surface position squitter (1/sec)
- Airborne velocity squitter (2/sec)
- Aircraft identification squitter (0.2/sec)
- Operational Status (0.4/sec)
- Target state (0.8/sec)

The ADS-B signal transmission is subjected to uncertainties and realities. First of all the location of the aircraft needs to be determined on-board. Therefore the Global Navigation Surveillance System (GNSS) and inertial systems are being used. Since inertial sensors drift with time, satellite based navigation such as GPS is considered the most important source for position determination. By (Ali, 2013) it is concluded that ADS-B is a significant more accurate method to determine positions than radar with horizontal position error smaller than 150m for 66.7% of the aircraft (Ali et al., 2013).

The range of the ADS-B broadcast message is limited due to several factors. Extensive measurements to the performance of the ADS-B extended squitter signal have been done in (Bernays et al., 2000) and (Ali, 2013) (Bernays et al., 2000; Ali et al., 2013). In these studies tha main focus was on accuracy and latency of the ADS-B message. In (Bernays et al., 2000) a quantitative assessment of the air to air range of ADS-B equipment is researched (Bernays et al., 2000). A decreasing reception probability is observed for an increasing range of aircraft. Besides range, aircraft message interference has to be considered since all ADS-B mode S communication is performed on the same 1090 MHz frequency. It is found in (Barhydt, 2004) the message interference resulting from overlapping messages at the receiver side can be modeled as the sum of multiple Poisson distributions(Barhydt et al., 2004) . The Poisson distribution is depending the following properties:

- Messeage transmitting aircraft in range
- Message frequency
- Message duration

In both (Barhydt, 2004) and (Chung, 2006) an ADS-B model is created with reception probability as main output (Barhydt et al., 2004; Chung & Staab, 2006). The message reception probability is modeled as a function of two variables: range between aircraft and level of interference due to surrounding aircraft.

It should be noted that the receiving aircraft does not have the real-time state information of the other aircraft. Aircraft A generates a position report and sends this to Aircraft B. However Aircraft A needs some time to send the ADS-B message and aircraft B needs some time to process the ADS-B message. Therefore latency affects the performance of the CD&R method. In Framework for ADS-B Performance Assessment: the London TMA Case Study it is found the latency due to processing is less than a second (Ali et al., 2013).
As sated above aircraft don't send their ADS-B report continuously. In (Barhydt, 2004) and (Chung, 2006) it is analyzed how the transmission frequency affects the message reception probability due to interference (Barhydt et al., 2004; Chung & Staab, 2006). However because of the transmission frequency of ADS-B message the aircraft is not aware of the aircraft state for a certain time interval. Therefore the transmit frequency is a trade-off between an allowable message reception probability caused by interference and a sufficient update rate of state information.
Only a specific amount of bits are reserved for a specific state in the ADS-B message. Therefore the accuracy of a state can not be described with infinite accuracy. The truncation effect should be considered.

It can be stated the general consensus is a transition of a ground-based controller to an airborne controller is expected. This will improve airspace capacity and enable the integration of UAVs in current airspace. Two important areas are defined for this research; CD&R and the

ADS-B system. Different type of conflict detection methods were found. Of those the nominal projection method with a fixed look-ahead time is identified as the most suitable one for en-route flight. Subsequently different type of CD&R methods were found and their general outline was discussed. However, all CD&R methods need state information of surrounding aircraft, which can be provided by the ADS-B system.

B-2-4 Research in current time framework

It should be noted there is a large research gap in the area of unmanaged airspace and conflict detection and resolution in the first decade of this millennium. This can be explained by the terrorist attacks on the world trade center in 2001. The ATM research field tended to be much more conservative after these attacks. Currently the research topics has gained more attention due to the developments in the UAV area. CD&R is a promising technology to integrate UAV technology with current air traffic. As stated above a key-technology for using airborne self separation is ADS-B technology. When an aircraft is aware of its surround air traffic it can apply conflict detection and resolution methods. However, the ADS-B system is not perfect. No extensive research is performed to assess the effect of ADS-B realities and uncertainties on conflict detection and resolution performance.

B-3 Results and Analysis

In several articles in section appendix B-2 it is concluded that a novel structure of airspace is needed to comply with future airspace demand due to increase in air traffic and developments in the UAV area (Conde et al., 2012). The vast majority of these studies predict a shift from ground-based centered control to airborne centered control (Ellerbroek, 2013; J. Hoekstra et al., 2003). Promising results is the unmanaged airspace, or free flight concept (J.M. Hoekstra, 1998). In this review the nominal projection has been used in combination with the modified voltage potential as a CDR methods. However also different CDR methods are proposed in (Kuchar et al., 1997) (Kuchar & Carpenter, 1997).

In general three different type of conflict detection are used in literature; nominal projection, worst-case projection and probabilistic projection. For each method a look-ahead time is being used to determining the future state of the aircraft using extrapolation. The nominal projections assumes one specific future location of the aircraft while the other two methods use an area where the the aircraft can be located. Each method is a trade-off between conservatism (safety) and false alarm rate (Kuchar & Carpenter, 1997). Several CDR methods are discussed and evaluated. This paper is a good reference to obtain a good overview of different CDR methods. The conflict resolution methods can be divided in four categories, namely prescribed, optimized, force field an manual.

Several studies are performed analyzing the ADS-B signal. (Ali, 2013) uses measurements are performed analyzing the accuracy and update rate of the ADS-B signal (Ali et al., 2013). In (Bernays, 2000) measurements are performed to analyze the reception probability between two aircraft with range as the independent variable (Bernays et al., 2000). Besides analyzing also different research is performed modeling the ADS-B signal. In (Barhydt, 2004) a reception probability model for an ADS-B message is generated based on range between two aircraft and number of surrounding aircraft causing interference (Barhydt et al., 2004). A similar approach is used by (Chung, 2006) (Chung & Staab, 2006). In this research the reception probability model is validated with real-life measurement data from (Bernays, 2000) (Bernays et al., 2000). The research done to modeling of the ADS-B and measurements can be used to analyze the ADS-B system limitation and generate a reception model. Subsequently this model can be used in CD&R methods and the effect of the ADS-B realities and uncertainties on CD&R performance can be analyzed.

B-4 Discussions and Conclusions

From the literature in this survey several conclusion can be made. First of all a new structure of airspace will enable more efficient, safer flight and higher airspace capacity. The general tendency in aviation is that the ground-based controller will be replaced in an airborne self separation system. The infrastructure foundation is available; such the implementation of the ADS-B system.

Secondly the different aspects involved in airborne self separation assurance are identified and discussed in appendix B-2; conflict detection and resolution methods and the ADS-B system. Conflict detection and resolution methods are based on state information of surrounding aircraft. In this research en-route traffic is analyzed. A nominal projection method, and a look-ahead time of around 5 minutes is optimal for CD&R for traffic during the en-route phase.

A recent development, ADS-B technology, enables sate information exchange between aircraft. However, the ADS-B system doesn't provide a continuous and perfect information link. The ADS-B system is subjected to realities and uncertainties such as a decreasing reception probability with increasing interference level and range between two aircraft. To develop a functional airborne self separation system, the effect of these system realities and uncertainties needs to be assessed. Al tough some literature was found analyzing the realities and uncertainties of the ADS-B system no research was found where its effects are related to the performance of CD&R methods. Therefore the research associated with this literature review aims to contribute to analyze the effect of these realities and uncertainties on different CD&R methods. An ADS-B reception model needs to be developed, implementing the situational and system related effects. Subsequently the performance of different CDR methods will be analyzed.

Appendix C

SESAR innovation days paper

A shortened paper (8 pages) will be submitted to the SESAR innovation days 2016. The sixth SESAR innovation days are hosted by the Technical University of Delft from the $8^t h$ to the $10^t h$ of November 2016. This appendix contains the to be submitted paper.

Effect of ADS-B Characteristics on Airborne Conflict Detection and Resolution

Thom Langejan, Emmanuel Sunil, Joost Ellerbroek and Jacco M. Hoekstra

***Abstract*—Most Free-Flight concepts rely on self-separation by means of airborne Conflict Detection and Resolution (CD&R) algorithms. A key enabling technology for airborne CD&R is the Automatic Dependent Surveillance-Broadcast (ADS-B) system, which is used for direct state information exchange between aircraft. Similar to other communication systems, ADS-B is affected by a number of limitations which can be broadly classified as system and situation related deficiencies. This research investigates the impact of these limitations on the viability of using ADS-B for airborne CD&R within the Free-Flight context. Here, 'state-based' conflict detection and the modified voltage potential conflict resolution algorithm are used as a case-study. An ADS-B model is developed, and its effect on the aforementioned CD&R method is measured using three fast-time simulation experiments. The experiments studied overall safety with ADS-B, as well as the specific effect of situation related characteristics, i.e., transmission range and interference, on safety. The results indicated that the overall safety with ADS-B was comparable to the case where perfect state information was assumed. Additionally, it was found that increasing ADS-B transmission range also increased signal interference, which in turn lowered safety. This suggests that the degrading effect of ADS-B signal interference should be considered in future airborne CD&R research, particularly for high traffic densities.**

***Index Terms*—ADS-B, Free Flight, Conflict Detection and Resolution (CD&R), Modified Voltage Potential (MVP), Air Traffic Management (ATM), Safety, Self-Separation, BlueSky ATM Simulator**

I. INTRODUCTION

THE Free-Flight Air Traffic Management (ATM) concept has been proposed as a means of increasing airspace safety, efficiency and capacity by permitting user defined trajectories. Most Free-Flight concepts rely on self-separation using airborne Conflict Detection and Resolution (CD&R) automation. As airborne CD&R requires information sharing between aircraft, a system for inter-aircraft communication is required. In Free-Flight literature, this information sharing is often achieved using the Automatic Dependent Surveillance-Broadcast (ADS-B) system. Aircraft equipped with ADS-B transmitters periodically broadcast their own state information, such as position and velocity, using data obtained from on-board sensors. Aircraft can also receive this information from neighboring traffic, which can in turn be used for detecting and resolving conflicts.

Similar to other data-link systems, ADS-B has a number of limitations that affect the quality of the transmitted and received information. These limitations can be broadly classified as system and situation related deficiencies. System related limitations affect the accuracy of the transmitted state information. This is not only affected by the accuracy of on-board sensors, but also by the number of bits available for (digital) data encoding. For example, ABS-B position messages are only accurate to within 30 meters of the true position, even though the Global Positioning System (GPS), which is the underlying system used for measuring aircraft position, is accurate up to 7.8 meters [1]. On the other hand, situation related deficiencies reduce ADS-B message detect and decode probability due to the distance between aircraft and due to signal interference[2].

Despite these limitations, much of the previous work on airborne CD&R, particularly studies related to the development of novel conflict resolution methods, have assumed perfect state information exchange between aircraft. Thus, it is as yet unknown whether the ADS-B system is actually capable of providing usable state information for airborne CD&R purposes. Furthermore, the extent to which the safety of CD&R methods is affected by ADS-B limitations is also unknown.

The research that is presented in this paper represents the initial work done towards understanding the effect of ADS-B on self-separation safety by focusing on one particular airborne CD&R method. Given the plethora of CD&R methods, the frequently used 'state-based' Conflict Detection (CD) method, and the Modified Voltage Potential (MVP) Conflict Resolution (CR) algorithm, have been selected as a case-study. An ADS-B model is developed, and its effect on state-based CD and the MVP CR algorithm are measured using three fast-time simulation experiments. The goal of the first experiment is to determine the overall safety with ADS-B. To this end, an ABS-B system based on Minimum Operational Performance Specifications (MOPS) [3] is compared to one that is based on measured actual performance [4], and to the case where perfect state information is used. The second and third experiments focus on the specific effect of situation related characteristics, i.e., transmission range and interference, on safety.

This paper is organized as follows. An overview of the Automatic Dependent Surveillance-Broadcast (ADS-B) system and its model derivation is described in Section II. Details of the three experiments used to study the safety impact of ADS-B, as well as a description of the Conflict Detection & Resolution (CD&R) method used are presented in Section III. The results are presented and discussed in Section IV. This paper ends with the main conclusions in Section V.

The authors are with the Control and Simulation Section, Faculty of Aerospace Engineering, Delft University of Technology, 2629HS Delft, The Netherlands. E-mail: T.P.langejan@student.tudelft.nl; e.sunil@tudelft.nl; j.ellerbroek@tudelft.nl; j.m.hoekstra@tudelft.nl

II. ADS-B Model

In this research, the focus is on the airborne ADS-B link between aircraft, enabled by ADS-B IN/OUT. ADS-B transmits specific state information in an omnidirectional manner, called squitter. The following different type of squitter messages exist, with their corresponding transmission rate:

- Airborne positions squitter (2 Hz)
- Surface position squitter (1 Hz)
- Airborne velocity squitter (2 Hz)
- Aircraft identification squitter (0.2 Hz)
- Operational Status (0.4 Hz)
- Target state (0.8 Hz)

The messages are transmitted using Pulse Position Modulation (PPM) on the 1090 MHz carrier frequency. Each message contains 120 bits and is transmitted at 1 Mbps, resulting in a message duration of 120 μs.

Two main elements can be identified affecting the ADS-B system performance; system and situational related elements. System related elements affect the accuracy of an ADS-B message, while situation related elements mostly affect the probability of proper detection and decoding of an ADS-B message. A schematic overview is shown in Figure 1. Both elements are discussed and modeled in the following subsections.

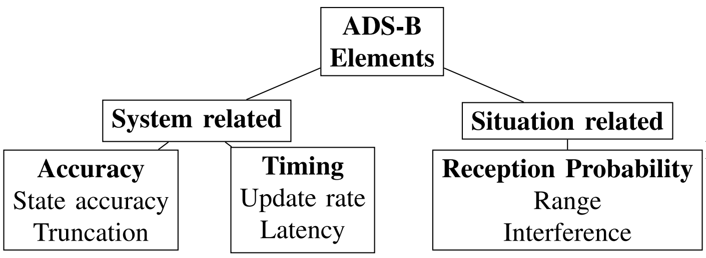

Figure 1: Schematic overview of elements degrading ADS-B performance.

A. System Related ADS-B Elements

The quality of an ADS-B message is affected by truncation, state accuracy and latency.

Truncation
The position reports contain latitude and longitude locations. Only 6 significant digits are available for transmission. Using the Haversine function, and a position described in longitude and latitude with a six digit significance level results in a accuracy ranging from 9 to 17 m, depending on the location on the earth.

State Accuracy
In addition to the truncation effect, the accuracy of the on-board measurement sensors affects the location precision. Location is determined using the Global Navigation Surveillance System (GNSS). In [1] it is that found a GPS measurement has an accuracy of $\leq$7.8 meter with a 95% confidence interval.

Latency
Generating and transmitting an ADS-B report results in a latency in the order of 20 milliseconds. This system delay results in a position error in the order of tens of meters.

Based on the truncation, accuracy and latency, the position accuracy of an ADS-B report can be modeled as a standard normal distribution with a standard deviation of 30 meters.

B. Situation Related ADS-B Elements

The situation related elements affect the detect and decode probability of an ADS-B report, caused by range and interference. Analytical models for these two aspects are discussed below.

Range
The derivation of an analytical model between distance and detect/decode probability is based on the 1090 Extended Squitter (ES) Minimum Operational Performance Specifications (MOPS) [3]. The general approach, described in [2], [5], is followed. This derivation consists of 5 steps.

Step 1: The derivation begins by computing the Free Space Path Loss (FSPL) for the 1090 MHz frequency.

$$FSPL(d) = \frac{4\pi df}{c}^2 \tag{1}$$

In Equation (1) c (speed of light) and f (carrier frequency) are constant. The FSPL per Nautical Mile (NM) is shown in Equation (2).

$$FSPL_{NM}(r) = 95.55 + 20 \cdot log_{10}(r)[\frac{dB}{NM}] \tag{2}$$

Step 2: The second step is to obtain the relation between distance and received power (S_{rec}) for a specific transmit power (S_{trans}), shown in Equation (3).

$$S_{rec} = S_{trans} - FSPL_{1NM} - 20 \cdot log(r) \tag{3a}$$

$$S_{rec} = S_{rec\_1NM} - 20 \cdot log(r) \tag{3b}$$

In Equation (3), $(S_{trans} - FSPL_{1NM})$ equals the received power at a distance of 1 Nautical Mile (NM), called S_{rec_1NM}, for a transmitted power of S_{trans}. Rewriting this equation, a relation between distance and received power is obtained, shown in Section II-B.

$$r = 10^{\frac{-(S_{rec} - S_{rec\_1NM})}{20}} \tag{4}$$

Step 3: In this step the detect and decode probability of an ADS-B report (without interference) is modeled as an exponential function of received signal power (S_{rec}). At the maximum reception distance, r_0, the detect and decode probability is set to zero. The received power at r_0 is defined as S_{rec0} [3]. The variable k is added to scale the curve of the reception probability function, resulting in Equation (5).

$$P(S_{rec}) = 1 - 10^{-k\frac{(S_{rec}-S_{rec0})}{20}}, S_{rec} \geq S_{rec0} \tag{5}$$

Step 4: The distance between transmitter and receiver for a detect and decode probability of zero, as a function of range (instead of received power), can be obtained by substituting Section II-B in Equation (5):

$$P(r) = 1 - \left(r \cdot 10^{-\frac{(S_{rec\ 1NM}-S_{rec0})}{20}}\right)^k, r \geq r_0 \tag{6}$$

The received power S_0 results in a zero detect and decode probability with the corresponding distance r_0. Using Section II-B, r_0 is obtained as shown in Equation (7)

$$r_0 = 10^{\frac{-(S_{rec0}-S_{rec\ 1NM})}{20}} \tag{7}$$

The inverse of Equation (7) is substituted in Equation (6) to obtain Equation (8).

$$P(r) = 1 - (\frac{r}{r_0})^k, r \geq r_0 \tag{8}$$

Equation (8) is used to determine the no-interference reception probability as a function range, using a fixed transmit power, S_{trans}.

Step 5: For the final step, the value of the scaling variable k is determined. In [3] a minimum triggering level (S_{MTL}) of -90 dBm for Class A3 equipped commercial transport is defined with the following requirements:

1) If link margin ($S_{rec} - S_{MTL}$) = 3dB the minimum reception probability should be ≥ 0.99.
2) If link margin ($S_{rec} - S_{MTL}$) = -3dB the minimum reception probability should be ≥ 0.15.

Substituting these values in Equation (5) results in a scaling factor k of 6.4314. In this model, it should be noted that the maximum reception distance, r_0, is a function of transmit power (S_{trans}) and sensor sensitivity (S_{rec0}).

The following assumptions are made in the detect and decode probability model derived with respect to range:

1) Omni-directional antenna used by transmitting and receiving aircraft.
2) A constant noise level on the 1090 MHz frequency is assumed, based on [3].
3) No multi-path effects.
4) Weather related effects are not taken into account.
5) No shielding by aircraft of ADS-B transmitter/receiver antenna.

Interference

If multiple ADS-B messages are received simultaneously at a receiver, it may not be possible to decode the received messages depending on the degree of overlap. This effect is called interference, and is visualized in Figure 2.

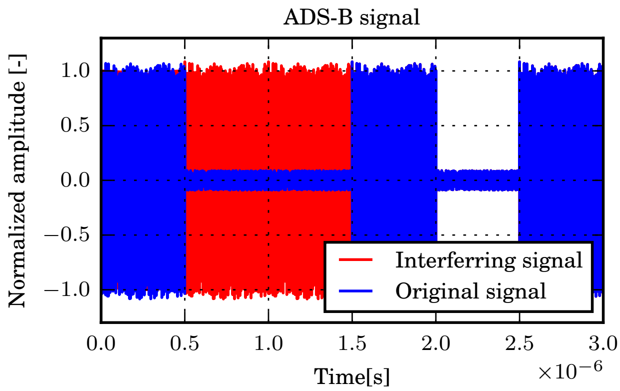

Figure 2: Interference effect; bits from the original signal cannot be decoded anymore due to interference.

To model the effect of interference on detect and decode probability, the Poisson distribution, shown in Equation (9), has been used. This probability distribution is generally used to calculate the number of events occurring during a specified time interval:

$$P[X = k] = (\lambda t)^k \frac{e^{-\lambda t}}{k!},\ k = 0, 1, 2, ... \tag{9}$$

In this equation, λ is the expected number of events occurring in unit time, t is the interval length, X is the number of events occurring in interval of length t, and P is the probability of X occurrences in an interval of length t.

The different ADS-B transmission rates, discussed in the previous section for the 6 different ADS-B reports, are considered. Each message has a duration of 120μ seconds and a total update rate of 6.4 Hz is obtained. The effect of the Traffic Collision Avoidance System (TCAS), transmitted on the same frequency is also added. The following assumptions are made:

1) No de-garbling is used. De-garbling can be modeled by selecting a lower message duration.
2) ADS-B message is modeled as 1 message, containing all the state information (instead of several different messages).

λ is calculated by the summation of the message update frequencies (F_{update}), multiplied by the number of aircraft within range (N_{ac}), shown in Equation (10).

$$\lambda = N_{ac} \cdot F_{update} \tag{10}$$

Assume a message is received at t=0. The duration of an ADS-B message τ is $120\mu s$, equal to the time variable in Equation (9).

To obtain the probability no other messages are received in this time interval the variable X in Equation (9) is set equal to 0, resulting in Equation (11).

$$P[X = 0] = (\lambda t)^0 \frac{e^{-\lambda t}}{0!} \tag{11a}$$

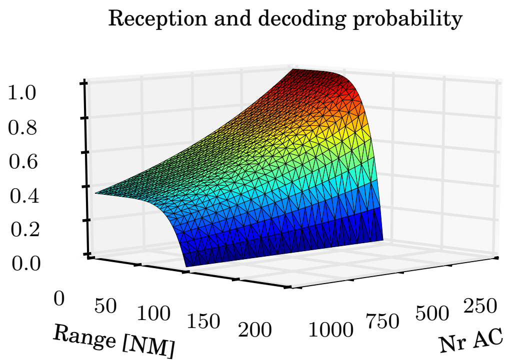

Figure 3: ADS-B detect and decode probability for MOPS specifications, based on number of interferring aircraft and range between aircraft.

$$P[X=0] = e^{-N_{ac}(\cdot F_{ADS-B}\cdot \tau_{ADS-B} + F_{TCAS}\cdot \tau_{TCAS})} \quad (11b)$$

C. Situation Related ADS-B Model

The detect and decode probabilities described in Section II-B can be combined. The corresponding detect and decode probability is shown in Equation (12). The probability $P_{T(i,j)}$ resembles the combined detect and decode probability of aircraft i receiving an ADS-B message from aircraft j, depending on range and interference. $P_{R(i,j)}$ is the detect and decode probability of aircraft i with respect to aircraft j due to range between the two aircraft. $P_{I(i,j)}(N_{acscaled})$ is the probability due to interference. The number of aircraft ($N_{acscaled}$) are scaled according to the distance of aircraft j at aircraft i. The model is shown in Figure 3.

$$\overbrace{P_{T(i,j)}(r, AC)}^{\text{Total probability}} = \overbrace{P_{R(i,j)}(r)}^{\text{Range}} \cdot \overbrace{P_{I(i,j)}(N_{acscaled})}^{\text{Scaled Interference}} \quad (12)$$

III. Experiment Design

In this section the design of three separate fast-time simulation experiments are described. The goal of the first experiment is to assess the overall safety of the ADS-B system. The aim of the second experiment is to study the effect of ADS-B range. The goal of the third experiment is to differentiate between the contribution of the range effect and the interference effect in the ADS-B model. Since experiment has a different goal, the independent variables for each experiment are different. But, the scenario settings, Conflict Detection (CD) and Conflict Resolution (CR) method, and dependent variables are similar between the experiments.

A. Simulation Environment

BlueSky, an open-source Python based Air Traffic Control (ATC) simulator developed at the Delft University of Technology, is used as simulation environment. Many useful features are already available in the simulator, such as CD and CR in the Airborne Separation Assurance System (ASAS) module. DataLog options, way-point routing and aircraft performance limitations (accelerations, bank angles etc.) are also implemented. The open-source characters enables easy implementation of new modules, such as an ADS-B model, in the simulator. For this research, the simulation update rate was set to 10 Hz. Further information regarding the simulator can be found in [6].

B. Conflict Detection

In the context of CD&R it is important to distinguish between intrusions and conflicts. An intrusion, also known as Loss Of Separation (LOS), occurs when the following minimum separation requirements are violated:

- 5 Nautical miles in the horizontal plane
- 1000 feet in the vertical plane

On the other hand, a conflict is a predicted intrusion within a certain look-ahead time; a five minute look-ahead time used in this work. To detect conflicts, the simple state-based CD method is used. Here, linear extrapolation of aircraft state vectors over the look-ahead time is used to detect conflicting trajectories.

C. Conflict Resolution - MVP

The Modified Voltage Potential (MVP) conflict resolution method is based on modeling aircraft as similarly charged particles that repel each other as described in [7], [8]. The determination of the MVP-based resolution vector is shown in more detail in Figure 4:

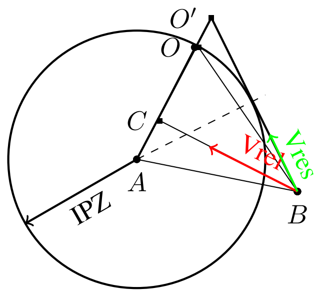

Figure 4: MVP-based conflict resolution for aircraft A and B in the horizontal plane. The relative velocity vector (V_{rel}) and the MVP-based resolution vector (V_{res}) are displayed.

The relative velocity vector with respect to a conflicting aircraft (A) is calculated (V_{rel}). This relative velocity vector results in a loss of separation without any intervention. Using this relative velocity and distance between the two aircraft, the Closest Point of Approach (CPA), point C, can be determined. Subsequently the closest distance out of the Intruder Protected Zone (IPZ), point O, is determined. The corresponding resolution vector CO still results in a LOS. Therefore Equation (13) is used to obtain the final resolution vector (V_{res}).:

$$\frac{|CO'|}{CO} = \frac{1}{|cos(arcsin(\frac{R}{AB}) - arcsin(\frac{AC}{AB})|} \quad (13)$$

Using the distance vector CO', the resolution velocity vector is calculated using Equation (14) [9]. In this equation, t_C is

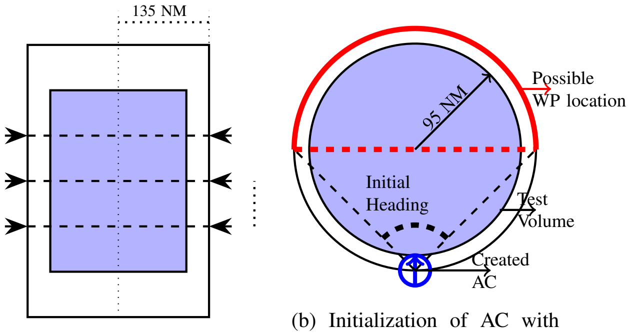

(a) Three flight levels

(b) Initialization of AC with 45° heading caption.

Figure 5: Scenario initialization.

the time required for aircraft B to reach point C when traveling with its pre-resolution velocity.

$$V_{MVP} = \frac{CO'}{t_C} + V_{current} \tag{14}$$

After a successful conflict resolution, aircraft are required to follow the heading back to their original destination, i.e., aircraft do not recover their original track but fly the heading that leads them directly to their destination. Other aircraft states, such as altitude and velocity, are also restored.

D. Traffic Scenarios

A common set of traffic scenarios were created for all three experiments. The testing region is discussed first, followed by the traffic demand.

Testing Region: A cylindrical region is used, consisting of an initialization volume and test volume. Aircraft are only logged while they are within the experiment area and deleted when leaving the experiment area. To maintain a constant air traffic density the experiment is divided in three phases.

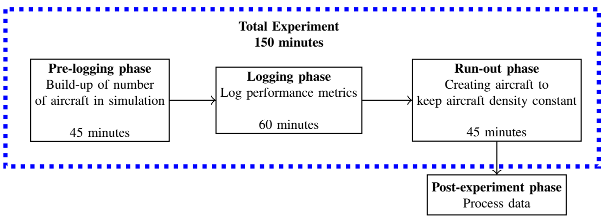

Traffic demand: A scenario generator is constructed to create similar air traffic scenarios (with different random number seeds). Aircraft are created on the edge of the initialization boundary at one of the 40 discrete points. Aircraft are created on three different flight levels and will randomly climb or descend to a different flight level or continue cruising at the current flight level. This results in conflicting aircraft from all possible directions. An overview is shown in Figure 5. Thee traffic densities are defined with their corresponding steady state number of aircraft, named Low (50), Medium (75) and High (100).

E. Independent Variables - Experiment I

The goal of this experiment is to assess the overall safety of the MVP method using ADS-B based state information. An overview of the independent variables is shown in Table I. Three ADS-B models are used; one based on the MOPS specifications (MOPS), one on measurements (Realistic) and one without ADS-B for perfect state information (Perfect).

Table I: Independent variables. Experiment - I

AC density	Low	Medium	High
ADS-B	MOPS	Realistic	Perfect

The ADS-B performance described in the previous section is based on the MOPS specifications. However, from measurements it is obtained that the ADS-B system has a larger range than the MOPS specifications [4]. Also the interference effect can be reduced using de-garbling. This can be modeled by reducing the specific message length in the Poisson distribution. Therefore two ADS-B models are assessed, one based on MOPS specifications and one on measurements. The parameters to determine the two ADS-B models are shown in Table II.

Table II: Parameters describing ADS-B detect and decode probability, based on MOPS [3] and measurements[4].

	ADS-B Assumptions Type	
	MOPS [3]	Realistic
$R_0[km]$	176	370
$R_0[NM]$	95	200
S_{trans} [dBm]	51	57
S_{trans} [W]	125	500 [4]
τ ADS-B μs	120	60
τ TCAS μs	64	32
State accuracy (Table III)	MOPS	Realistic

The resulting range and interference detect and decode probability curves are shown in Figure 6.

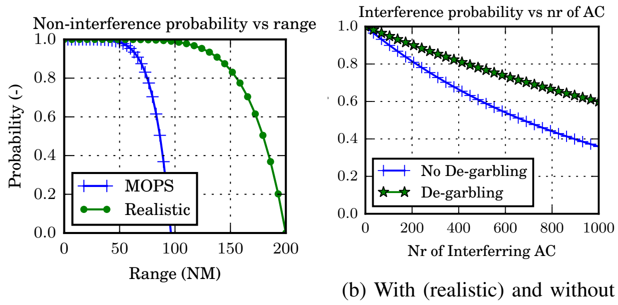

(a) MOPS and Realistic. Range related.

(b) With (realistic) and without (MOPS) degarbling, interference related.

Figure 6: Detect and decode probability for MOPS and Realistic model.

The different system related inaccuracies used in the MOPS and realistic model are shown in Table III.

Table III: System related inaccuracies

System related inaccuracies			
		Cases	
Parameters	Distribution	Realistic	MOPS
Position [m]	Normal	$\mu = 0, \sigma = 30$	$\mu = 0, \sigma = 50$
Velocity $\frac{m}{s}$	Normal	-	$\mu = 0, \sigma = 10$
Heading [^{o}]	Normal	-	$\mu = 0, \sigma = 3$

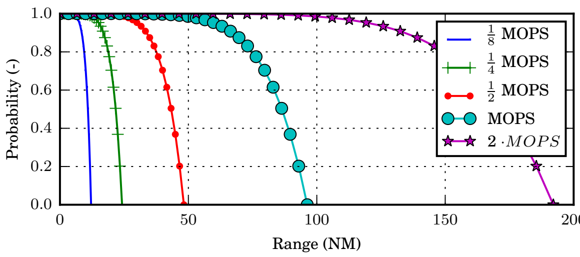

Figure 7: MOPS based reception models defined as fraction of MOPS range. Non-interference probability vs range.

Five repetitions were performed for each independent variable combination, using a different traffic scenario for each repetition. This resulted in 45 separate runs for Experiment I (3 ADS-B settings x 3 traffic densities x 5 repetitions).

F. Independent Variables - Experiment II

The goal of the second experiment is to study the effect of changing the maximum reception distance. From Section II it can be obtained that an increase in range results in a stronger interference effect. Therefore different ADS-B ranges are assessed and compared. The same traffic densities are used. The range of these ADS-B models, based on the MOPS model, are shown in Table IV. The maximum reception range can be modified by adapting the transmit power.

Table IV: Independent variables Experiment II (range analysis).

MOPS fraction	$\frac{1}{8}$	$\frac{1}{4}$	$\frac{1}{2}$	1	2
ADS-B Range [NM]	12	24	48	96	192
AC density	Low	Medium	High	-	-

The corresponding reception probability curves (defined as fractions of the MOPS range) are shown in Figure 7.

Once again, five repetitions were performed. This resulted in 75 separate runs for Experiment II (5 range settings x 3 traffic densities x 5 repetitions).

G. Independent Variables - Experiment III

An experiment is performed to asses the individual contribution of the two situation related properties; range and interference. Three traffic densities are assessed. An overview of the dependent variables is shown in Table V.

Table V: Independent variables. Experiment - III

AC density	Low	Medium	High
ADS-B	MOPS	MOPS interference	MOPS range

The following ADS-B settings are used as independent variables:

1) **ADS-B MOPS settings**, interference and range effect.
2) **Range effect only**.
3) **Interference effect only**.

For this experiment, five repetitions were also performed. This resulted in 45 separate runs for Experiment III (3 ADS-B models x 3 traffic densities x 5 repetitions).

H. Dependent variables

The conflicts detected, based on ADS-B state information are being logged. Additionally the conflicts detected when perfect state information would be available are logged. From these two metrics the false alerts (false positives) and missed conflicts (false negatives) can be obtained. Besides conflicts detected, the intrusions are logged.

Data representation: Each observed dependent variable is shown in a figure. The different traffic densities are shown on the x-axis, and the dependent variable on the y-axis. The legend indicates the ADS-B model. The 95% confidence interval is shown with the error bar for the 5 repetitions of each experiment setting.

IV. Results and Discussion

In this section the results of the three different experiments are discussed and presented.

A. Results Experiment - I

The goal of this experiment is to identify the overall effect on safety when ADS-B is used for inter-aircraft information sharing. An overview of the type of detected conflicts is shown in Table VI.

Table VI: Type of conflicts detected as percentage of total conflicts for the MOPS and Perfect ADS-B settings.

ADS-B model	Conflict type	Traffic density			Cumulative
		Low	Medium	High	
MOPS	Real Conflict	92	88	89	89
	False Positive	8	12	11	11
	False Negative	5	4	5	5
Realistic	Real Conflict	95	94	94	94
	False Positive	5	6	6	6
	False Negative	3	3	4	4

It can be observed that the percentage of false positive conflicts increases with traffic density. The percentage of false alerts is larger for the MOPS based ADS-B model than the Realistic ADS-B model. The detected number of conflicts per aircraft are shown in Figure 8. It is shown that more conflicts are detected for the ADS-B based state information cases.

The number of intrusions per aircraft is shown in Figure 9. The number of intrusions when perfect state information is used is larger than the case where the ADS-B model is used for the medium and high traffic density situation. However, no significant differences are observed.

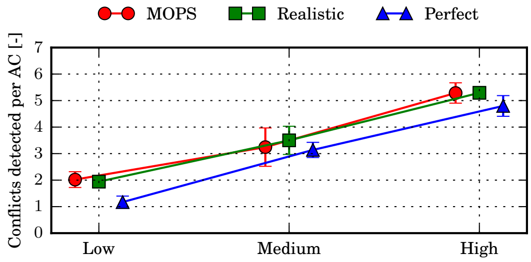

Figure 8: Number of detected conflicts per aircraft. Experiment - I.

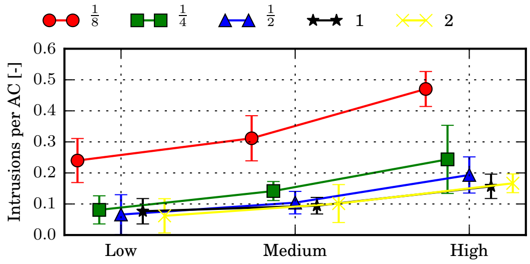

Figure 11: Number of intrusions per aircraft. Experiment - II.

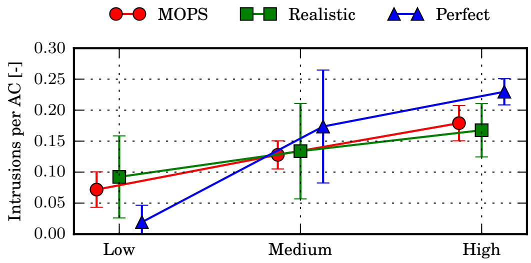

Figure 9: Number of intrusions per aircraft. Experiment - I.

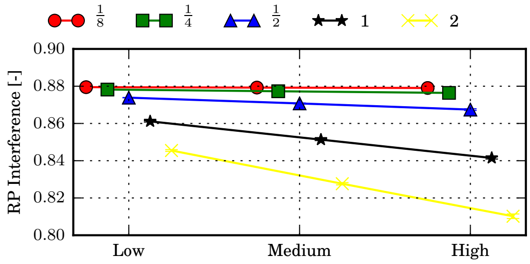

Figure 12: Mean interference reception probability. Experiment - II.

B. Results Experiment - II

In addition to the simulations, described in Section IV-A, a range analysis is performed. The goal of this analysis is to assess the effect of an increase in range, which also results in an increasing interference effect. The legend indicates the ADS-B model as fraction of the MOPS range. The number of detected conflicts for each model are shown in Figure 10. The models with $\frac{1}{8}^{th}$ and $\frac{1}{4}^{th}$ of the MOPS range show a smaller amount of detected conflicts.

Figure 11 shows the number of intrusions. Large differences start to occur between $\frac{1}{8}^{th}$ and $\frac{1}{4}^{th}$ of the range of the MOPS performance (12 NM and 24 NM). At 25% of the MOPS range, the number of intrusions show about a 50% increase, while at 12.5% of the MOPS range the number of intrusions increases with 250% for the highest traffic density.

From the number of intrusions it is found that the performance difference for the single MOPS model, with a range of 96 NM ("1") is slightly better than the model with double the MOPS model, with a range of 190 NM ("2") regarding number of intrusions. With the 5 minutes look-ahead time, for both ADS-B models, the range dependent detect and decode probabilities are in the linear region, close to 1. However, the effect of interference increases. This is clearly shown in Figure 12; where the decreased detect and decode probability caused by interference is shown. The increased range results in a decrease of detect and decode probability due to additional interference. Therefore it can be concluded that the interference effect should be taken into account in extremely high traffic density situations.

C. Results Experiment - III

The goal of this final experiment is to differentiate between the two main situation related effects; interference and range. The number of detected conflicts are shown in Figure 13. It is obtained that the number of detected conflicts for the range only model is slightly lower than for the other two.

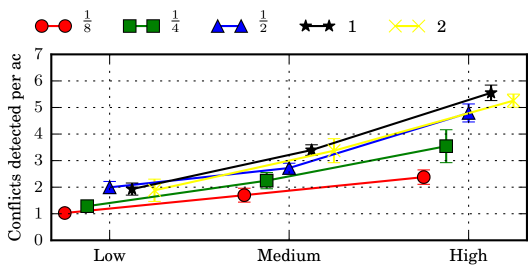

Figure 10: Number of detected conflicts per aircraft. Experiment - II.

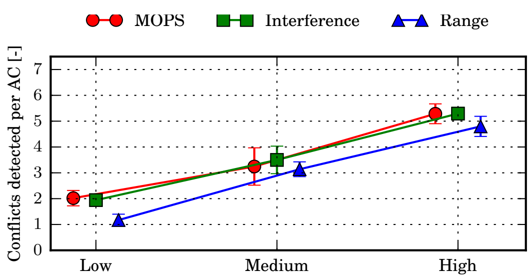

Figure 13: Number of detected conflicts per aircraft. Experiment - III.

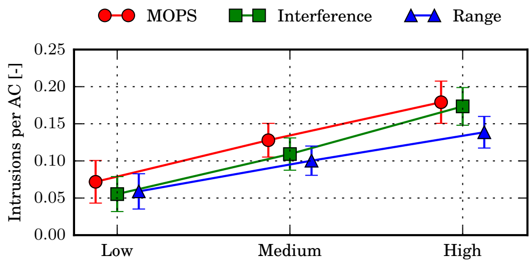

Figure 14: Number of intrusions per aircraft. Experiment - III.

The number of intrusions while using the interference only model is higher than the range model, especially at the higher traffic densities. The interference effect has a more negative impact than the range effect, especially at the High traffic density.

D. Discussion

From the first experiment it can be concluded that the effect of ADS-B based state information is small for the MVP method for the assessed traffic densities, compared to using perfect state information. This is partly due to the look-ahead time of 5 minutes, resulting in a detect and decode probability close to one. Also the position accuracy is high with respect to the dimensions of the IPZ. However, the interference effect should be taken into account. A larger transmit power increases the number of aircraft within range causing interference. Additionally, the impact of each aircraft increases, due to the higher transmitted power level. Also in the sensitivity analysis (Experiment - III) the effect of interference became larger at higher traffic densities. The detect and decode probability decreases with increasing number of aircraft according to the Poisson distribution. Additionally an increase in maximum reception range (i.e. transmit power) decreases this probability even further. Current Air Traffic Management (ATM) research aims to increase air traffic capacity. Therefore the interference result is a valuable observation and could be incorporated in future research.

V. Conclusion

In this paper, an ADS-B model based on system and situation related characteristics was presented. The effect of these characteristics on airborne Conflict Detection and Resolution (CD&R) was studied using fast-time simulation experiments. Here, sate-based conflict detection and the Modified Voltage Potential (MVP) conflict resolution algorithm was used as a case-study. For the studied conditions, the following conclusions can be drawn:

- The difference in safety between using ADS-B based state information and perfect state information was small.
- The range analysis showed that the combination of sate-based conflict detection and MVP is a very robust CD&R method, even when the maximum range was artificially reduced to $\frac{1}{4}^{th}$ of the ADS-B minimum ADS-B specifications.
- An increase in maximum reception range (by increasing transmission power) decreases the total detect and decode probability. This is because increasing range also increases signal interference as additional aircraft are detected.
- The interference effect becomes more dominant than the range effect for higher traffic densities. It is likely to play a more severe effect at very high traffic densities.
- The ADS-B system should not be considered as a direct limiting factor for self-separation or Free Flight. However, the interference effect at high traffic densities should be taken into account. The use of a single carrier frequency, increase in transmit power and high traffic density increase the interference effect.
- Future research will investigate the effect of ADS-B characteristics on additional CD&R methods and for higher densities.

References

[1] Global positioning system standard positioning service performance standard (2008). [Online]. Available: http://www.gps.gov/technical/ps/2008-SPS-performance-standard.pdf
[2] R. Barhydt, M. T. Palmer, and N. Langley, "Ads-b within a multi-aircraft simulation for distributed air-ground traffic management," *AIAA Digital Avionics Systems Conference*, 2004.
[3] RTCA Special Committee 186, "Minimum Aviation System Performance Standards for Automatic Dependent Surveillance Broadcast (ADS-B)," *RTCA/Do-242a*, 2002.
[4] B. S. Y. D. Ali, W. Schuster, W. Ochieng, A. Majumdar, and T. K. Chiew, "Framework for ADS-B Performance Assessment : the London TMA Case Study," *AIAA*, pp. 39–52, 2013.
[5] W. Chung and R. Staab, "A 1090 Extended Squitter Automatic Dependent Surveillance - Broadcast (ADS-B) Reception Model for Air-Traffic-Management Simulations," *AIAA 2006-6614, Modeling and Simulation Technologies Conference and Exhibit*, no. August, pp. 1–11, 2006.
[6] J. M. Hoekstra and J. Ellerbroek, "BlueSky ATC Simulator Project : an Open Data and Open Source Approach," *ICRAT 2016*.
[7] J. Hoekstra, R. van Gent, and R. Ruigrok, "Designing for safety: the free flight air traffic management concept," *Reliability Engineering & System Safety 75*, pp. 215–232, 2002.
[8] M. S. Eby, "A Self-Organizational Approach for resolving Air Traffic Conflicts," *The Lincoln Laboratory Journal*, vol. 7, no. 2, pp. 239–253, 1994.
[9] J. Maas, E. Sunil, J. Ellerbroek, and J. Hoekstra, "The effect of swarming on a voltage potential-based conflict resolution algorithm," *ICRAT*, 2016.

Bibliography

Aerial, M., Formation, V., & Swarm, U. (2003). Aiaa 2003-5729. (August).

Ali, B. S. Y. D., Schuster, W., Ochieng, W., Majumdar, A., & Chiew, T. K. (2013). Framework for ADS-B Performance Assessment : the London TMA Case Study. *AIAA*, 39–52.

Aviation, C. (2008). Capacity declaration amsterdam airport schiphol ; summer 2008 available number of slots distribution of aircraft movements over a twenty-four hours period. , *2008*, 20–22.

Ballin, M. G., Wing, D. J., Hughes, M. F., & Conway, S. R. (1999). Airborne Separation Assurance And Traffic Management : Research Of Concepts And Technology. *AIAA*(c), 1–12.

Barhydt, R., Eischeid, T., Palmer, M., & Wing, D. (n.d.). Use of a Prototype Airborne Separation Assurance System for Resolving Near-term Conflicts During Autonomous Aircraft Operations. In *Aiaa guidance, navigation, and control conference and exhibit.* American Institute of Aeronautics and Astronautics. Available from `http://arc.aiaa.org/doi/abs/10.2514/6.2003-5401`

Barhydt, R., Palmer, M. T., & Langley, N. (2004). ADS-B Within A Multi-aircraft Simulation For Distributed Air-ground Traffic Management Ads-b Message Generation Air Traffic Operations Simulation. *AIAA*.

Bernays, D. J., Thompson, S. D., & Harman, W. H. (2000). Measurements of ADS-B Extended Squitter performance in the Los Angeles basin region. In *Digital avionics systems conference, 2000. proceedings. dasc the 19th* (Vol. 2, pp. 7B1/1—-7B1/8 vol.2).

Bilimoria, K., Sheth, K., Lee, H., & Grabbe, S. (2000). Performance evaluation of airborne separation assurance for free flight. In *18th applied aerodynamics conference.* American Institute of Aeronautics and Astronautics. Available from `http://arc.aiaa.org/doi/abs/10.2514/6.2000-4269`

Chung, W., & Staab, R. (2006). A 1090 Extended Squitter Automatic Dependent Surveillance - Broadcast (ADS-B) Reception Model for Air-Traffic-Management Simulations. *AIAA 2006-6614, Modeling and Simulation Technologies Conference and Exhibit, August*(August), 1–11.

Conde, R., Alejo, D., Cobano, J. A., Viguria, A., & Ollero, A. (2012). Conflict Detection and Resolution Method for Cooperating Unmanned Aerial Vehicles. *Journal of Intelligent & Robotic Systems*, *65*(1-4), 495–505. Available from http://link.springer.com/10.1007/s10846-011-9564-6

Delahaye, D., , A. Vidosavljevic, A., Sunil, E., Hoekstra, J., Ellerbroek, J., et al. (n.d.). Metropolis urban airspace design.

DoD. (2016). *Global positioning system standard positioning service performance standard.* Available from http://www.gps.gov/technical/ps/2008-SPS-performance-standard.pdf

Duong, V., Hoffman, E., & Nicolaon, J.-p. (1997). Initial Results of Investigation into Autonomous Aircraft Concept (FREER-1). *1st USA/Europe Air Traffic Management Research and Development Seminar (ATM1997)*, 1–12.

Eby, M., & Kelly, I., W.E. (1999). Free flight separation assurance using distributed algorithms. *1999 IEEE Aerospace Conference. Proceedings (Cat. No.99TH8403)*, *2*.

Eby, M. S. (1994). A Self-Organizational Approach for resolving Air Traffic Conflicts. *The Lincoln Laboratory Journal*, *7*(2), 239–253.

Ellerbroek, J. (2013). *Airborne Conflict Resolution In Three Dimensions.*

Eurocontrol. (n.d.). ADS-B Overview year = 2004.

European Organisation for the Safety of Air Navigation (EUROCONTROL). (2013). *Challenges of Growth 2013* (Tech. Rep.).

Francisco, S., & Louisville, A. (2014). NextGen Update: 2014. *NextGen Update: 2014*(August).

Harman, W., Gertz, J., & Kaminsky, A. (1998). Techniques of improving reception of 1090 mhz ads-b signals.

Hoekstra, J. (2015). *Bluesky open air traffic simulator homepage.* Available from http://homepage.tudelft.nl/7p97s/BlueSky

Hoekstra, J., Gent, R. van, & Ruigrok, R. (2002). *Designing for safety: the free flight air traffic management concept* (Vol. 75) (No. november).

Hoekstra, J., Gent, R. V., & Groeneweg, J. (2003). Airborne separation assurance validation with multiple humans-in-the-loop. *5th USA/Europe air traffic management R&D seminar*, *251*, 1–10.

Hoekstra, J. M., Ruigrok, R. C. J., Gent, R. N. H. W. van, Visser, J., Gijsbers, B., Clari, M., et al. (2000, May). *Overview of NLR Free Flight Project* (Tech. Rep. No. NLR-CR-2000-227). Amsterdam: NLR.

Introduction, I. (2006). Fast-time Simulation of an Automated Conflict Detection and Resolution Concept. *Management*(September), 25–27.

J.M. Hoekstra, R. R. et al. (1998). Conceptual Design of Free Flight With Airbrone Separation Assurance.

Krozel, J., & Peters, M. (1997, December). Strategic conflict detection and resolution for free flight. In *Proceedings of the 36th ieee conference on decision and control, 1997* (Vol. 2, pp. 1822—-1828 vol.2).

Krozel, J., Peters, M., Bilimoria, K., Lee, C., & Mitchell, J. S. B. (2001, December). System performance characteristics of centralized and decentralized air traffic separation strategies. In *4th {USA}/{Europe} {Air} {Traffic} {Management} {R}\&{D} {Seminar}*. Santa Fe.

Kuchar, J. K., & Carpenter, B. D. (1997). Airborne Collision Alerting Logic for Closely-Spaced Parallel Approach. *Air Traffic Control Quarterly*(5), 2.

Kuchar, J. K., & Yang, L. C. (2000). A Review of Conflict Detection and Resolution Modeling Methods. *IEEE Transactions on Intelligent Transportation Systems*, *1*, 179–189.

Lachner, R. (1997). Collision avoidance as a differential game: real-time approximation of optimal strategies using higher derivatives of the value function. *1997 IEEE International Conference on Systems, Man, and Cybernetics. Computational Cybernetics and Simulation*, *3*, 2308–2313. Available from `http://ieeexplore.ieee.org/lpdocs/epic03/wrapper.htm?arnumber=635270`

Maas, J. (2015). A Quantitative Comparison of Conflict Resolution Strategies for Free Flight.

Magazine, A., & Engineers, E. (2012). Increasing autonomy of UAVs.

Prandini, M., Hu, J., Lygeros, J., & Sastry, S. (2000). A Probabilistic Approach to Aircraft Conflict Detection. *IEEE Transactions on Intelligent Transportation Systems*, *1*(4), 199–219.

RTCA Special Committee 186. (2002). Minimum Aviation System Performance Standards for Automatic Dependent Surveillance Broadcast (ADS-B). *Rtca/Do-242a*.

SESAR Consortium. (2012). European ATM Master Plan - Edition 2. *The Roadmap for Sustainable Air Traffic Management*(October), 1–100.

Soediono, B. (1989). No Title No Title. *Journal of Chemical Information and Modeling*, *53*(February), 160.

Tadema, J., Theunissen, E., & Kirk, K. M. (2010). Self Separation Support for UAS. *AIAA Infotech@ Aerospace Conference*(April), 1–15.

Valenti Clari, M. S. V., Ruigrok, R. C. J., & Hoekstra, J. M. (2000). Cost-benefit study of free-flight with airborne separation assurance. *Proceedings of the AIAA Guidance, Navigation and Control Conference*, 1–27.